EGG-TMI-7785
September 1987

INFORMAL REPORT

ASSESSMENT OF TMI-2 I AND Cs CHEMISTRY DURING CORE DEGRADATION

August W. Cronenberg
Sidney Langer

Idaho National Engineering Laboratory

Managed by the U.S. Department of Energy

EG&G Idaho

Work performed under DOE Contract No. DE-AC07-76ID01570

EGG-TMI-7785

ASSESSMENT OF TMI-2 I AND Cs CHEMISTRY DURING CORE DEGRADATION

August W. Cronenberg[a]
Sidney Langer

Published September 1987

EG&G Idaho, Inc.
Idaho Falls, Idaho 83415

Prepared for the
U.S. Department of Energy
Idaho Operations Office
Under DOE Contract No. DE-AC07-76ID01570

---

a. ESA, Inc., 836 Clair View Lane, Idaho Falls, ID 83402

ABSTRACT

Data from the TMI-2 accident has shown that only small amounts of iodine (I) and cesium (Cs) escaped the plant, on the order of tens of curies. To further the understanding of the chemical and physical processes which were responsible for such limited release, a detailed investigation of fission product I and Cs behavior during the core degradation phase of the TMI-2 accident was initiated. Specifically, analyses are presented of I and Cs release from the severely damaged fuel, chemical reaction processes with the steam/hydrogen effluent, and transport/deposition behavior within the primary coolant system.

Results indicate that although elemental I and Cs release from fuel can be expected, the effluent chemical environment was such as to favor predominantly CsI and CsOH formation in the high-temperature effluent. Subsequent CsI reaction with boric acid released with reflood water is predicted to have resulted in partial conversion of CsI to Cs-borate and HI. Residual transport of CsI is predicted to condense and chemisorb in the upper reactor plenum, forming additional HI in the process. HI is therefore assessed to be the principal form of iodine transport leaving the reactor vessel during core degradation, which was subsequently dissolved in water to produce iodide ions in solution with coolant.

CONTENTS

FIGURES

TABLES

ASSESSMENT OF TMI-2 I AND Cs CHEMISTRY DURING CORE DEGRADATION

1. INTRODUCTION

From measurements of off-site TMI-2 radiation, it has been estimated that about 2.1 million curies (Ci) of the noble fission gases (largely Xe-133) escaped to the environment. Since the calculated inventory of Xe-133 in the TMI-2 core at the time of the accident was ≈220 million Ci, this corresponds to a noble-gas release fraction of approximately 1%. On the other hand, only about 15 curies of iodine-131 was released to the environment, where the total core inventory was ≈65 million curies. Similar limited release of Cs and other risk-dominant fission products have also been estimated.[1,2] Such limited releases are significant with respect to assessment of the risk associated with nuclear power, since radioiodine and cesium (along with tellurium) have the highest potential for biological insult to the public health. The formation of water-soluble chemical species of iodine and cesium (e.g., CsI, HI, CsOH) and the fact that containment isolation was maintained during the accident, are considered the primary reasons for limited iodine and cesium release from the TMI-2 plant. The purpose of this report is to assess I and Cs chemistry during the TMI-2 accident, where I/Cs release characteristics from the fuel, chemical reaction potential in the steam/H_2 effluent, and transport/deposition processes are evaluated.

Initially it was postulated[2-4] that the formation of CsI and CsOH largely controlled iodine and cesium behavior during the TMI-2 accident. However, recent evidence from various programs being conducted to study fission product behavior during severe accidents, call into question the contention that iodine is *a priori* bound to Cs, and that CsI primarily controls iodine release, transport, and deposition behavior.

With respect to the chemical form of I and Cs released from fuel, recent experimental results from fission product release studies at Battelle Columbus Laboratories[5] show that the activation energies for release of Cs and I from UO_2 fuel are on the order of 140 and

109 Kcal/mole, respectively. This difference indicates that Cs and I may be released from the fuel separately and at different rates, not as molecular CsI. The burnup condition of the test fuel samples was in the range of 35,000 MWd/t. Data from the PBF Severe Fuel Damage Test data[6] also indicate that for low-burnup fuel, atomic I and Cs release from fuel is favored. Because both elemental I and Cs are quite volatile at elevated fuel temperatures (see Table 1-1), early release from overheated fuel would be expected. On the other hand, CsI is less volatile and can be expected to have a lower diffusivity than atomic species,[6] thus it may be retained in the fuel longer than its constituents.

Once released from fuel, I and Cs will mix and chemically react with the steam and hydrogen effluent. Thermochemical equilibrium and kinetics analysis of gas-phase chemistry indicates that the chemical forms of I and Cs in a steam/H_2 gas environment are largely controlled by fission product concentration conditions and H/O mole ratio. For low concentrations of I and Cs in the more abundant steam/H_2 gas effluent ($<10^{-7}$ moles fission product per mole steam), the formation of CsOH and HI is favored. At high concentrations ($>10^{-4}$), CsI formation can be expected.

An interdependence also exists between chemical form and transport/deposition behavior through the primary coolant system for reactive species. Results of recent experiments indicate that gaseous effluent composed primarily of CsOH, CsI, HI, steam, and hydrogen will react with stainless steel surfaces, where Cs compounds are deposited and HI is released.[7,8] Boric acid (boron being present in reflood water as a neutron absorber) also tends to destabilize CsI, liberating HI in the process.[9]

Despite initial speculation that CsI was the dominant chemical form governing iodine behavior during the TMI-2 accident, the above cited data call this assumption into question. In fact, there is very little evidence from the TMI-2 accident to indicate what the true chemical form of the iodine was during transport through the primary coolant system. The release to the containment was at all times scrubbed through a pool of hot

TABLE 1-1. MOLECULAR PROPERTIES AND TRANSITION TEMPERATURES

Species	Molecular or Atomic Number	Molecular or Atomic Weight	Molecular or Atomic Radius (A)	Transition Temperature at 1 atm (K)
Cs	55	132.9	2.35	T_{mp} = 301 T_{bp} = 951
I	53	126.9	1.33	T_{mp} = 387 T_{bp} = 457
Xe	54	131.3	2.05	T_{mp} = 161 T_{bp} = 166
CsI	108	259.8	3.68	T_{mp} = 894 T_{bp} = 1553

water in the pressurizer. The only evidence for iodine chemical form was deduced from sump water samples showing high concentrations of ionic species (i.e., I^- and IO_3^- ions in solution). These results were interpreted[2] as indicating iodine was in the form of CsI-salt before entering solution, but HI is a soluble acid and would also form an ionic solution when exposed to water. However, HI is more volatile than CsI and would transport as a vapor through much of the reactor coolant system (RCS) system before dissolving in water (most likely in the pressurizer), while CsI would condense at higher temperatures (equivalent to temperatures estimated in the reactor plenum). The purpose of this investigation is to reevaluate the TMI-2 findings on I and Cs behavior, where an in-depth assessment is made of internal fuel morphology and microstructural effects on fission-product release from fuel, fission product/steam/hydrogen concentration conditions which govern effluent chemistry, and transport/deposition behavior in the primary coolant system.

An assessment of I and Cs chemical behavior during the core degradation phase of the TMI-2 accident requires knowledge of the following:

1. The chronology of significant events affecting the escape of fission products from the damaged fuel.

2. The release behavior of I and Cs from fuel, and the steam/hydrogen chemical environment into which such fission products are released.

3. Characterization of the effluent flow path and thermalhydraulic conditions governing condensation and chemisorption processes.

In Section 2, the TMI-2 accident sequence is summarized, with core damage and thermalhydraulic conditions presented and the steam/H_2 chemical environment estimated. The release of I and Cs from the damaged TMI-2 fuel are then estimated in Chapter 3. Thermochemical equilibrium and chemical kinetics analyses are performed in Chapter 4, to assess the gas-phase chemistry of I and Cs in the steam/H_2 effluent. Transport and

deposition chemistry within the primary system are evaluated in Chapter 5. Conclusions concerning overall I and Cs chemical behavior during the the TMI-2 accident are then summarized in Chapter 6.

1.1 References

1. J. G. Kemeny, et al., Report of the President's Commission on the Accident at Three Mile Island, October 1979.

2. D. O. Campbell, A. P. Malinauskas, and W. R. Stratton, "The Chemical Behavior of Fission Product Iodine in Light Water Reactor Accidents," Nuclear Technology, 53, 1981, pp. 111-119.

3. C. A. Pelletier, et al., "Iodine-131 Behavior During the TMI-2 Accident," NSAC-30, September 1981.

4. T. Moore, "Reactor Accidents: A Global Reassessment of Consequences," EPRI Journal, August 1983, pp. 10-23.

5. C. Alexander, "High-Temperature/High-Pressure Mass Spectrometry for Fission Product Release Evaluation," Proc. NRC Severe Fuel Damage and Source Term Research Program Review Mtg., Idaho Falls, Idaho, April 16-19, 1985.

6. A. W. Cronenberg and D. J. Osetek, "Fuel Morphology Effects on Chemical Form of Iodine Release From Severely Damaged Fuel," J. Nucl. Materials, 1987.

7. C. A. Alexander and J. S. Ogden, "CsI-H_2O-Stainless Steel Chemistry," Proc. NRC Severe Fuel Damage Partners Meeting, Rockville, MD, October 21-24, 1986.

8. O. Gotzmann, C. E. Johnson, and D. C. Fee, "Attack of Stainless Steel by Liquid and Vaporized CsOH," J. Nucl. Matl. 74, 1978, pp. 68-75.

9. I. R. Beattie, B. R. Bowsher, T. R. Gilson, and P. J. Jones, The Interaction of CsI with Boric Acid, Winfrith Laboratory Report: AEEW-R-1974, June 1985.

2. ACCIDENT SEQUENCE AND STEAM/HYDROGEN ENVIRONMENT

In this section the chronology of TMI-2 core degradation is summarized, with emphasis on identifying the most important events thought to have governed fission product release from the damaged TMI-2 fuel. Based on current knowledge of the TMI-2 accident scenario, code-predicted core heatup and thermalhydraulic conditions are then used to define the steam/hydrogen environment into which I and Cs are released and react.

2.1 Overview of Accident Sequence Affecting I/Cs Release

The TMI-2 accident scenario and major events thought to have influenced fission product release from the damaged core are summarized in Table 2-1. As discussed in Ref. 1, the accident was initiated by cessation of secondary feedwater flow. The resultant reduction of primary-to-secondary heat exchange caused primary coolant heatup and an increase in primary system pressure. The pressurizer pilot-operated relief valve (PORV) then opened to relieve pressure, but failed to close, releasing coolant in the process. However, during this period the core remained covered with coolant.

At 100 min into the accident, the plant operator turned off the reactor coolant pumps, resulting in accelerated core heatup and uncovery. By 150 min the zircaloy-steam exothermic reaction dramatically increased core heatup and degradation. The zircaloy melting temperature (≈2250 K) was exceeded, resulting in relocation of the molten zircaloy and liquefied fuel into a coherent mass of uncoolable material as illustrated in the top portion of Figure 2-1. During this period (≈150-174 min), significant I and Cs release would be expected from the liquified fuel.

At 174 min, the reactor 2B-pump was turned on and coolant was briefly (≈1 min) pumped into the reactor vessel. The resultant thermal-mechanical forces are believed to have shattered the oxidized fuel rod remnants in the upper regions of the core, forming a rubble bed on top of the consolidated core materials. The core conditions after the 2B-pump transient are illustrated in the middle portion of Figure 2-1. Significant

TABLE 2-1. TMI-2 ACCIDENT EVENT SEQUENCE

Time	Event(s)
0-100 min (0-1.7 hr)	Cessation of secondary feedwater flow; loss of primary coolant from pressurizer; core remained covered; reactor coolant pump turned off at 100 min.
100-150 min (1.7-2.5 hr)	Core uncovery to about core half-height by 138 min; rod ballooning and rupture; rod gap-release of fission products.
150-174 min (2.5-2.9 hr)	Autocatalytic zircaloy-steam reaction became significant; initiation of significant hydrogen generation and fission product release; zircaloy melt temperature (2250 K) exceeded; molten zircaloy and liquefied fuel relocation and formation of uncoolable consolidated debris material; significant release of fission products from liquefied fuel.
174-175 min (2.9 hr)	The 2B-pump was energized at 174 min and pumped coolant for less than a minute; fragmentation of oxidized fuel rods in upper region of core; formation of porous rubble bed on top of consolidated debris region; additional release of fission products from shattered fuel in upper region of core.
175-200 min (2.9-3.3 hr)	Continued heatup of consolidated/uncoolable debris material.
200-267 min (3.3-4.4 hr)	The High-Pressure Injection (HPI) pumps were operated intermittently during this period; additional shattering of fuel and release of fission products.
224 min (3.7 hr)	Remelting and breakout of molten material from the uncoolable consolidated debris region; relocation of core material to the flooded lower plenum region; additional fission product release due to debris fragmentation.
960 min (16 hr)	Generally stable conditions were achieved at approximately 16 hour into the accident when a reactor coolant pump was restarted. Cold shutdown with natural circulation was achieved about one month later, on April 27, 1979.

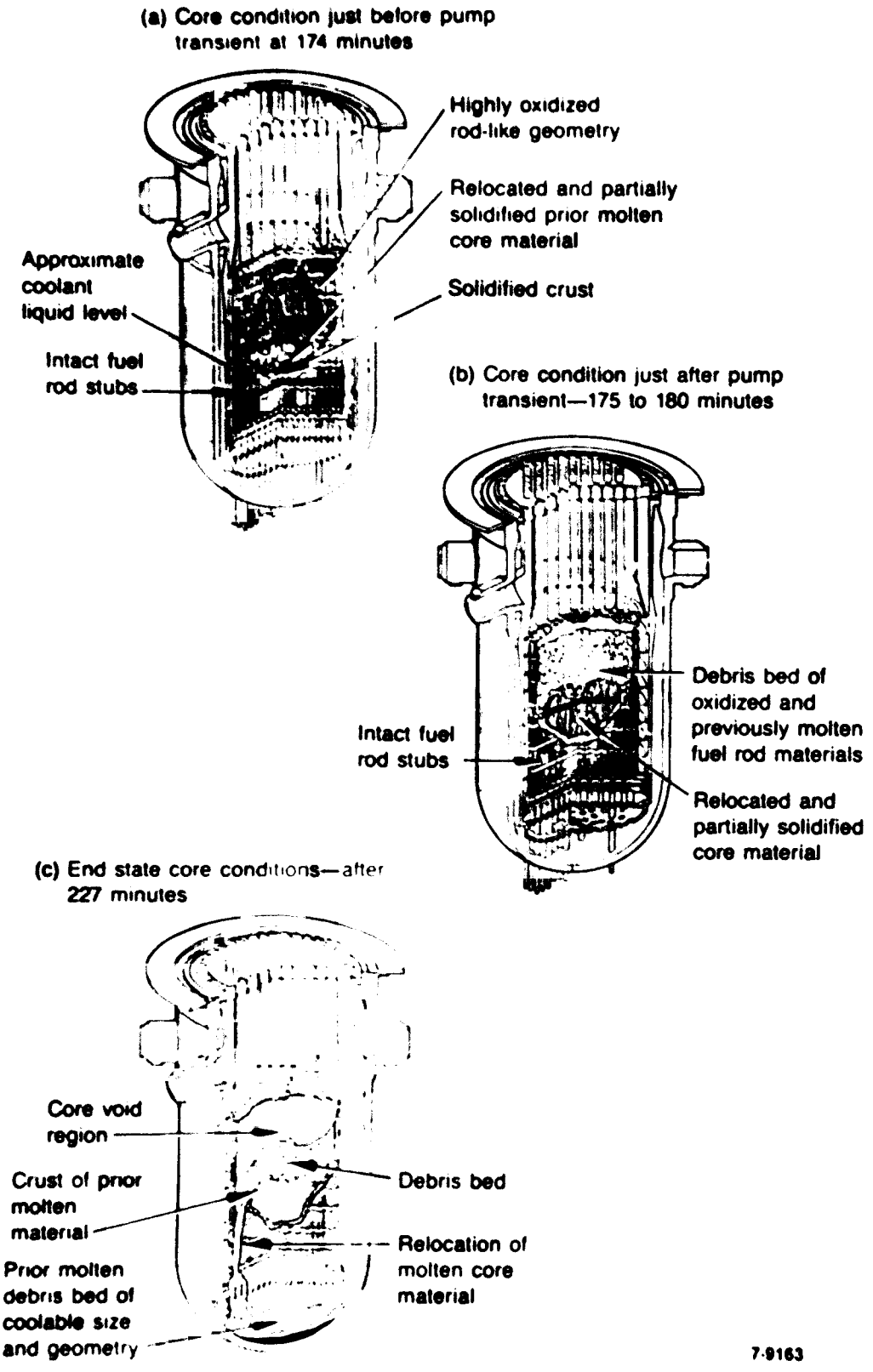

Figure 2-1. Hypothesized stages of the TMI-2 accident progression.

fission product release is also thought to have occurred as a result of such fuel shattering, based on finding from the PBF-severe fuel damage experiments.[2]

The consolidated, partially solidified core material continued to heat up during the next 50 min (174 to 224 min), although coolant delivery to the reactor vessel (from the pump transient and emergency core cooling injection) is estimated to have covered the core by approximately 210 min. By 224 min, much of the consolidated region had reached temperatures sufficient to cause remelting of this material. On-line data recorded during the accident[3] indicate that the consolidated core material relocated to the lower plenum between 224 and 226 min. Additional fission product release may have occurred during molten debris quenching and fragmentation in the lower plenum. Debris fragmentation resulted in the formation of a coolable configuration in the lower plenum. The best-estimate final damage configuration of the core is illustrated in the bottom of Figure 2-1.

Based on the current understanding of the TMI-2 accident sequence described above, three major periods of volatile fission product release are through to have occurred (excluding gap release of noble gases on initial rod failure). The three events leading to major I and Cs releases are considered to be:

150-174 min	Volatile fission product release during zircaloy oxidation induced fuel liquefaction and relocation.
174 min	Release from shattered fuel rods during the 2B-pump reflood transient.
224 min	Release from fragmented debris during quenching in lower plenum.

The last event (at 224 min) is thought to be of less importance to I and Cs transport chemistry with steam/H_2 effluent, since such a release would be directly into a water environment. For present purposes, the first two

events are considered dominant with respect to I and Cs vapor transport chemistry. Detailed consideration of core thermalhydraulic and fuel temperature conditions during this time period are presented in the following subsection.

2.2 SCDAP Predicted Core Damage and Thermalhydraulic Conditions

Although the general progression of events during the TMI-2 accident and overall core damage sequence are known, considerable uncertainty exists with respect to the details of core heatup and associated thermalhydraulic conditions relative to coolant boiloff and hydrogen generation history. The relative rates of steam and hydrogen production, however, largely control the effluent chemical environment (i.e. H/O mole ratio) and resultant I and Cs chemical form during vapor transport.

At the time of this study, no definitive steam/H_2 generation history has been defined for the TMI-2 accident. Instead, a range of conditions is estimated, based on code-predicted core behavior for various assumptions regarding coolant makeup flow, core reconfiguration and cladding surface area available for oxidation, core nodalization scheme, degree of flow blockage, extent of fuel liquefaction, etc. Differences in assumed makeup flow and available zircaloy surface area for oxidation and attendant H_2 release, can have a significant effect on estimated H_2/steam concentration conditions, which in turn largely control I/Cs/effluent chemistry. In this study, an attempt is made to assess a reasonable range of steam/H_2 environmental conditions during the time period from 150-180 min, when the major fraction of I and Cs release from fuel is expected. Having assessed such a range, a "base-case" effluent chemical environment is defined to establish a basis for calculation of the expected I and Cs chemical forms during vapor transport with such effluent. Variations in H/O mole ratio and I/Cs concentration conditions from the "base-case" problem are also considered, to establish a range of uncertainty in the chemical form of I/Cs vapor transport.

For present purposes, two SCDAP predicted core-damage sequences are considered. The first is based on an early SCDAP analysis of core damage

assuming core uncovery at 100 min (here called the "SCDAP-1985" calculation), and a more recent investigation using a coupled SCDAP/RELAP calculation of system behavior (here called "SCDAP/RELAP-1987" calculation). Details of these calculations are presented in Refs. 4 and 5 and summarized below.

2.2.1 SCDAP-1985 Calculation

The SCDAP/MOD1 computer code[6] was used to predict the core damage progression sequence and core thermalhydraulic conditions. The SCDAP-1985 results summarized here are based on core uncovery at about 100 min, which was designated the "early-uncovery" scenario in Ref. 4. Details of the core nodalization scheme and other code input parameters are presented in Reference 4. The intent of this study was to make core thermalhydraulic, fuel temperature, and damage progression predictions as a function of accident time.

The core makeup flow, pressure, and liquid-level histories are shown in Figure 2-2. The core is indicated to have uncovered to about the 0.7 m elevation by the time the 2B-pump was actuated at 174 min. Operation of the 2B-pump is predicted to result in only partial core reflooding to about the 2.5 m elevation, so that the top third of the core is predicted to have remained uncovered and subject to continued zircaloy oxidation and fuel heatup. The average system pressure between 160 and 180 min is predicted to be about 1500 psi (10.3 MPa), while the nominal makeup flow through the core at a time just after termination of the 2B-pump event is on the order of 2.5 kg/s.

As indicated in Figure 2-3, the core heatup rate is predicted to be accelerated at the time when fuel temperatures of 1500 K were calculated due to enhanced cladding oxidation. Fuel temperatures in excess of 2500 K are indicated at times greater than 170 min. The cumulative code-predicted hydrogen production is also shown in Figure 2-3 as a function of time. The maximum rate of hydrogen production due to zircaloy oxidation is predicted to occur just after partial core flooding at 176 min, due to enhanced boiloff, steam oxidation of the cladding, and rapid escalation to high

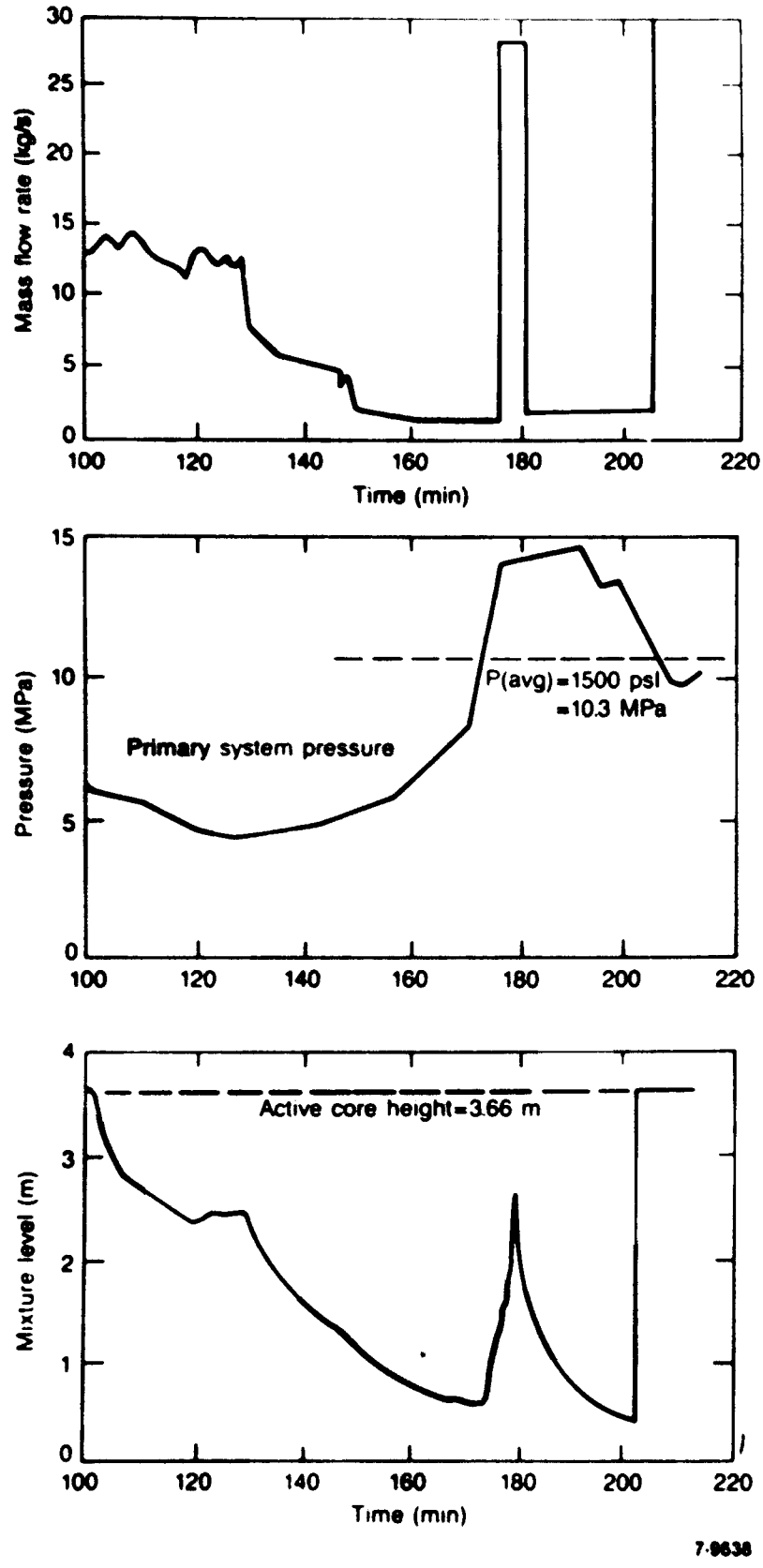

Figure 2-2. SCDAP calculated coolant mass flow rate, system pressure, and hydrogen generation history for the TMI-2 accident.

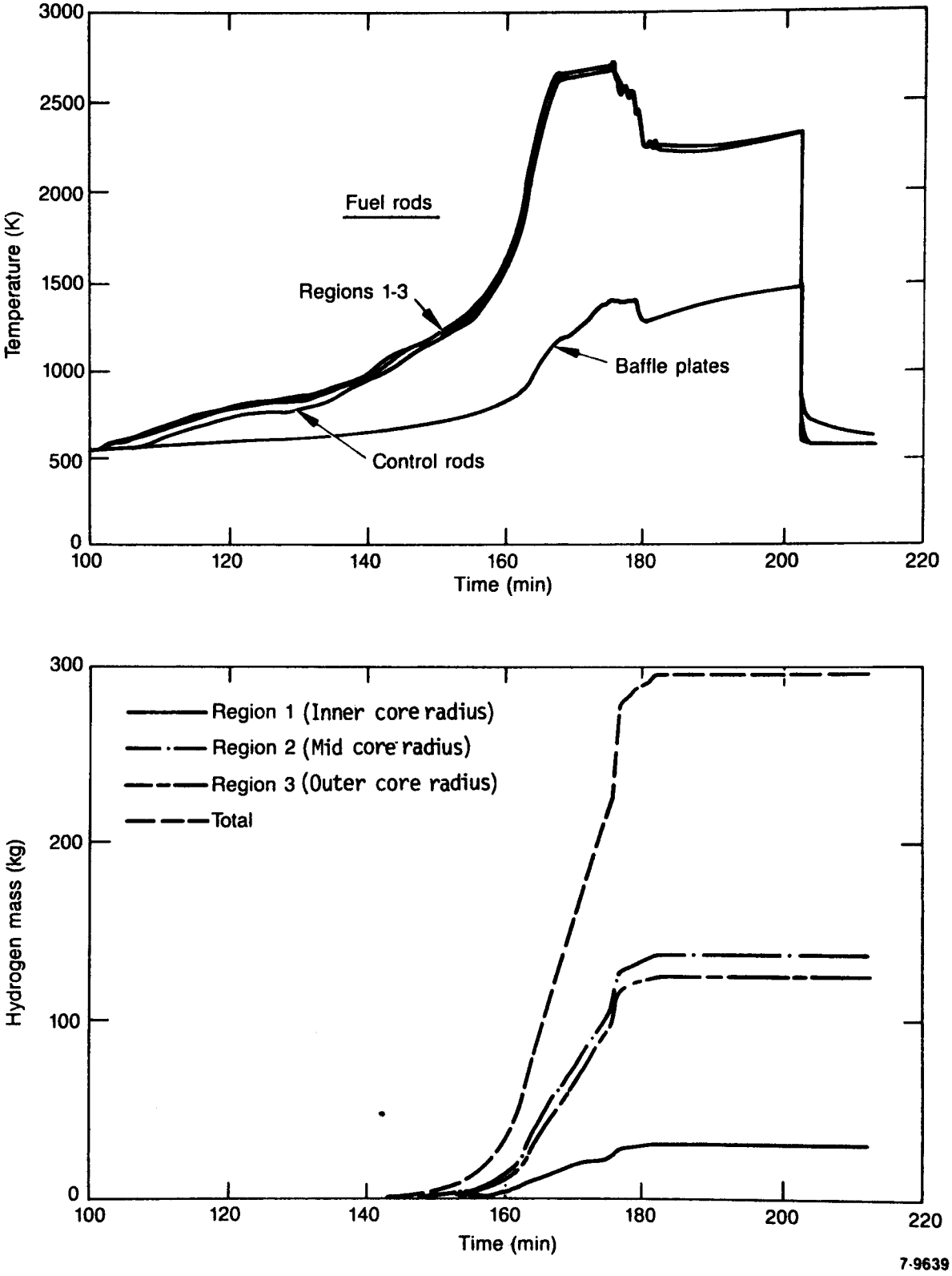

Figure 2-3. SCDAP-1985 predicted core temperatures and hydrogen generation histories.

temperatures in the upper region of the core. The total SCDAP-1985 predicted hydrogen production is approximately 300 kg.[a] Noting that complete zircaloy cladding (23,000 kg) oxidation would give approximately 1010 kg total hydrogen, the SCDAP-1985 calculation translates to about 30% oxidation. The hydrogen generation rate during core heatup (from 160 to 180 min) is estimated to be:

$$H_2\text{-rage} = \frac{(290-20)}{20\ \text{min}} = 13.5\ \text{kg/min} = 0.225\ \text{kg/s} \quad .$$

For the SCDAP-1985 predicted thermalhydraulic conditions, the steam/H_2 chemical environment can be estimated as follows. Assuming a steam production rate equivalent to the water makeup flow just after termination of the 2B-pump transient (≈2.5 kg/s, see Figure 2-2) and an average hydrogen production rate of 0.225 kg/s, the H_2/H_2O mole ratio is estimated in Table 2-2 to be on the order of 4.26. Thus, a hydrogen-rich effluent environment is predicted at an accident time just after the 2B-pump transient, when significant fission product release would be expected as a consequence of fuel shattering from rod remnants as well as from liquified fuel.

2.2.2 SCDAP/RELAP-1987 Calculation

A coupling of the SCDAP and RELAP codes has recently been used to predict the core damage progression sequence and thermalhydraulic conditions,[5] as part of the Standard Problem effort.[b] The results presented here are based on core uncovery at about 100 min after reactor scram. Details of the core nodalization scheme and other code input

---

a. Other estimates of the total hydrogen mass generated during the TMI-2 accident range from 450 to 580 kg [see Refs. 7, 8].

b. The TMI-2 Standard Program effort involves benchmarking of RELAP/SCDAP code-predicted accident progression and core degradation, with data findings from core debris removed and vessel inspection efforts.

TABLE 2-2. ESTIMATION OF THE TMI-2 H_2/H_2O MOLE RATIO FOR THE SCDAP-1985 CALCULATION

Nominal Flow Conditions:

H_2O - makeup flow rate = 2500 g/s

H_2 - generation rate = 225 g/s

Calculation of H_2/H_2O Molar Ratio:

H_2O molar boiloff rate = $\frac{2500\ g/s}{18\ g/mole}$ = 138.9 moles/s

H_2 molar generation rate = $\frac{225\ g/s}{2\ g/mole}$ = 112.5 moles/s

Unreacted H_2O molar flow rate = 138.9 - 112.5 = 26.4 moles/s

Mole fraction of Free H_2 = $\frac{112.5}{138.9}$ = 0.81

Mole fraction of Unreacted H_2O = $\frac{26.4}{138.9}$ = 0.19

Free-H_2/Unreacted-H_2O Mole ratio = $\frac{112.5}{26.4}$ = 4.26

[(Free-H_2 + H_2-from Unreacted H_2O)/Unreacted H_2O] Mole ratio

= $\frac{138.9}{26.4}$ = 5.26

Calculation of Effluent Concentration:

Effluent Conditions: 10.3 MPa
2000 K

$$\text{Effluent concentration} = \frac{10.3\ E{+}06\ Pa}{8.314\ E{+}03\ \frac{Pa\text{-}m^3}{kgmole\text{-}K}\ (2000\ K)}$$

$$= 6.19\ E{-}01\ kgmoles/m^3 = 6.19\ E{-}04\ gmoles/cm^3$$

Free-H_2 concentration = 0.81(6.19 E-04) = 5.014 E-04 moles/cm^3
= 3.018 E+20 molecules/cm^3

Unreacted-H_2O concentration = 0.19(6.19 E-04) = 1.176 E-04 moles/cm^3
= 7.08 E+19 molecules/cm^3

---

parameters are presented in Reference 5. Of interest are core thermalhydraulic, fuel temperatures, and damage progression predictions as a function of accident time.

Various best-estimate conditions have been used to assess the range of uncertainties associated with TMI-2 thermalhydraulic behavior. Makeup flow prior to 100 min was assumed to be ≈2 kg/s and a letdown (loss from pressurizer) of 9 kg/s. The predictions presented in Figures 2 4 through 2-6 are based on a core axial nodalization of six 2-ft evenly spaced nodes. Because of differences in SCDAP/RELAP predicted versus plant measured thermalhydraulic conditions, the makeup flow beyond 100 min was varied from 1.0 kg/s to 5.2 kg/s.

Figure 2-4 presents the predicted core-central region cladding temperatures as a function of time for the different makeup flow conditions, up to the time of the 2B-pump transient (174 min). Accelerated heatup occurred above 1500 K, driven by steam-induced cladding oxidation. Fuel heatup to temperatures in excess of the $Zr(O)/UO_2$ liquefaction temperature (≈2170 K) are predicted at a time between 150-160 min. In general the uncovered upper core axial node is shown to reach peak temperatures in the range of 2500-3000 K depending upon makeup flow, while lower core nodes show a stronger dependence on makeup flow rate.

Figure 2-5 shows the elevation of the liquid level above the bottom of the core as a function of time for various assumed makeup flow conditions. The core is predicted to have uncovered to below the bottom of the core at the 1 kg/s makeup flow condition; however, at 4 kg/s and 5.2 kg/s, complete core uncovery is not predicted.

The cumulative hydrogen production up to the initiation of the 2B-pump transient (at 174 min) is shown in Figure 2-6. Noting that oxidation of

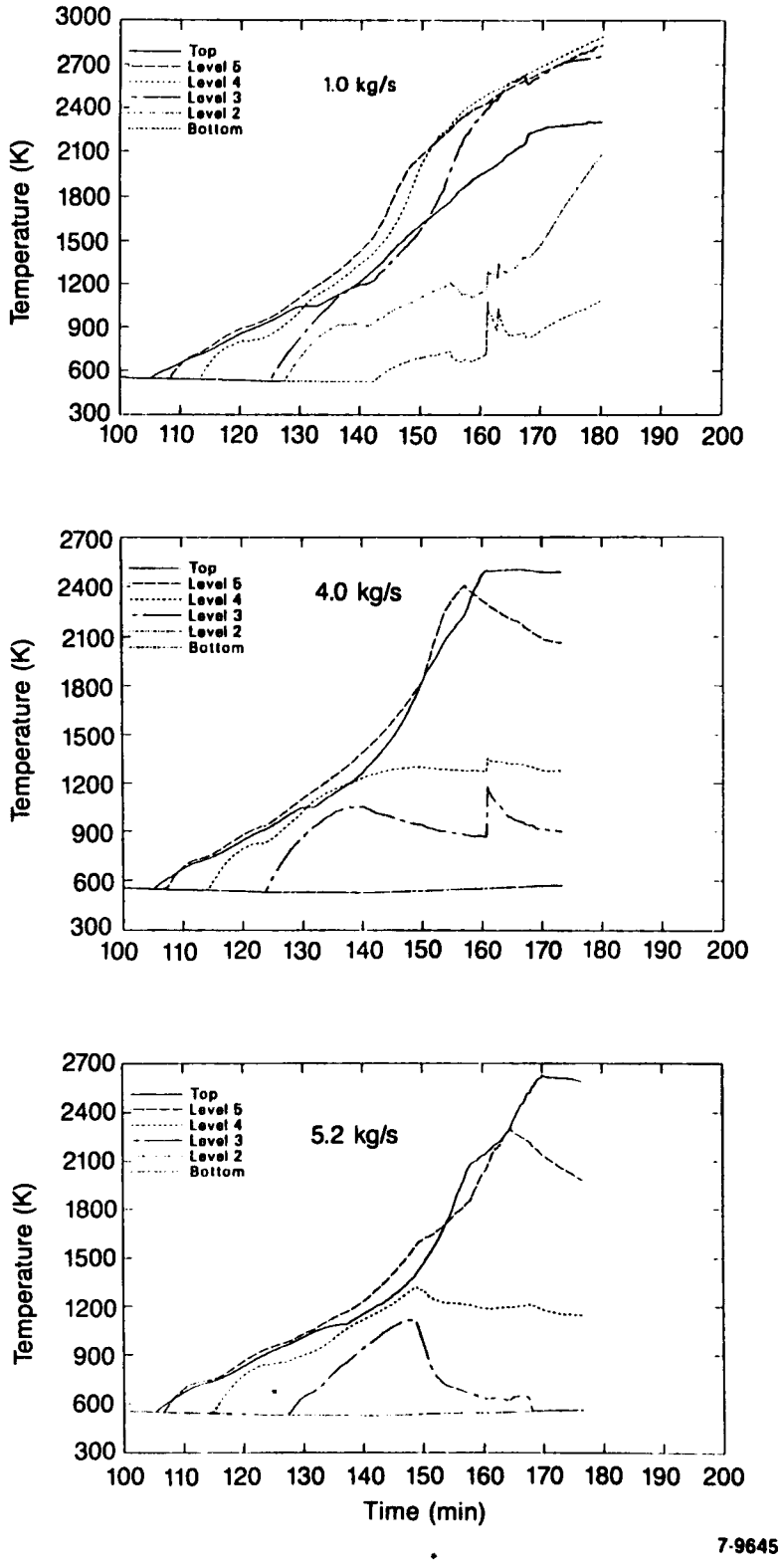

Figure 2-4. SCDAP/RELAP-1987 predicted cladding temperatures in center core node.

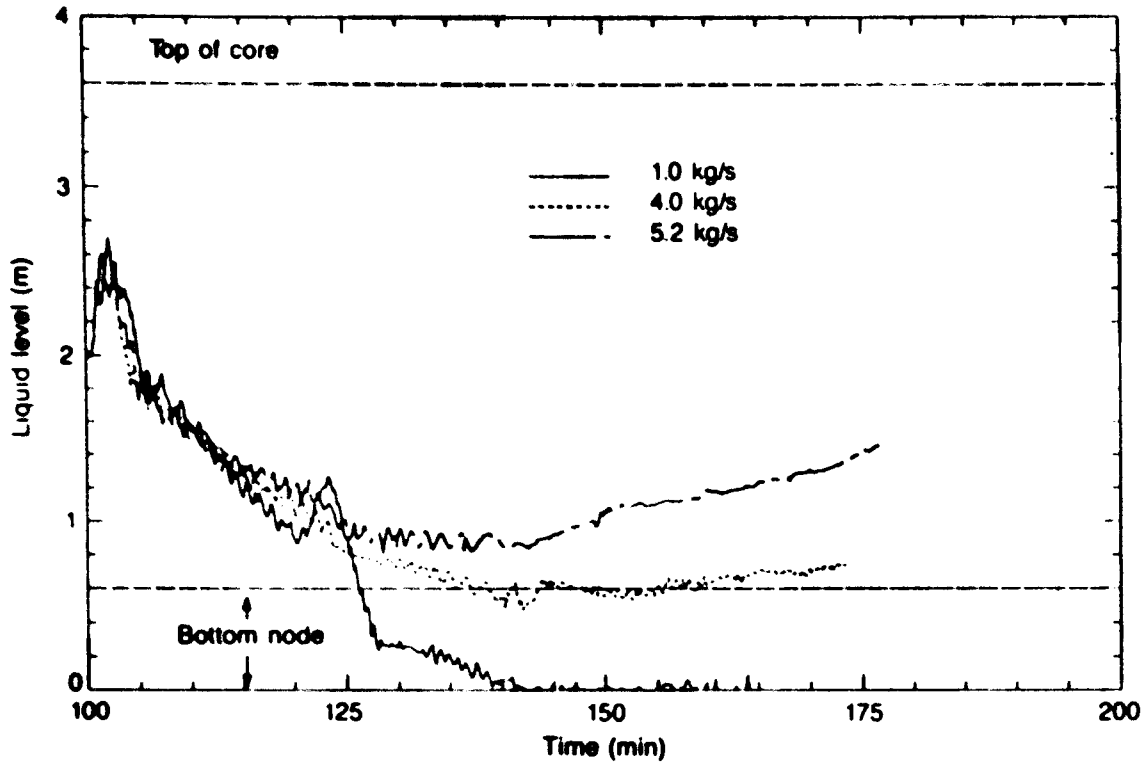

Figure 2-5. SCDAP/RELAP-1987 predicted core liquid-level versus assumed coolant makeup flow rate.

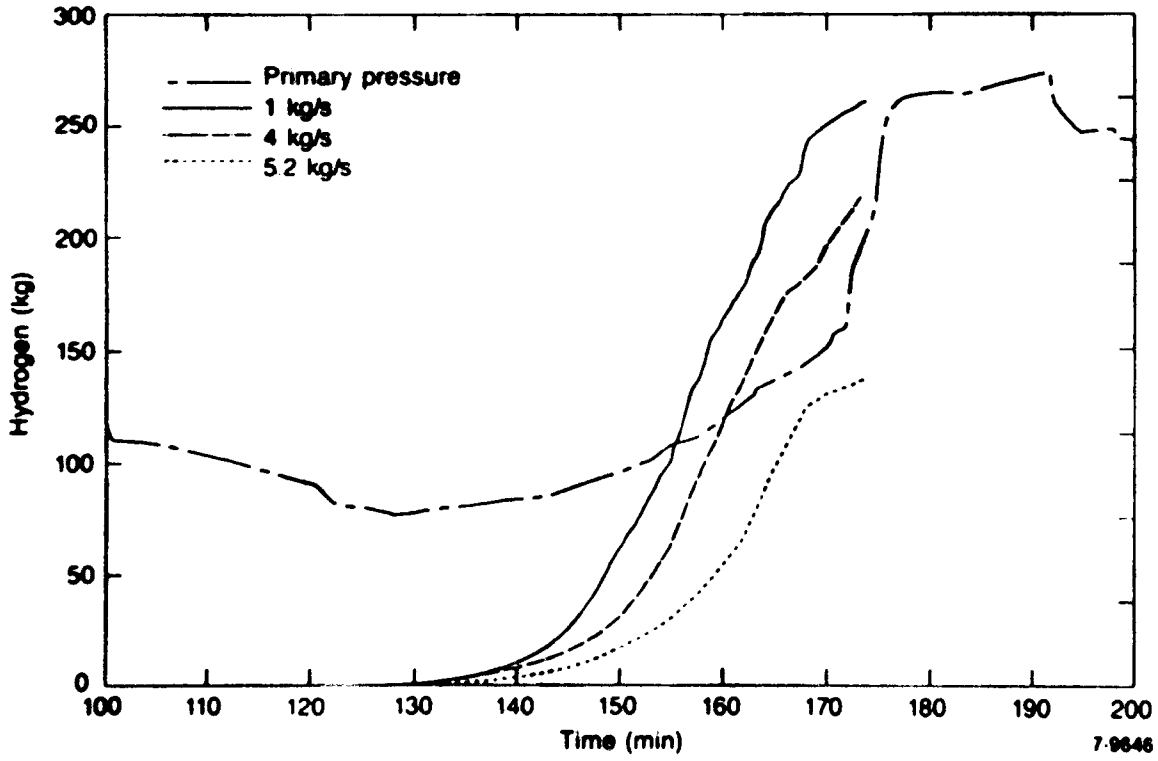

Figure 2-6. SCDAP/RELAP-1987 predicted total hydrogen generation versus makeup flow.

all 23,000 kg of zircaloy cladding would give approximately 1010 kg of hydrogen, the percentages of maximum for the different makeup flow rates are:

Estimate	H_2 Release, kg	Percent of Maximum
SCDAP/RELAP-1987 (1 kg/s)	260	26 (to 174 min)
SCDAP/RELAP-1987 (4 kg/s)	220	22 (to 174 min)
SCDAP/RELAP-1987 (5.2 kg/s)	140	14 (to 174 min)

During the 150 to 174 min time period of core heatup, the associated average rates of H_2 production are estimated to be:

$$H_2\text{-Rate (at 1 kg/s)} = \frac{(260-70)}{24 \text{ min}} = 7.9 \text{ kg/min} = 0.13 \text{ kg/s} \quad ,$$

$$H_2\text{-Rate (at 4 kg/s)} = \frac{(220-20)}{24 \text{ min}} = 8.3 \text{ kg/min} - 0.14 \text{ kg/s} \quad ,$$

$$H_2\text{-Rate (at 5.2 kg/s)} = \frac{(140-10)}{24 \text{ min}} = 5.4 \text{ kg/min} = 0.09 \text{ kg/s} \quad .$$

Noting that total conversion of the makeup flow (1-5.2 kg/s) to hydrogen corresponds to 0.11-0.58 kg/s (divide makeup flow by 9), it can be seen that for the 1.0 kg/s makeup flow condition, additional boiloff of core coolant is required to produce the estimate 0.13 kg/s H_2 production rate. For the 4.0 and 5.2 kg/s makeup flow conditions, complete consumption of the makeup coolant is not predicted. Thus, depending upon boiloff and H_2 production conditions, a range of steam/H_2 chemical environment conditions could have existed based on the SCDAP/RELAP-1987 results.

Assuming a steam production rate equivalent to the water makeup flow rate, the estimated H/O mole ratio for the 1.0 kg/s and 4.0 kg/s SCDAP/RELAP-1987 calculations are presented in Tables 2-3 and 2-4. As indicated for the 1.0 kg/s case, complete steam reduction is predicted (all oxygen is consumed by zircaloy oxidation), so that the effluent H/O mole ratio exiting the core is assessed to be infinite. However, for the 4.0 kg/s case, a H_2/H_2O mole ratio of 1.46 is estimated, indicating some excess of free hydrogen in a predominantly steam environment. A similar result would exist for the 5.2 kg/s makeup flow condition.

2.3 "Nominal TMI-2" Steam/H_2 Chemical Environment

As indicated, considerable differences exist with respect to boiloff and H_2-generation characteristics as predicted from the various SCDAP calculations presented, where such conditions largely control the chemical environment for fission product/effluent interaction. Because of such uncertainties, a "Nominal" set of TMI-2 effluent conditions is specified for detailed analysis of I/Cs chemical form. Parametric variations from the "base-case" conditions are also investigated, to assess parameter effects (e.g. H/O-mole ratio and I/Cs/H_2O concentration conditions) on predicted I and Cs chemical form.

Table 2-5 summarizes the assumed boiloff, H_2-generation, and effluent conditions estimated from the various SCDAP calculations. As can be seen, the SCDAP-1985 effluent H_2/H_2O mole ratio lies between that predicted for the 1.0 and 4.0 kg/s SCDAP/RELAP-1987 calculations. On this basis, the SCDAP-1985 results are used here as the "Nominal" for estimating I and Cs chemical reactions with the TMI-2 steam/H_2 effluent.

The SCDAP-1985 effluent conditions are summarized in the second column of Table 2-5. The peak cladding temperatures in the core before the 28-pump transient were calculated to reach in excess of 2500 K, while the baffle plate temperature at the core radial periphery was estimated to be on the order of 1300 K. Because the steam temperature can be expected to be closer to the cladding temperature, a value of 2000 K is chosen for the purposes of estimating concentration conditions for ideal gas behavior.

TABLE 2-3. ESTIMATION OF THE H_2/H_2O MOLE RATIO FOR THE SCDAP/RELAP-1987 PROBLEM AT 1 kg/s MAKEUP FLOW

Nominal Flow Conditions:

H_2O-makeup flow = 1000 g/s

H_2-generation rate = 110 g/s

Calculation of H_2/H_2O Molar Ratio:

H_2O molar flow rate = $\frac{1000\ g/s}{18\ g/mole}$ = 55.5 moles/s

H_2 molar generation rate = $\frac{111\ g/s}{2\ g/mole}$ = 55.5 moles/s

Unreacted H_2O molar flow rate = 55.5 - 55.5 = 0.0 moles/s

Mole fraction of Free H_2 = 1.0

Mole fraction of Unreacted H_2O = 0.0

(Free-H_2/unreacted-H_2O) Mole ratio = Infinite

[(Free-H_2 + H_2 from Unreacted-H_2O)/Unreacted-H_2O] Mole ratio = Infinite

Calculation of Effluent Concentration

Effluent Conditions: 6.5 MPa
2000 K

$$\text{Effluent concentration} = \frac{6.5\ E+06\ Pa}{8.314\ E+03\ \frac{Pa\text{-}m^3}{kgmole\text{-}K}\ (2000\ K)}$$

$$= 3.9\ E-01\ kgmoles/m^3 = 3.9\ E-04\ gmoles/cm^3$$

Free-H_2 concentration = 3.9 E-04 moles/cm^3 = 2.35 E+20 molecules/cm^3

Unreacted-H_2O concentration = 0.0 moles/cm^3 = 0.0 molecules/cm^3

TABLE 2-4. ESTIMATION OF THE TMI-2 H_2/H_2O MOLE RATIO FOR THE SCDAP/RELAP-1987 PROBLEM AT 4 kg/s MAKEUP FLOW

Nominal Flow Conditions:

H_2O - water (boiloff rate) = 4000 g/s

H_2 - gas (estimated) = 140 g/s

Calculation of H_2/H_2O Molar Ratio:

H_2O molar boiloff rate = $\frac{4000\ g/s}{18\ g/mole}$ = 222 moles/s

H_2 molar generation rate = $\frac{140\ g/s}{2\ g/mole}$ = 70 moles/s

Unreacted H_2O molar flow rate = 222 - 70 = 152 moles/s

Mole fraction of free H_2 = $\frac{70}{222}$ = 0.32

Mole fraction of Unreacted H_2O = $\frac{152}{222}$ = 0.68

(Free-H_2/Unreacted-H_2O) Mole ratio = 70/152 = 0.46

[(Free-H_2 + H_2 from Unreacted-H_2O)/Unreacted-H_2O] Mole ratio

= $\frac{222}{152}$ = 1.46

Calculation of Effluent Concentration

Effluent Conditions: 6.5 MPa
2000 K

$$\text{Effluent concentration} = \frac{6.5\ E+06\ Pa}{8.314\ E+03\ \frac{Pa\text{-}m^3}{kgmole\text{-}K}\ (2000\ K)}$$

$$= 3.9\ E-01\ kgmoles/m^3 = 3.9\ E-04\ gmoles/cm^3$$

Free-H_2 concentration = 0.32(3.9 E-04) = 1.248 E-04 moles/cm^3
= 7.5 E+19 molecules/cm^3

Unreacted-H_2O concentration = 0.68(3.99 E-04) = 2.65 E-04 moles/cm^3
= 1.60 E+20 molecules/cm^3

TABLE 2-5. RANGE OF EFFLUENT STEAM/H_2 CONDITIONS

Parameter	SCDAP-1985 Calculation (Nominal)	SCDAP/RELAP-1987 Calculation (1 kg/s)	SCDAP/RELAP-1987 Calculation (4 kg/s)
Effluent Temperature	≈2000 K	≈2000 K	≈2000 K
Effluent Pressure	1500 psi; 10.3 MPa (at t = 180 min)	940 psi; 6.5 MPa (at t = 170 min)	940 psi; 6.5 MPa (at t = 170 min)
Steam Boiloff Rate	2.5 kg/s	1 kg/s	4 kg/s
H_2-Generation	0.225 kg/s	0.11 kg/s	0.14 kg/s
H_2/H_2O-Mole Ratio (Free-H_2/ Unreacted-H_2O)	4.26	Infinite	0.46

The effluent pressure is estimated from Figure 2-2 to be on the order of 1500 psi. The SCDAP-1985 boiloff rate is taken as equal to the estimated makeup flow rate (2.5 kg/s) at 180 min, although it should be recognized that additional steam can be produced by boiloff of residual coolant left in the core. The H_2-generation rate is also based on SCDAP-1985 predicted results, yielding a H_2/H_2O (Free-H_2/Unreacted-H_2O) mole ratio of 4.26.

2.4 References

1. E. L. Tolman, et al., TMI-2 Accident Scenario Update, EGG-TMI-7484, December 1986.

2. A. W. Cronenberg, et al., "An Assessment of Liquefaction and Quench-Induced I, Cs, and Te Release from Low and High Burnup Fuel," Proc. Intern. Mtg. on Light Water Reactor Severe Accident Evaluation, Cambridge, MA, August 28-September 1, 1983.

3. P. Kuan, Core Relocation in the TMI-2 Accident, EGG-TMI-7402, November 1986.

4. C. M. Allison, S. T. Polkinghorn, and M. S. Sokal, SCDAP/MOD1 Analysis of the Progression of Core Damage During the TMI-2 Accident, EGG-SAR-7104, June 1984.

5. D. W. Golden and A. Takizawa, "Standard Problem Demonstration Calculation," CSNI Standard Problem Workshop, Idaho Falls, ID, February 6, 1987.

6. C. M. Allison, G. A. Berna, and L. J. Siefken, "Draft Preliminary Report for Comment SCDAP/MOD1 Theory and Models," EGG Report FIN-A6360, January 1985.

7. M. P. Sherman, et al., The Behavior of Hydrogen During Accidents in Light Water Reactors, NUREG/CR-1561, SAND 80-1495, August 1980.

8. Electrical Power Research Institute, Analysis of the Accident at TMI-2, EPRI Report NSAC-80-1, March 1979.

3. ESTIMATED IODINE AND CESIUM RELEASE RATES FROM FUEL

To define the chemical form and timing of iodine and cesium release from the TMI-2 fuel during core degradation, a brief review is presented of the internal fuel rod chemistry governing fission product behavior in UO_2. Previous literature indicates that I/Cs chemistry in UO_2 is closely tied to fuel oxidation state and burnup-related morphology effects. These data, as well as the SCDAP-predicted fuel temperature and TMI-2 core damage history, form the basis for definition of I/Cs fission product release behavior from fuel during the TMI-2 accident.

3.1 Internal Fuel Rod Chemistry

Reactive fission products (such as Cs and I) can participate in chemical interactions with each other, as well as with the UO_{2+x} fuel. Their transport behavior through the fuel microstructure is also closely tied to the physical state of the fuel, where grain size, microbubble concentration, pore density, and microcracking can influence release behavior. The principal questions of interest are the rates and chemical form of I and Cs release from fuel. Evidence is presented indicating that the fuel oxidation potential (i.e. UO_{2+x} stoichiometry) and burnup-related morphology exert a strong influence on I and Cs release behavior.

The primary evidence (indirect) for formation of CsI within fuel rods is the observations of Cubicciotti and Sanecki,[1] who identified the compound as deposits on the inside cladding surface of irradiated UO_2 fuel rods. However, it is uncertain as to whether I and Cs were released separately from the fuel and subsequently reacted in the fuel-cladding gap to form CsI deposits, or whether CsI was released directly from the UO_2 fuel matrix.

Thermochemical analyses[2,3] indicate that the chemistry of fission products Cs and I in irradiated fuel is complex, due in part to various sequestering reactions, where cesium uranate (Cs_2UO_4), cesium iodide (CsI), cesium-molybdate (Cs_2MoO_4), and various cesium oxides can form

in irradiated UO_2. A qualitative guide to the chemical state of fission products in UO_2 is facilitated by use of Figure 3-1. Fission product compounds with free energies below that of the fuel result in oxide formation, while stable elements are predicted for compounds with free energies above that of the fuel. Clearly lanthanum (La) and cerium (Ce) have a high propensity to form oxides, while ruthinium (Ru) should always be found as a metal. Little potential exists for oxides of iodine at normal fuel temperatures. However, uncertainty exists with respect to such important fission products as molybdenum (Mo) and Cs, because the free energies of Cs and Mo oxides are close to that of the fuel. As indicated, the potential to form oxides of cesium depends upon fuel oxidation state. At normal fuel rod operating temperatures of about 1200 K and stoichiometric (O/U=2.00) conditions, cesium-oxide formation would not be predicted, thus Cs is available to form CsI and other compounds. However, the oxidation potential of the fuel changes rapidly with small changes in stoichiometry; where oxides of cesium are predicted for $UO_{2.1}$ freeing iodine in the process via the following example reactions:

$$CsI + 20[UO_{2.1}] = CsUO_4 + 19[UO_{2.0}] + I$$

$$CsI + 20[UO_{2.1}] = 20[UO_{2.0}] + CsO_2 + I$$

Hofmann and Spino[4] have also shown that the fuel oxygen potential can have a pronounced affect on CsI stability. The results of isothermal creep rupture tests, with UO_{2+x} fuel clad in zircaloy, indicate that at initial oxygen potentials of -230 kJ/mol O_2 (which corresponds to an O/U ratio of about 2.04 at 700°C), CsI dissociates in sufficient quantity to cause iodine attack on zircaloy cladding. Radiation-induced dissociation of CsI would also contribute to dissociation of the CsI molecule in fuel, as demonstrated in Ref. 5. In addition to radiation and fuel oxidation effects, empirical evidence also indicates that burnup-related morphology can impact fission product release behavior.

As discussed by Tam[2] and others[6,7] the most favorable sites for volatile fission product compound formation are within microbubble sites and the open porosity of the fuel. Consider the situation illustrated in

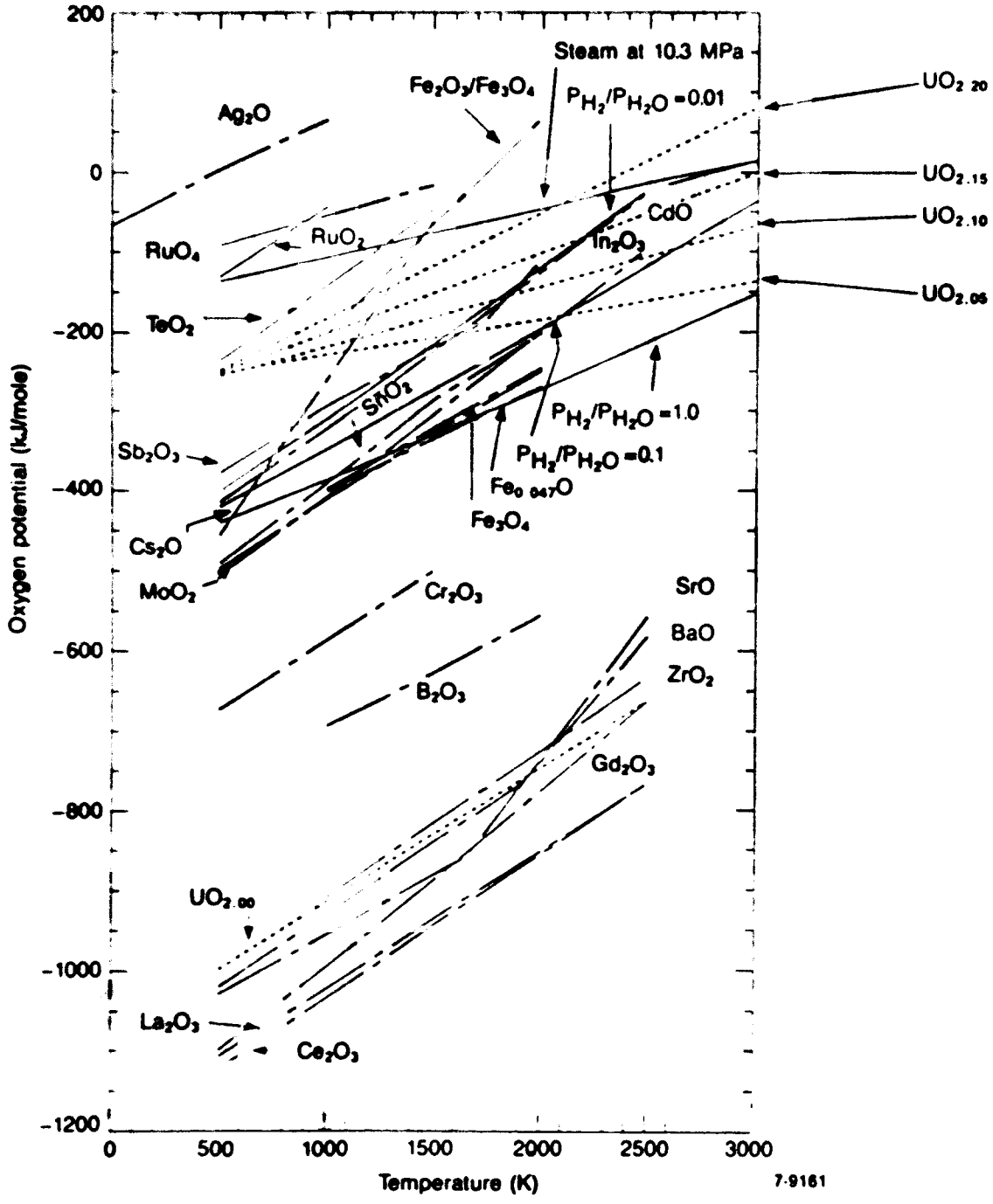

Figure 3-1. Standard free energies of formation of high-yield fission products and UO_{2+x}.

Figure 3-2. Individual atoms of I and Cs (and their precursors) are born separately within the UO_2 crystal lattice, such that at low-burnups relatively wide dispersion of these solute atoms can be expected. Therefore CsI compound formation would not be expected. However, as burnup increases, gaseous (Xe, Kr) and volatile (I, Cs) fission products nucleate into small intragranular bubbles within the fuel grain interior. These bubbles grow and migrate to the grain boundaries, forming larger intergranular bubbles, which in turn migrate and collect in the open porosity. Microbubbles and the open porosity in high-burnup fuel can serve as the primary reaction sites for CsI formation.

Although direct evidence of burnup-related morphology effects on the chemical form of I and Cs release is lacking, general observations can be inferred by comparing data on fission product release behavior. Appelhans and Turnbull[8] made in-pile measurements of the release rates of xenon, krypton, and iodine from low-burnup UO_2 pellets (≈3800-7000 MWd/t). Results showed that iodine release fractions were of the same order of magnitude as the noble gases for burnup conditions below 5 MWd/kg-UO_2. Prussin and Olander[9] also observed that at trace-irradiations (≈10^{-18} atom-percent burnup), UO_2 samples release a high fraction of I. Parker, et al.,[10] noted similar high iodine release behavior for low-burnup (≈1000-4000 MWd/t) UO_2 fuel pellets. Fission product release data for the PBF-SFD Scoping Test (ST) also supports an atomic release mode of I and Cs at trace-irradiation conditions (≈90 MWd/t). Analysis of such data[6] indicates that at low-burnup conditions (<5000 MWd/t) an atomic mode of I and Cs release from the fuel matrix is favored rather than release in compound form.

With respect to the TMI-2 accident, two conditions favor elemental iodine and cesium release: (a) the low-burnup condition (average ≈3175 MWd/t, Ref. 11), and (b) fuel oxidation. Retrieved TMI-2 fuel debris samples indicate a change in fuel stoichiometry from initially $UO_{2.0}$ to UO_{2+x} plus U_4O_9 precipitates.[12] Several samples were examined by Scanning Auger Spectroscopy (SAS) where detailed information was obtained on the concentrations and local distributions of key elements (U, Zr, and O). Quantitative SAS data indicated an average oxygen

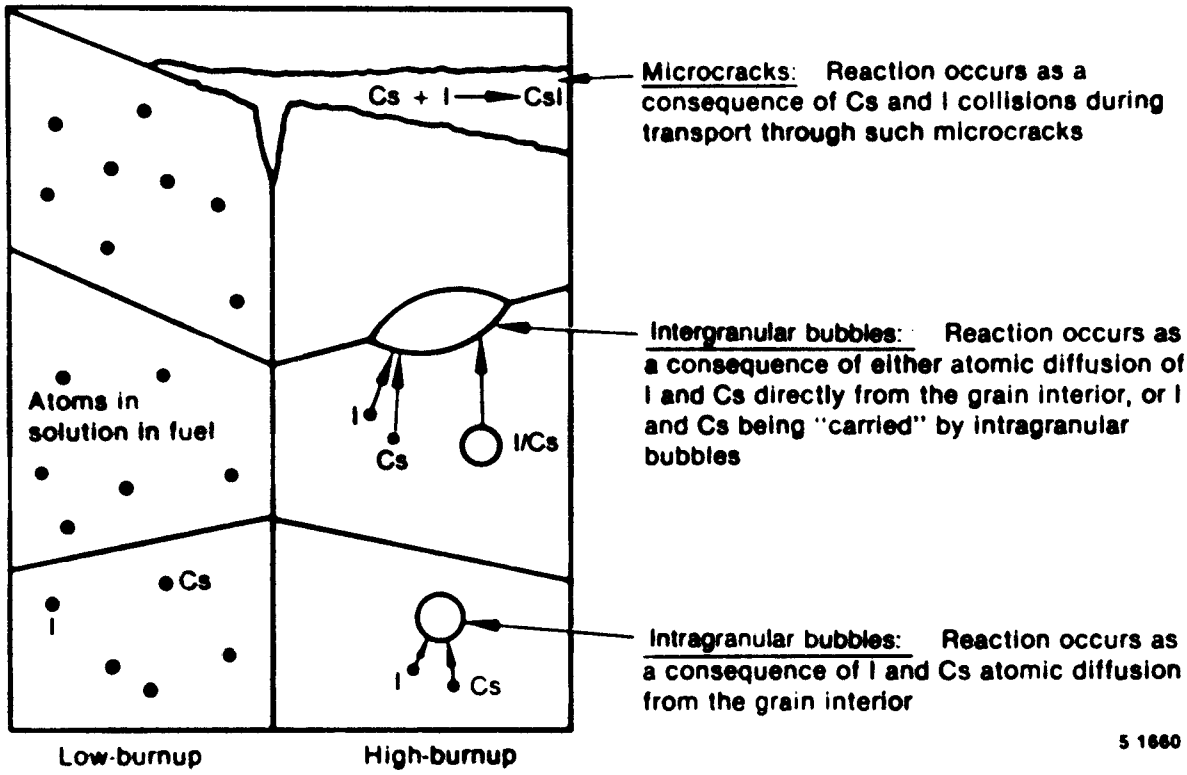

Figure 3-2. Illustration of potential reaction sites for Cs + I to form CsI.

concentration in the fuel matrix of 71 atom-percent, which converts to $UO_{2.44}$, well above stoichiometric UO_2. Similar oxidation of the PBF-SFD-ST fuel to a hyperstoichiometric condition of $UO_{2.4}$ has also been observed.[13] As discussed by Olander,[14] $UO_{2.0}$ fuel can oxidize to $UO_{2.6}$ in steam at elevated temperature and pressure conditions.

Because of the above, atomic diffusion of I and Cs is considered to be the primary mode of release rather than molecular CsI. The release rates of atomic iodine and cesium are estimated in the following section.

3.2 I and Cs Fuel Release Rates

Within this section the fission product inventories of I and Cs for the TMI-2 burnup conditions are assessed, as well as the fuel temperatures and damage state. These factors provide the basis for estimation of I and Cs release rates from fuel.

3.2.1 Fission Product Inventory

The ORIGEN-2 code[15] was used to develop a fission product inventory map of the TMI-2 core at the time of the accident. Table 3-1 contains the estimated[11] isotopic inventory (in moles) for fission product I and Cs. The total elemental inventories of I and Cs are presented in Table 3-2, where values are quoted at the time of core shutdown, indicating the following core-averaged Cs to I ratios:

Cs/I - Mole ratio = 165.23/18.68 = 8.85

Cs/I - Mass ratio = 22.47/2.43 = 9.25

Besides knowledge of the initial fission product inventory, the fuel damage and temperature conditions must be known to estimate the timing and magnitude of I and Cs fission product release from fuel. A brief description of the fuel thermal and damage characteristics is presented next.

TABLE 3-1. ISOTOPIC INFORMATION FOR FISSION PRODUCT I AND Cs AT THE TIME OF TMI-2 SHUTDOWN

Isotopic Number	Inventory[a] Iodine (moles)	Half-Life	Cesium (moles)	Half-Life
127	2.53	Stable	--	
128	--		--	
129	9.49	1.7 E+7 y	--	
130	1.12	12.3 h	--	
131	4.13	8 d	--	
132	7.48 E-02	2.4 h	--	
133	9.96 E-01	20.3 h	71.5	Stable
134	4.70 E-02	52 min	1.15	2.1 y
135	2.96 E-01	7 h	20.88	2.0 E+6 h
136	--		6.96 E-02	13 d
137	--		71.6	30 y
138	--		2.48 E-02	32 min
139	--		6.87 E-03	9.5 min
140	--		--	
141	--		-	
Total	18.68		165.23	

a. Includes only isotopes greater than 10^{-3} moles.

TABLE 3-2. TOTAL ELEMENTAL FISSION PRODUCT INVENTORIES OF I AND Cs AT THE TIME OF TMI-2 SHUTDOWN

Element	Moles	Average Molar Mass	kg
I	18.68	130	2.43
Cs	165.23	136	22.47

3.2.2 Core Conditions Governing Release

Fission product release from the TMI-2 fuel is complicated by a number of factors. Axial and radial temperature gradients exist within the core, which affect the fuel damage state as well as release behavior and timing. Likewise, axial and radial power profiles result in variations in the inventory of short- and long-life fission products. However, detailed consideration of temperature and fission product variations within the core greatly complicate the prediction of release behavior and are not necessary if accuracy within an order-of magnitude will suffice, as is the case in this study.

The core heatup and damage predictions presented in Section 2 form the basis for estimation of I and Cs release rates from the TMI-2 fuel. One of the more commonly used methods for estimating fission product release from damaged and overheated fuel is via NUREG-0772 correlations.[16] In this approach, the rate of release of fission products from fuel is expressed as a function of fuel temperature:

$$dM_x^t/dt = k_x(T)M_x^{t-1}$$

where M_x^{t-1} is the mass inventory of fission product species x in the fuel at the prior time step (t-1), t is time, and the proportionality constant (k_x) is assumed to be a function of temperature only. The fractional release rate constants (k_x) are shown in Figure 3-3. The NUREG-0772 correlations are applied to the TMI-2 core heating transient to estimate the I and Cs elemental release rates and release fractions.

As discussed in Section 2, the release of fission product I and Cs is thought to have occurred during the 150-180 min time period of core heatup, when extensive zircaloy oxidation, molten α-Zr(O) induced UO_2 dissolution, melt debris relocation, and fuel fracturing occurred as a consequence of the 28-pump transient. As indicated in Figure 3-4, fuel dissolution for oxygen-saturated alpha-zircaloy commences at about 2150 K, at which point melt debris relocation would be expected. The SCDAP

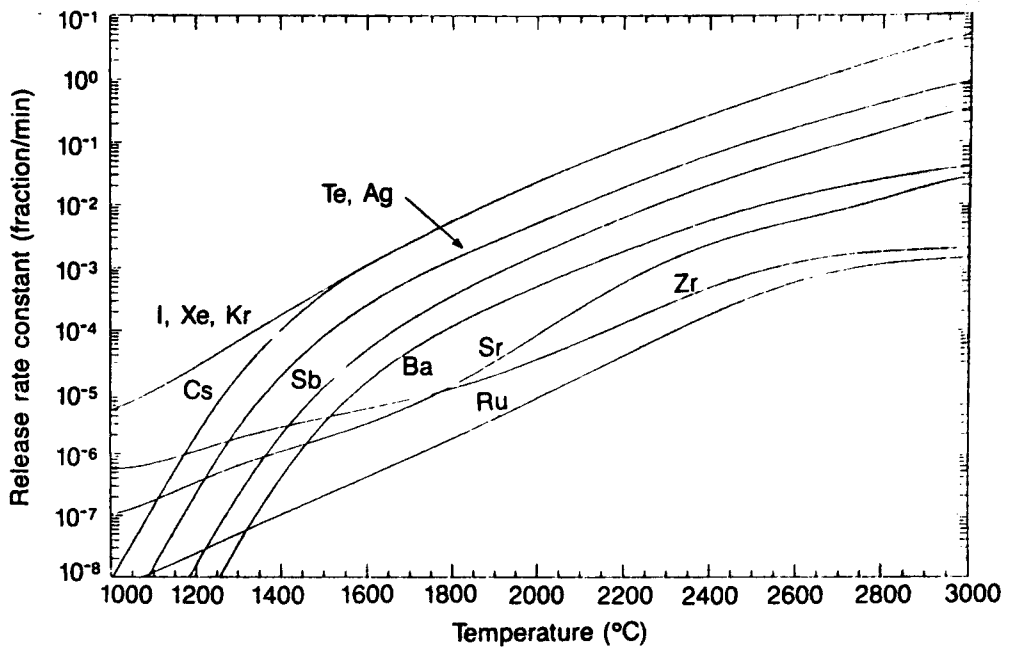

Figure 3-3. Fission product release rate constants from NUREG-0772.

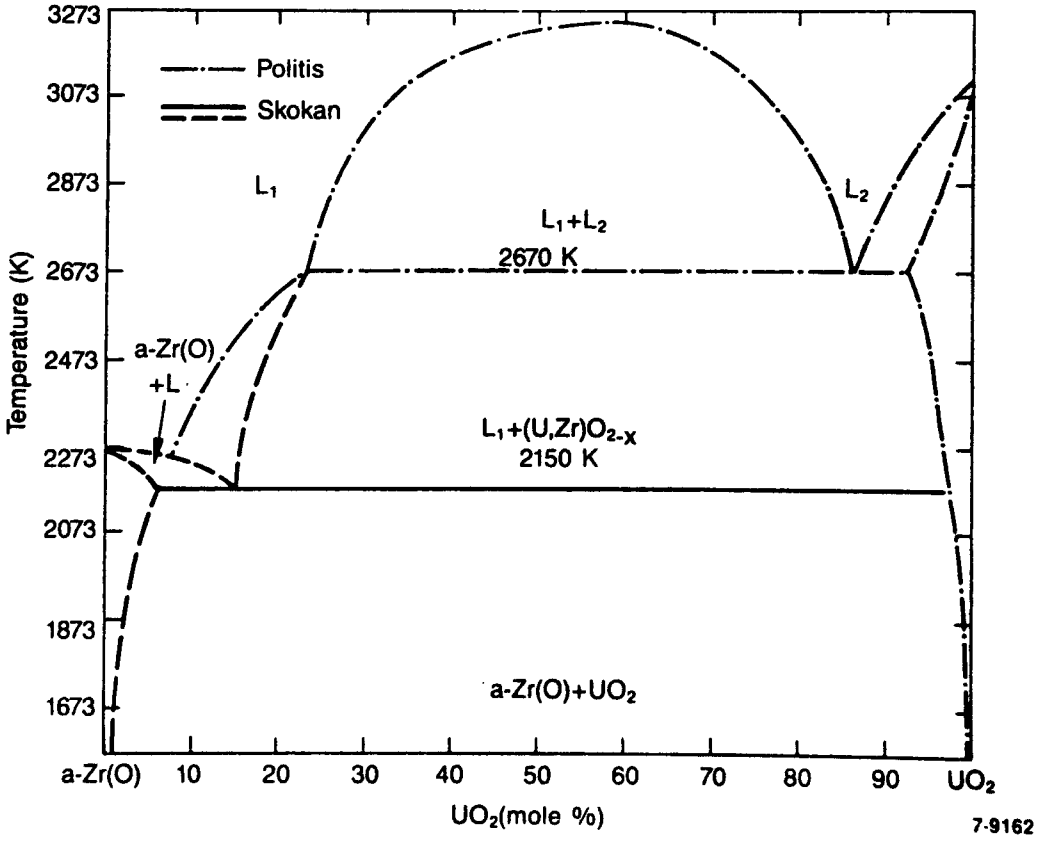

Figure 3-4. Equilibrium pseudo binary phase diagram between UO_2 and oxygen-saturated alpha-phase zircaloy-4.

predictions of fuel rod temperatures, shown previously in Section 2, assume that intact geometry is maintained until the monoeutectic melting temperature is achieved (≈2673 K). This assumption results in high core temperatures due to the extended time allowable for intact cladding oxidation. Although maintenance of rod-like geometry and continued zircaloy oxidation at elevated temperatures (>2500 K) may have occurred at localized core regions, core-wide maintenance of rod geometry beyond the α-Zr(O)/UO_2 liquefaction temperature of ≈2150 K appears unrealistic. For present purposes, the release rate coefficients for I and Cs are based upon a molten α-Zr(O)/UO_2 liquefaction temperature of ≈2150 K, i.e.,

T_f ≈ 2150 K (1877°C) .

At this temperature, the release rate coefficients (k) shown Figure 3-3 are the same for I, Cs, Kr, and Xe and have an approximate value of

k ≈ 0.1 fraction/min .

Thus, within a 10 minute period, the entire inventory of I, Cs, Xe, and Kr is predicted to be released from core nodes which experience temperatures in excess of 2200 K. However, based upon PBF-SFD experience,[17,18] it is noted that for low-burnup fuel (<5000 MWd/t), the NUREG-0772 correlations result in an overprediction of noble gas and volatile (I, Cs) fission product release. This is due to morphology considerations governing release, where for low-burnup conditions fission products may be retained longer within the fuel grain structure. Consequently, for the low-burnup TMI-2 fuel (≈3175 MWd/t), the NUREG-0772 release rates are reduced by an order-of-magnitude. A "Nominal" release rate of

k(TMI-2) ≈ 0.01 fraction/min

is used in this study. In addition, release rates that span the "Nominal" value by a factor of ten are also investigated with respect to effluent chemisty, i.e.,

K(TMI-2) ≈ 0.1-0.0001 fraction/min .

Having estimated fractional release rate, the absolute release rates in grams per unit time can also be estimated. Table 3-3 presents the absolute release rates for I and Cs at the TMI-2 conditions, where the top quarter of the core fuel is assumed to contribute to fission product release, indicating effective mass release rates of

$I \simeq 6$ g/min $= 0.1$ g/s

$Cs \simeq 56$ g/min $= 0.93$ g/s .

It is instructive to compare the above estimated release rates with the inventory of I and Cs found in water samples taken from the TMI-2 containment. The water samples[19] indicate that a total of about 20% of fission product iodine and 40% of cesium reached the containment as water soluble species. Assuming a release period of 30 min during core degradation, the above estimated release rates correspond to about 180 g (or 7.4%) for iodine and 1680 g (or 7.5%) of the cesium inventory. The difference may be due to additional release after debris relocation to the lower plenum, higher release rates during core heatup, or a combination of these and other factors. For the present order-of-magnitude assessment of fission product chemistry during the core degradation period (150-180 min), the above estimated release rates are used.

Once I and Cs are released from the damaged TMI-2 fuel, they will mix and react with the high-temperature steam/hydrogen effluent, forming various chemical compounds which can alter their transport and deposition characteristics. The iodine and cesium concentrations for the "Nominal" steam/H_2 effluent conditions are estimated as follows.

3.3 "Nominal TMI-2" I/Cs/Effluent Concentration Conditions

Since both iodine and cesium do not affect (to any measurable degree) the total pressure of the system, their concentrations can be estimated directly by comparing their release rates to the total effluent

TABLE 3-3. ESTIMATION OF TMI-2 IODINE AND CESIUM "NOMINAL" RELEASE RATE

Iodine Release Conditions:

Assumption: During the initial fuel heatup phase, little release occurs until the fuel undergoes liquefaction at a fuel temperature (T_f) of ~2150 K, where the fractional release rate (F) is approximately 10^{-2} 1/min. Considering that negligible release occurs prior to this time, the absolute release rate can be estimated knowing the initial inventory and fractional release rate; i.e.:

Iodine

M_I = Total I Inventory = 2430 g
k_I = Fractional Release Rate Constant = 10^{-2} 1/min
F = Fraction of Core at Temperature = 0.25
F_I = I Mass Release Rate = $M_I \times F_I \times k_I$
= 2430 x 0.25 x 0.01 ≈ 6.08 g/min

Cesium

M_{Cs} = Total Cs Inventory = 22,470 g
k_{Cs} = Fractional Release Rate Constant = 10^{-2} 1/min
F_C = Fraction of Core at Temperature = 0.25
F_{Cs} = Cs Mass Release Rate = $M_{Cs} \times F_C \times k_{Cs}$
= 22,470 x 0.25 x 0.01 ≈ 56 g/min

(H_2 + steam) flow rate, as indicated in Table 3-4. The Cs-I-O-H concentration conditions in the high-temperature region of the core for the "Nominal TMI-2" conditions can be summarized as follows:

Temperature: 2000 K

Pressure: 10.3 MPa (1500 psi)

H_2/H_2O mole ratio: 4.3

I/H_2O mole ratio: 5.536 E-06

Cs/H_2O mole ratio: 4.89 E-05

Having defined an appropriate set of initial conditions, thermochemical equilibrium and reaction kinetics studies are presented in the following chapter to assess the predominant chemical forms of I and Cs in the steam/H_2 effluent exiting the TMI-2 core.

TABLE 3-4. ESTIMATION OF THE "NOMINAL TMI-2" I AND Cs CONCENTRATIONS

Molar Release Rates:

$$M_I = \frac{0.1\ g/s}{130\ g/mole} = 7.96\ E\text{-}04\ moles/s$$

$$M_{Cs} = \frac{0.93\ g/s}{137\ g/mole} = 6.69\ E\text{-}03\ moles/s$$

Fission Product/Effluent Molar Ratio:

$$I/Effluent\ \frac{7.69\ E\text{-}04\ moles\text{-}I/s}{138.9\ moles\text{-}effluent/s} = 5.563\ E\text{-}06$$

$$Cs/Effluent\ \frac{6.79\ E\text{-}03\ moles\text{-}Cs/s}{138.9\ moles\text{-}effluent/s} = 4.89\ E\text{-}05$$

Fission Product Concentrations:

I concentration = 5.536 E-06(6.19 E-04) = 3.43 E-09 moles/cm^3
= 2.06 E+15 atoms/cm^3

Cs concentration = 4.89 E-05(6.19 E-04) = 3.03 E-08 moles/cm^3
= 1.82 E+16 atoms/cm^3

3.4 References

1. D. Cubicciotti, and J. E. Sanecki, "Characterization of Deposits on Inside Surfaces of LWR Cladding," J. Nucl. Mater., 78, 1978, pp. 96-111.

2. S. W. Tam, P. E. Blackburn, and C. E. Johnson, "Effect of Core Chemistry on Fission Product Release," Proceedings of International Meeting on Thermal Nuclear Reactor Safety, Chicago, IL, August 29-September 2, 1982, pp. 101-110.

3. H. Kleykamp, "The Chemical State of the Fission Products in Oxide Fuels," J. Nucl. Mater. 131, 1985, pp. 221-241.

4. P. Hofmann and J. Spino, "Conditions Under Which CsI Can Cause SCC Failure of Zircaloy Tubing," J. Nucl. Mater., 127, 1985, pp. 205-220.

5. K. Konashi, T. Yato, and H. Kaneko, "Radiation Effect on Partial Pressure of Fission Product Iodine," J. Nucl. Mater., 116, 1983, pp. 86-93.

6. A. W. Cronenberg and D. J. Osetek, "Fuel Morphology Effects on Chemical Form of Iodine Release from Severely Damaged Fuel," J. Nucl. Mater., 149, No. 2, July 1987.

7. J. Rest, "Evaluation of Volatile and Gaseous Fission Product Behavior in Water Reactor Fuel Under Normal and Severe Core Accident Conditions," Nuclear Technology, 61, 1983, pp. 33-48.

8. A. D. Appelhans and J. A. Turnbull, Measured Release of Radioactive Xenon, Krypton, and Iodine from UO_2 at Typical Light Water Reactor Conditions, and Comparison with Release Models, NUREG/CR-2298, 1981.

9. S. G. Prussin, D. R. Olander, P. Goubeault, and D. Bayen, "Release of Volatile Fission Products from UO_2," Proc. ANS Topical Mtg. on Fission Product Behavior and Source Term Research, Snowbird, Utah, July 15-19, 1984.

10. G. W. Parker, et al., Out-of-Pile Studies of Fission-Product Release from Overheated Reactor Fuels at ORNL: 1955-1965, ORNL-3981, 1967.

11. B. G. Schnitzler and J. B. Briggs, TMI-2 Isotopic Inventory Calculations, EGG-PBS-6798, August 1985.

12. D. W. Akers, TMI-2 Core Debris Grab Samples: Examination and Analysis, EGG-TMI-6853, 1985, pp. 75-76.

13. A. D. Knipe, S. A. Ploger, and D. J. Osetek, PBF Severe Fuel Damage Scoping Test: Test Results Report, NUREG/CR 4683, EGG-2413, August 1986.

14. D. R. Olander, "Oxidation of UO_2 by High Pressure Steam," Nuclear Technology, 74, 1986, pp. 215-217.

15. A. G. Groff, ORIGEN-2--A Revised and Updated Version of the Oak Ridge Isotope Generation and Depletin Code, ORNL-5621, July 1980.

16. U.S. Nuclear Regulatory Commission, Technical Bases for Estimating Fission Product Behavior During LWR Accidents, NUREG-0772, June 1981.

17. D. J. Osetek, A. W. Cronenberg, and R. R. Hobbins, "Fission Product Behavior During the First Two PBF Severe Fuel Damage Tests," Proc. Topical Mtg. on Fission Product Behavior and Source Term Research, Snowbird, Utah, July 15-19, 1984.

18. D. J. Osetek, A. W. Cronenberg, D. L. Hagrman, J. Rest, and J. M. Broughton, "Fission Product Release from Severly Damaged Fuel," Proc. ANS/ENS Light Water Reactor Safety Mtg., Karlsruhe, W. Germany, September 10-13, 1984.

19. J. G. Kemeny, et al., Report of the President's Commission on the Accident at Three Mile Island, October 1979.

4. ANALYSIS OF I-Cs-O-H CHEMISTRY

Elemental Cs and I have valence states of +1 and -1 respectively, so that chemical interaction of these species can be expected. This chapter concentrates on an assessment of I and Cs gas-phase chemistry, when these fission products mix with the TMI-2 steam/hydrogen effluent. To define chemical form, thermochemical equilibrium analysis is first employed, where temperature and species concentrations largely govern the partitioning of I and Cs into various compound forms. For dilute fission product concentrations, collision probabilities are reduced. Thus the question arises as to whether thermochemical equilibrium predictions are sufficiently accurate for the low-burnup TMI-2 fuel. Chemical kinetics predictions are also examined to assess the time dependence of chemical form.

4.1 Thermochemical Equilibrium Predictions

4.1.1 General Observations

In most studies of fission product transport, thermochemical equilibrium is assumed. The premise of this type of analysis is that the minimum free energy of the system is achieved in the time span of interest, where the various reactant species have reached an equilibrium state resulting in no net change in concentration condition. The value of such calculations lies in their simplicity, where initial concentrations of the interacting species and their reaction free energies are the only data needed. Specific reaction mechanisms need not be specified and results are independent of the initial assumed chemical form of the reactants.

Although various equilibrium studies of I/Cs chemistry under severe accident conditions have been conducted,[1-5] such studies have not been directly applied to the specific chemical environment of the TMI-2 accident. In this section a review is presented of the general trends indicated by earlier studies, followed by predictions specific to the TMI-2 conditions (see Section 4.1.2).

Results of earlier studies (Ref. 1) are shown in Figures 4-1 and 4-2. These figures are based on predicted species partitioning using the SOLGASMIX thermochemical equilibrium code.[6] Figure 4-1 shows the effect of fission product concentration on the distribution of the primary iodine species at different temperatures, where the equilibrium concentrations of 17 potential reaction products (see Table 4-1) for the four-component Cs-I-O-H chemical system were predicted. The low-concentration condition is at an I/steam mole ratio of (2.0 E-7), while the high-concentration condition is at an I/steam mole ratio of (2.0 E-3). Both calculations are for a H/O mole ratio of 3.0 and a Cs/I mole ratio of 10. At low concentrations, HI and I are shown to be the dominant iodine species at elevated temperatures, while at the high fission product concentration level, CsI is the dominant iodine species. A change in concentration, therefore, has a marked effect on species chemical form.

Figure 4-2 illustrates the effect of a change in H/O mole ratio on the partitioning of the primary iodine species at an iodine concentration level of 2 E-05 moles per mole of H_2O, where results are again taken from Ref. 1. At a low H/O-mole ratio, CsI dissociation at elevated temperatures results in the formation of free iodine rather than HI (see Figure 4-2a). However, for hydrogen-rich environments (H/O > 2; see Figures 4-2c and d), CsI is stable to higher temperatures with subsequent dissociation resulting in HI formation. At high temperatures, HI in turn dissociates, resulting in an increased inventory of free I. In the following section, such equilibrium analysis is applied to the TMI-2 concentration conditions.

4.1.2 TMI-2 Predictions

Th SOLGASMIX code[6] is used here to assess the dominant I and Cs chemical forms in the TMI-2 gaseous effluent. In this study the equilibrium concentrations of the same 17 potential species listed in Table 4-1 are predicted at the "Nominal TMI-2" environmental conditions estimated in the previous chapters, as well as at parametric variations from these conditions. Results are presented in Table 4-2, indicating that temperature and concentration conditions largely affect iodine species partitioning. At the "Nominal-TMI-2" concentration conditions, almost

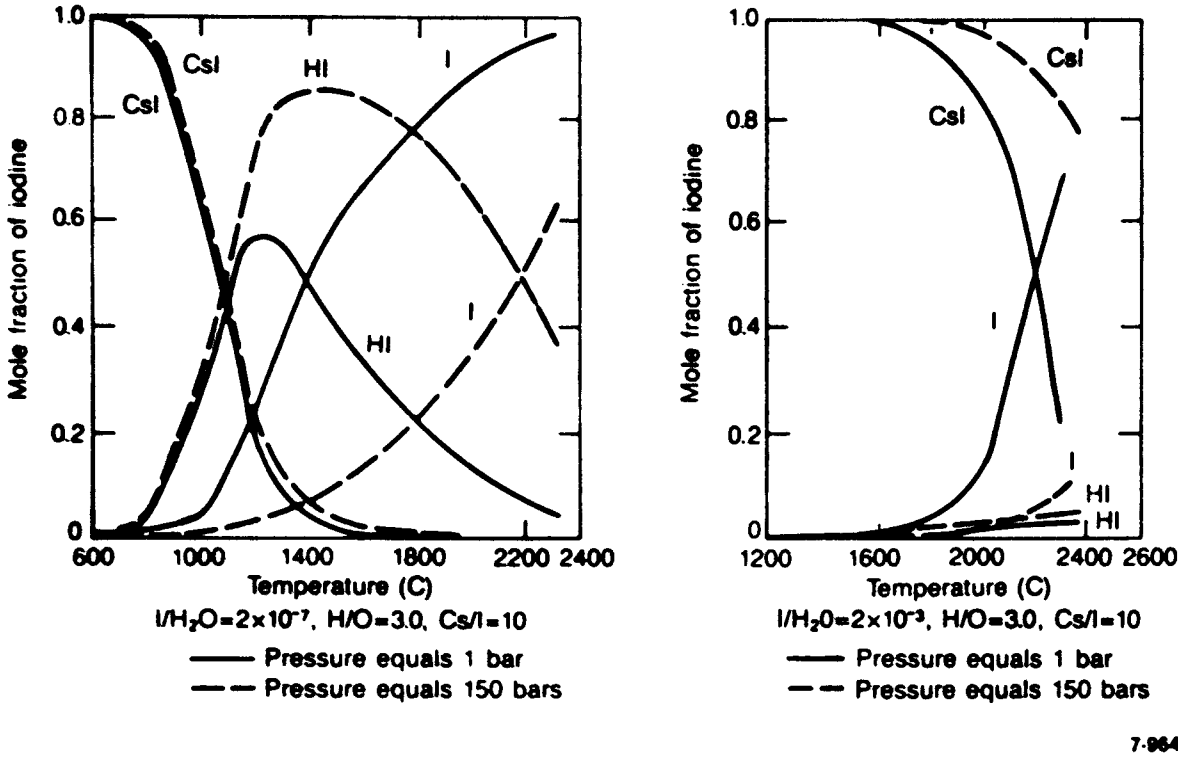

Figure 4-1. Thermochemical equilibrium predictions of the principal chemical forms of iodine in a steam/hydrogen mixture at low (E-7) and high (E-3) I/steam ratios (Ref. 1).

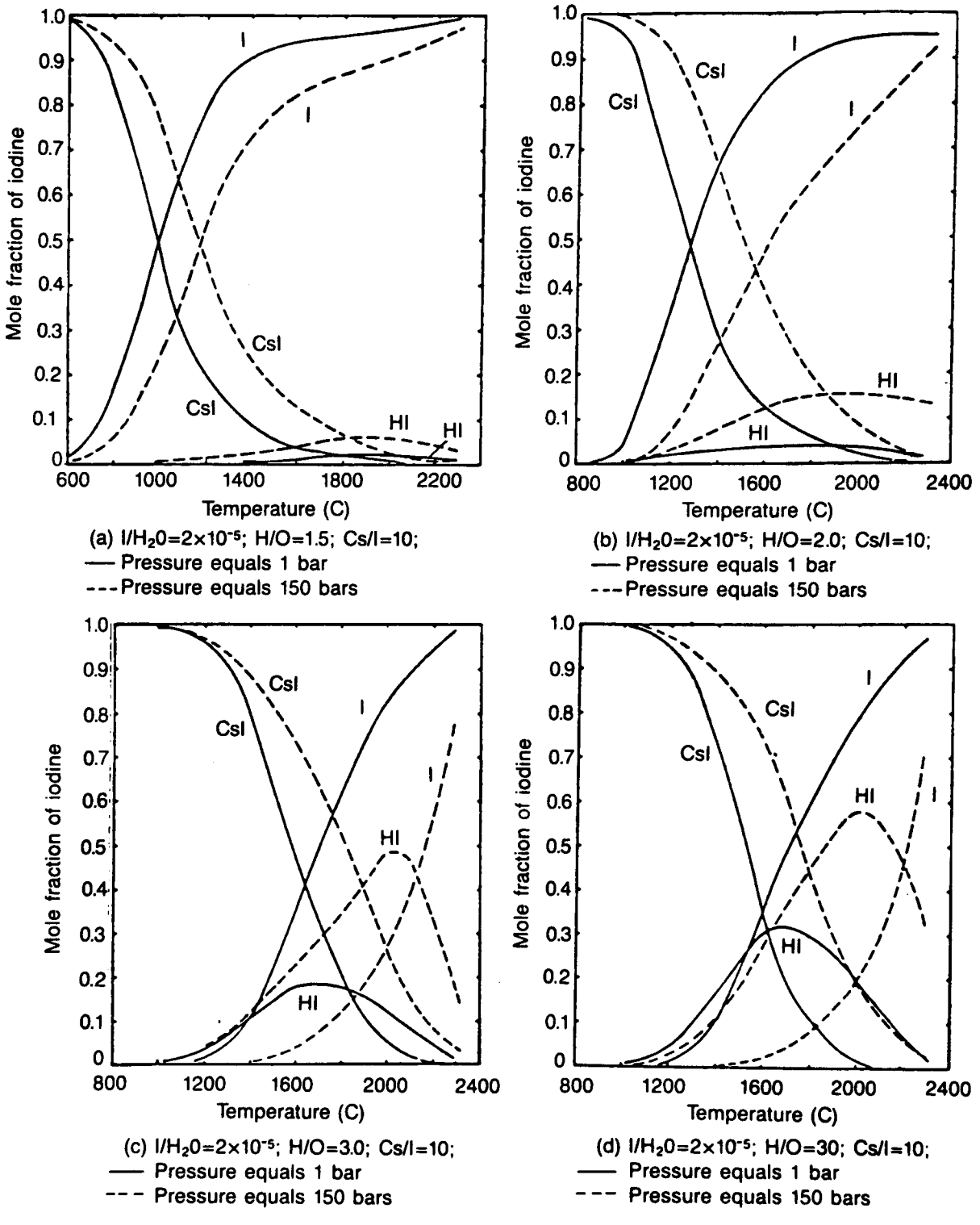

Figure 4-2. Relative abundance of iodine species in the Cesium-Iodine-Hydrogen-Oxygen System for the conditions given.

TABLE 4-1. PRINCIPAL VAPOR SPECIES FOR THE Cs-I-H-O SYSTEM

Elements (4):

H, O, I, Cs

Reaction Products (17):

H_2O, H_2, O_2, H, O, OH, HO_2, Cs, CsI, CsOH, $(CsOH)_2$, Cs_2O, CsO, Cs_2, I, HI, I_2

TABLE 4-2. SOLGASMIX RESULTS AT TMI-2 CONDITIONS

Nominal TMI-2 Condition

P	=	10.3 MPa	H_2O	=	1.176 E-04 moles/cc
I	=	3.43 E-09 moles/cc	H_2	=	5.014 E-04 moles/cc
Cs	=	3.03 E-08 moles/cc	H_2/H_2O	=	4.26

Calculational Results

Initial I/Cs Concentration Conditions	H_2/H_2O Mole Ratio	Temperature (K)	SOLGASMIX Prediction of Iodine Species Partitioning (%)					
Nominal TMI-2	4.3	2000	I	=	6	HOI	=	0
			I_2	=	0	CsI	=	65
			HI	=	29	Cs_2I_2	=	0
		1500	I	=	0	HOI	=	0
			I_2	=	0	CsI	=	98.6
			HI	=	1.4	Cs_2I_2	=	0
		1000	I	=	0	HOI	=	0
			I_2	=	0	CsI	=	96.2
			HI	=	0	Cs_2I_2	=	3.8
1/10 x Nominal TMI-2	4.3	2000	I	=	13.0	HOI	=	0
			I_2	=	0	CsI	=	17.0
			HI	=	70.0	Cs_2I_2	=	0
		1500	I	=	0	HOI	=	0
			I_2	=	0	CsI	=	88.6
			HI	=	11.4	Cs_2I_2	=	0
		1000	I	=	0	HOI	=	0
			I_2	=	0	CsI	=	100
			HI	=	0	Cs_2I_2	=	0
Nominal TMI-2	1.0	2000	I	=	11	HOI	=	0
			I_2	=	0	CsI	=	42.3
			HI	=	46.7	Cs_2I_2	=	0
		1500	I	=	0	HOI	=	0
			I_2	=	0	CsI	=	96.7
			HI	=	3.3	Cs_2I_2	=	0
		1000	I	=	0	HOI	=	0
			I_2	=	0	CsI	=	97.6
			HI	=	0	Cs_2I_2	=	2.4

total CsI formation (≈98.6%) is predicted at the relatively low effluent temperatures associated with above-plenum conditions ($T \leq 1200$). However, at the elevated temperatures (≈2000 K) associated with the effluent environment within the core, significant HI (29%) is predicted in conjunction with CsI (65%).

The effect of concentration level is also shown in Table 4-2, where a decrease in iodine concentration by a factor of 10 below "Nominal TMI-2" concentration results in an increased trend toward HI formation. For example, at 1500 K and the "Nominal TMI-2" iodine concentration, CsI is predicted to be the predominant form of iodine (98.6%), while a factor of 10 reduction in initial iodine concentration results in a reduction in CsI formation to 88.6% and an increase in HI formation to 11.4%. This trend appears reasonable, since at reduced fission product concentrations, I and Cs reactions with the more predominant steam and hydrogen species can be expected. As will be shown, kinetic predictions are consistent with these observations. It should be noted that for the TMI-2 conditions, any Cs not bound to iodine is predicted to be CsOH. Since the Cs/I mole ratio for TMI-2 burnup conditions is estimated to be ≈8.8, most cesium reacts with the effluent H_2/H_2O to form cesium hydroxide (CsOH).

In addition to a parametric study of concentration and temperature effects, the effect of a diminished H_2/H_2O mole ratio is also shown in Table 4-2. As discussed in Ref. 7, an indication of peak core exit effluent temperature and its oxidation potential have been obtained from metallurgical analysis of the stainless-steel control rod drive leadscrews.[8,9] The leadscrews, illustrated in Figure 4-3, were in the upper plenum during the accident and extended from just above the core upper grid support. Temperature characterization was based on leadscrew hardness and grain size data. Peak temperatures in the range of 1200-1380 K were established near the bottom of the plenum at the radial center and about 1000 K near the periphery. Temperatures of about 700 K have been determined near the top of the plenum, at both the radial center and periphery.

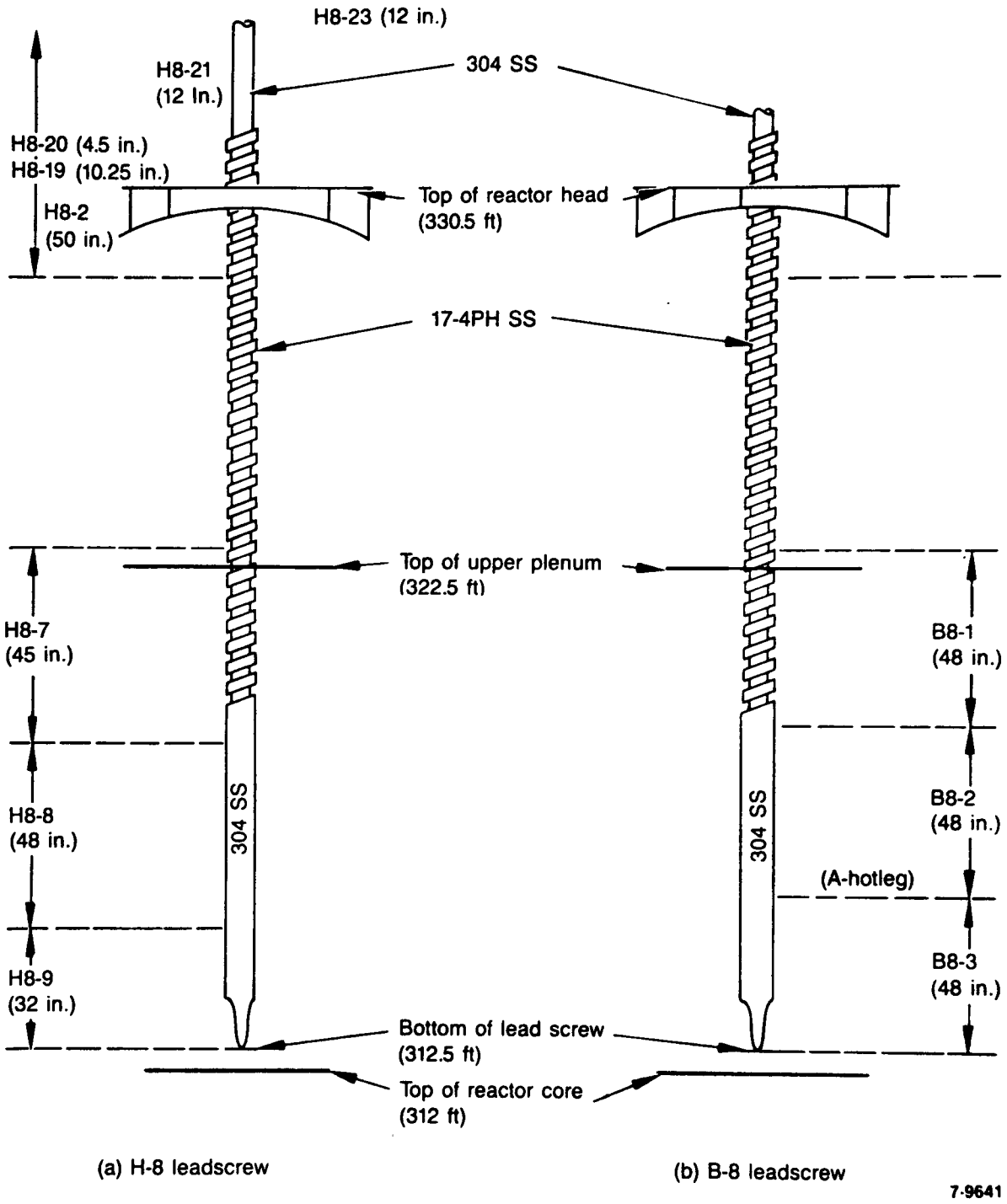

Figure 4-3. Sectioning and sampling diagram for the H8 and B8 leadscrews.

Information on the oxide scale present on the leadscrews was analyzed to provide insight on the hydrogen/steam ratio (and therefore oxygen potential) of the gas exiting the core during the high-temperature portion of the accident. A comparison of the 48 μ thick oxide layer found on the leadscrews with kinetics data[10,11] on oxidation of stainless steel, indicates that such oxidation can only occur at a H_2/H_2O mole ratio less than unity and that it would take approximately 70 to 80 minutes at 1255 K to produce an oxide layer thickness of 48 μ. It is also noted that the SCDAP calculations presented in Chapter 2 show that the vast majority of hydrogen was generated over a 26 min period (i.e., 150 to 180 min), indicating that the gaseous effluent exiting the core was steam-rich during most of the accident (i.e., except during 150-176 min time period). Because of this, an H_2/H_2O mole ratio of 1.0 was also investigated.

As shown in Table 4-2, a change in H_2/H_2O mole ratio from 1.0 to 4.3 somewhat affects iodine species partitioning. At an H_2/H_2O mole ratio of 4.3, less HI is formed. This result is due to the coupled effects of reactions of Cs and I with each other and with the steam/H_2 effluent. Because the concentration of cesium for TMI-2 conditions is estimated to exceed that of iodine by a factor of approximately 8.8, the reaction of Cs with H_2O to form CsOH largely controls the overall partitioning of cesium species. As the relative concentration of steam is diminished at a higher H_2/H_2O mole ratio, more Cs is available to form CsI, so that the concentration of HI is diminished somewhat. In other words, because Cs is in greater concentration than I, Cs reaction behavior controls (somewhat) that of iodine. Thus, if the potential to form CsOH is reduced due to a lower H_2O concentration, then the probability to form CsI is increased, which reduces the potential for HI formation. However, the effect of H_2/H_2O mole ratio on the chemical form of I and Cs in the TMI-2 effluent is not as great as the influence of temperature and fission product concentration conditions. At 1500 K, a mole ratio of H_2/H_2O = 1.0 gives 96.7% CsI while 98.6% CsI is predicted at H_2/H_2O = 4.3.

The boiling points of these species at 1 and 70 atm are presented in Table 4-3. As indicated, HI and iodine are quite volatile and can be

TABLE 4-3. NORMAL BOILING POINTS OF I AND Cs SPECIES

	Species				
	HI	I_2	Cs	CsOH	CsI
T_{vap} (K) at 1 atm	238	457	951	1263	1553
T_{vap} (K) at 70 atm	411	860	2275	2180	2745

expected to be transported further through the plant system. CsI and CsOH are less volatile, and therefore can be expected to condense during transport to low temperature regions of the reactor vessel.

The above I and Cs species-partitioning estimates are based on thermochemical equilibrium analysis. The results of these calculations are independent of the fission-product chemical form initially released from fuel and depend only the system temperature, pressure, species concentration conditions, and the assumption of rapid gas-phase kinetics. However, for dilute mixtures, collision probabilities are reduced, thus the question arises as to whether such thermochemical equilibrium predictions are applicable to the low fission-product concentration conditions of the TMI-2 accident. To assess this concern, investigations of collision rates and overall reaction kinetics were performed at the TMI-2 concentration conditions. Details of this analyses are found in Appendix A and the results are summarized below.

4.2 Chemical Kinetics Predictions

For any chemical reaction, the rate of change in concentration of a particular component in a reacting mixture can be expressed in terms of its generation minus consumption rates. Thus, for a reaction of the form:

$$A + B \underset{k_d}{\overset{k_r}{=}} C + D$$

the rates of change in concentrations for species A and C can be expressed as:

$$\frac{dA}{dt} = -k_r[A][B] + k_d[C][D]$$

$$\frac{dC}{dt} = +k_r[A][B] - k_d[C][D]$$

In the above expressions, k_r and k_d are the reaction and dissociation rate constants, respectively, while the brackets [ ] denote concentration in molecules or atoms per cubic centimeter. For the TMI-2 conditions, the following system of chemical reactions were investigated to assess overall I/Cs/effluent kinetics behavior:

$$Cs + I + X \underset{k_{d1}}{\overset{k_{r1}}{=}} CsI + X$$

$$Cs + H_2O \underset{k_{d2}}{\overset{k_{r2}}{=}} CsOH + H$$

$$I + H_2 \underset{k_{d3}}{\overset{k_{r3}}{=}} HI + H$$

$$I + H + X \underset{k_{d4}}{\overset{k_{r4}}{=}} HI + X$$

$$H + H_2O \underset{k_{d5}}{\overset{k_{r5}}{=}} HOI + H$$

$$I + I + X \underset{k_{r6}}{\overset{k_{r6}}{=}} I_2 + X$$

$$CH_4 + I_2 \underset{k_{d7}}{\overset{k_{r7}}{=}} CH_3I + HI$$

$$Cs + HI \underset{k_{d8}}{\overset{k_{r8}}{=}} CsI + H$$

$$CsOH + HI \underset{k_{d9}}{\overset{k_{r9}}{=}} CsI + H_2O$$

$$H + H + X \underset{k_{d10}}{\overset{k_{r10}}{=}} H_2 + X$$

Several features are noted, relative to the above system of equations, which are considered to dominate I and Cs chemistry in steam-hydrogen mixtures. First, the above reactions are (in general) exothermic, so that a second reaction product is probably required to stabilize the reaction. One can visualize that if a single product molecule is formed in an excited state, it would dissociate spontaneously unless a second species is available to carry a portion of the reaction energy. Second and third order reactions are chosen so as to produce, in all cases, a second excited product that stabilizes the reaction. For reactions which result in a single product species, the neutral molecule (X) is added to the reaction

to dissipate the heat of reaction.[a] In addition, methyl-iodide (CH_3I) formation was also considered, due to the potential for carbon release from degraded structural materials at elevated temperatures and potential C-H reactions. Detailed information of kinetics data and other system parameters are presented in Appendix A. Results are summarized as follows.

Figure 4-4 presents results for the "Nominal TMI-2" concentration conditions as listed in Table 4-2, at a temperature of 1500 K. Concentration-versus-time results are plotted on a logarithmic scale, assuming zero initial concentration of methane. As indicated, I and Cs are shown to react quickly to form CsOH, CsI, and HI, where equilibrium is attained in approximately 10^{-2} seconds for these species. Essentially no formation of HOI (hypoiodous acid) is predicted. The ultimate (steady-state) partitioning of iodine between CsI and HI, as predicted for the TMI-2 environmental conditions, is CsI = 98.5% and HI = 1.5%. This partitioning compares favorably with SOLGASMIX[6] thermochemical equilibrium predictions (see Table 4-2) indicating approximately 98.5% CsI and 1.4% HI. It should be noted that the kinetics results should converge to the same values as the thermochemical equilibrium predictions if all reaction mechanisms are included in the kinetics study. The discrepancy of less than 1% indicates that the primary reactions governing I and Cs behavior have been considered.

The fact that equilibrium concentrations are predicted from kinetics to be reached on a scale of ≈0.01 seconds, indicates that thermochemical equilibrium predictions can be used to assess gas-phase I and Cs reaction behavior within the core. Such thermochemical equilibrium predictions indicate that the predominant forms of iodine and cesium in the core effluent are CsI and CsOH. However, as discussed in the following section, changes in chemical form can occur as the effluent is cooled and exposed to structural surfaces during transport through the primary system.

---

a. In the present analysis, the concentration of the collision molecule (X) that carries the reaction energy is considered to be H_2.

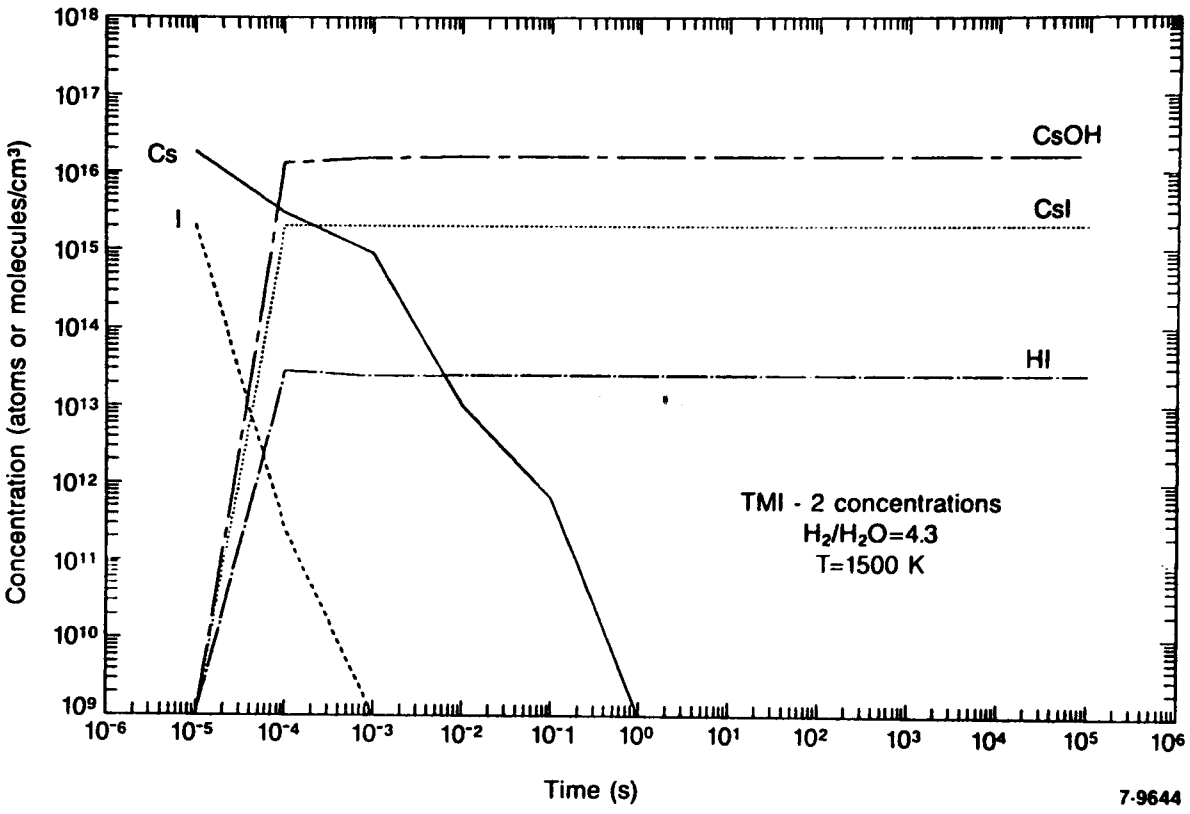

Figure 4-4. Illustration of I and Cs gas-phase reaction behavior in the TMI-2 core effluent at t = 180 min.

4.3 References

1. U.S. Nuclear Regulatory Commission, Technical Bases for Estimating Fission Product Behavior During LWR Accidents, NUREG-0772, June 1981.

2. R. A. Sallach, Chemistry of Fission Products Elements in High Temperature Steam; Thermodynamic Calculations of Vapor Composition, SAND 81-0534/1, 1981.

3. D. Cubicciotti and B. R. Sehgal, "Vapor Transport of Fission Products in Postulated Severe LWR Accidents," Nuclear Technology, 65, 1984, pp. 266-291.

4. R. Han and H. J. Ache, "Thermochemical Calculations on the Behavior of Gaseous Iodine Species Following a Hypothetical Severe Light Water Reactor Accident," Nuclear Technology, 67, 1984, pp. 407-410.

5. D. F. Torgerson, et al., "Fission Product Chemistry Under Reactor Accident Conditions," Proc. of Inter. Mtg. of Thermal Reactor Safety, Chicago, IL., August 29-September 2, 1982, pp. 1069-1077.

6. T. M. Besmann, SOLGASMIX-PX, A Computer Program to Calculate Equilibrium Relationships in Complex Chemical Systems, ORNL/TM-5775, 1977.

7. R. R. Hobbins, A. W. Cronenberg, S. Langer, and D. E. Owen, "Insights on Severe Accident Chemistry from TMI-2," Proc. Am. Chem. Society Mtg: Severe Accident Chemistry Symposium, Anaheim, CA, September 7-12, 1986.

8. K. Vinjamuri, D. W. Akers, and R. R. Hobbins, Examination of H8 and B8 Leadscrews from Three Mile Island Unit 2 (TMI-2), GEND-INF-052, September 1985.

9. K. Vinjamuri, D. W. Akers, and R. R. Hobbins, "TMI-2 Leadscrew Radionuclide Deposition and Characterization," Proc. ANS Topical Mtg on Fission Product Behavior and Source Term Research, Snowbird, Utah, July 15-19, 1984.

10. D. A. Powers, "A Review of Steam Oxidation of Steels - The Forgotten Source of Hydrogen," Proceedings of the Workshop on the Impact of Hydrogen on Water Reactor Safety, Vol. 2, NUREG/CR-2017, SAND 81-0661, September 1981.

11. J. Bittel, L. H. Sjodahl, and J. F. White, Corrosium-NACE, 25, 7, 1969.

5. VAPOR TRANSPORT CHEMISTRY OF CsI and CsOH

Although thermochemical equilibrium and kinetics predictions indicate CsI and CsOH to be the primary fission product vapor species exiting the core, changes in chemical form can occur as the effluent is cooled and exposed to structural surfaces during transport through the primary coolant system. To assess the potential alteration of chemical form during transport, a simplified model of the reactor coolant system and effluent flow path is presented, where the structural materials and temperature conditions are defined. The effects of effluent condensation, chemisorption, and boron chemistry are then assessed in terms of alteration of CsI and CsOH transport chemistry.

5.1 Effluent Flow Path

Figure 5-1 is a simplified sketch of the TMI-2 primary coolant flow path. Effluent cooldown first occurred in the plenum space above the core. The presence of additional structures within the upper plenum (e.g., control-rod guide tubes and leadscrews, plenum barrel, grid plate) adds to the total surface area for deposition. Thus, the plenum region would be expected to have experienced significant deposition of condensable and reactive vapor species. Upon exit from the plenum, the effluent would then be transported through hot-leg connecting piping to the steam generators and pressurizer. The steam generators and pressurizer probably contained residual water during the accident, which would have scrubbed fission products from effluent, forming water soluble ionic species and possibly hydrosol. Previous studies[1,2] have adequately dealt with the question of iodine and cesium water chemistry. The present analysis is thus restricted to an assessment of condensation and chemisorption behavior in regions upstream of the steam generators and condenser (i.e., within the plenum and hot-leg connecting pipe).

5.1.1 Upper Plenum Characteristics

Indicators of peak temperatures in the plenum have been obtained from metallurgical analyses of the control-rod drive leadscrews.[3] Peak

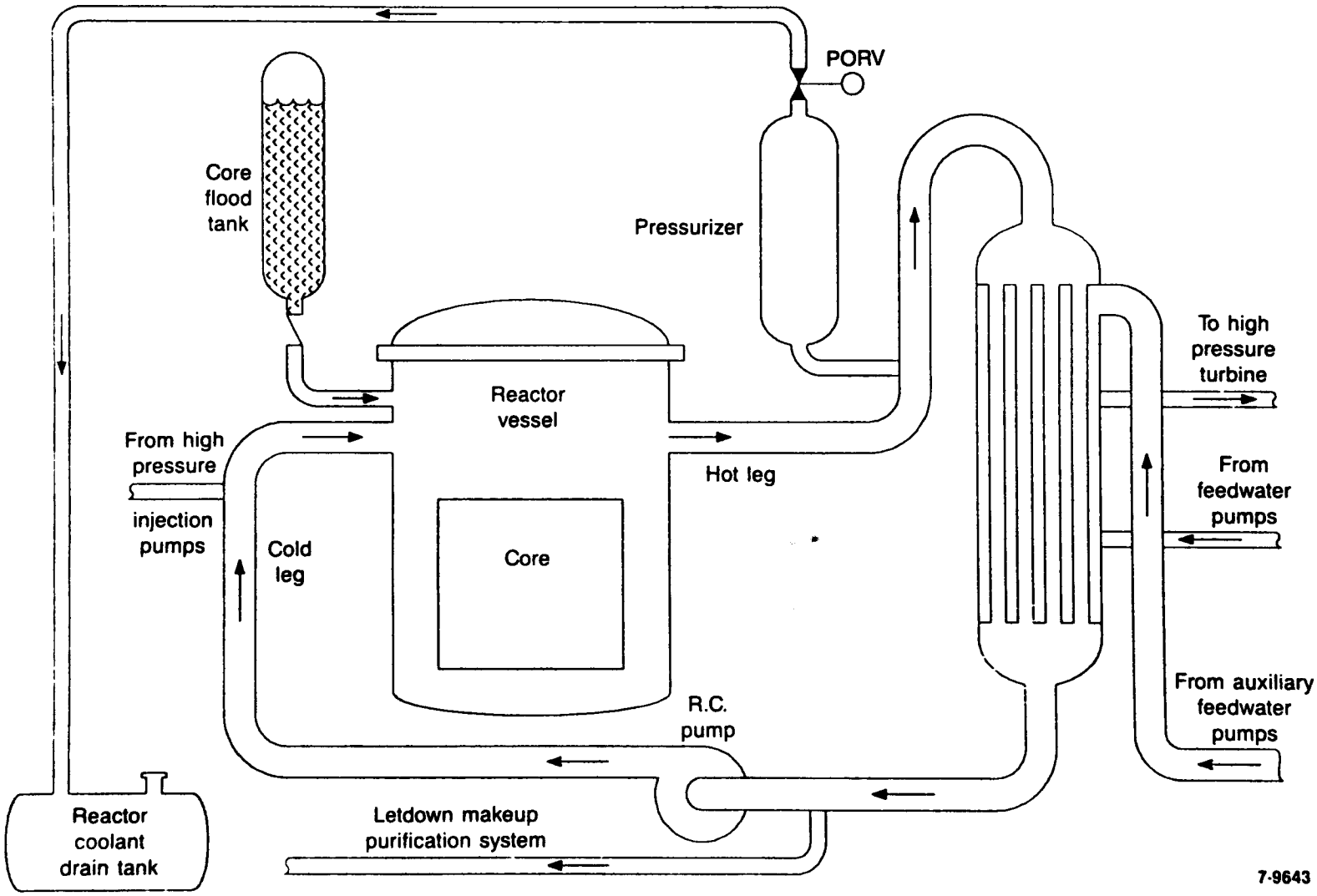

Figure 5-1. Illustration of primary reactor coolant system.

temperatures of 1255 K were determined near the bottom of the plenum at the radial center and 1033 K near the periphery. Temperatures of about 700 K were determined near the top of the plenum at both the radial center and peripheral positions. Based on these data, the plenum can be nodalized into three characteristic temperature regions as shown in Figure 5-2, namely the upper half of the plenum volume at 700 K, a central lower region at 1255 K comprising about 1/6th the plenum volume, and the lower peripheral regions at 1033 K.

Besides temperature characterization of the plenum, the total surface area and material composition of the various plenum components must be specified. The plenum assembly consists of a 304-stainless steel flanged cylinder. Inside the plenum cylinder are 61 control rod guide tubes which house stainless-steel leadscrews. An estimate of the plenum surface area for deposition is presented in Table 5-1 for the following components; the dome-shaped head, the inside plenum cylinder surface, the outside surface of the control rod guide tubes, and the leadscrew surface area. For these plenum components, a surface area of $4.02(10^6)$ cm^2 is estimated, which compares favorably with $4.25(10^6)$ cm^2 quoted in Ref. 3 (see footnote-a, Table 36). For present purposes, a total plenum surface area of about $4.0(10^6)$ cm^2 is used, with a partitioning of surface area (A_s) at the temperatures indicated from the leadscrew data as illustrated in Figure 5-2.

5.1.2 Hot-Leg Pipe Characteristics

Figure 5-3 presents a sketch of the A and B loop hot let pipe, connecting the reactor vessel and steam generators. The pipe is carbon steel lined with stainless steel, where the surface area of the hot leg is $9.7(10^5)$ cm^2 (see Refs. 5 and 6). For this study, the hot-leg pipe temperature is taken to be equal to the mid-height above-core plenum temperature as assayed from the leadscrew data (i.e., approximately 1000 K).

Having identified plenum and hot-leg pipe temperatures and deposition surface area characteristics, condensation and chemisorption effects are assessed in terms of CsI and CsOH transport chemistry in the following subsections.

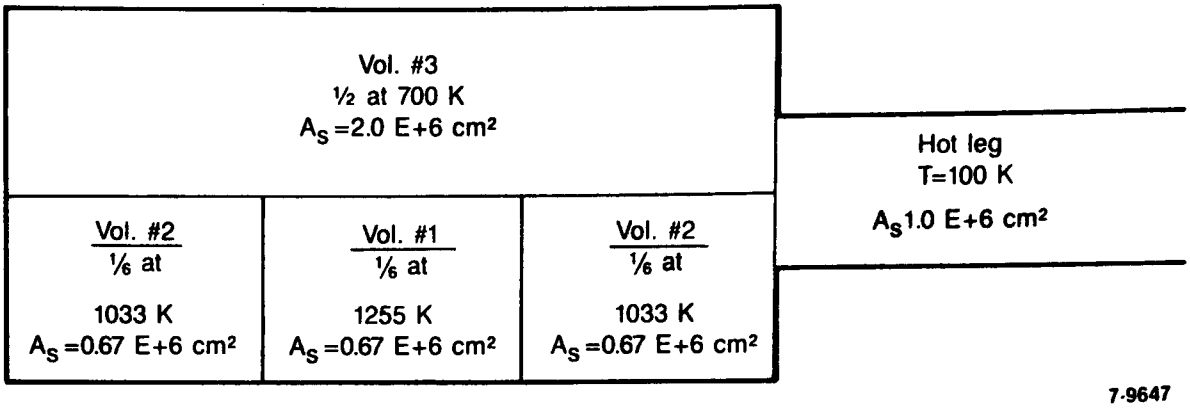

Figure 5-2. Characterization of upper plenum volume according to leadscrew temperature data.

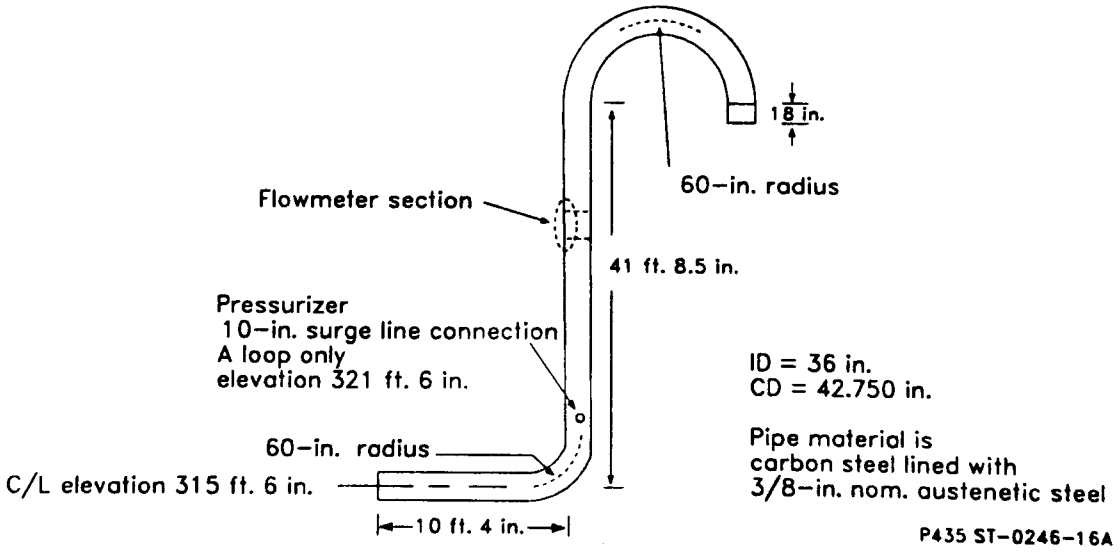

Figure 5-3. Dimensional and material characteristics of loop A and B hot-leg pipe.

TABLE 5-1. ESTIMATED PLENUM SURFACE AREA FOR FISSION PRODUCT DEPOSITION

Dome-Shaped Head (Carbon Steel)

ID = 150 in. (380 cm)
Surface Area = $\frac{1}{2}$ Sphere = $\frac{\pi}{2}$ (ID^2) =2.3 E+5 cm^2 Area

Inside Plenum Cylinder Surface (Stainless Steel)

ID = 140 in. (355 cm)
Height (H) = 10 ft = 304 cm
Surface Area = π(ID) H = 3.4 E+5 cm^2

Outside Surface of Control Rod Drive Tubes (Stainless Steel)

Number of Guide Tubes = 61
Guide Tube Diameter (D) =8.625 in. (21.9 cm)
Height (H) =24 ft (730 cm)
Surface Area =61(π D) H =3.1 E+6 cm^2

Leadscrew (Stainless Steel)

Number of leadscrews = 61
Leadscrew diameter (D) =1 in. (2.5 cm)
Height (H) =730 cm
Surface Area =61(π D) H =3.5 E+5 cm^2

Total Plenum Surface Area

A_S = 4.03 E+6 cm^2

5.2 Condensation Effects

5.2.1 Condensation Model

As illustrated in Figure 5-4, condensation can be modeled as a gas-phase mass transfer process where the time rate of change of species-A in a control volume element can be written in terms of a mass transfer flux (J, g/cm^2 s), i.e.,

$$\frac{dC_a}{dt} = \begin{matrix}\text{Rate of mass condensation} \\ \text{in control volume element}\end{matrix} = JA = A\left[\frac{C_{bulk} - C_{eq}}{R_{gb}}\right] \qquad (5\text{-}1)$$

where A is the surface area (cm^2) for condensation, R_{gb} is the effective resistance of the gas boundary layer, C_{bulk} is the concentration of species-A in the bulk flow stream, and C_{eq} is the equilibrium concentration at the wall surface temperature. If the bulk concentration (C_{bulk}) of species-A exceeds the wall equilibrium concentration (C_{eq}), the mass transfer flux is directed toward the liquid-vapor interface indicating condensation.

The condensation resistance through the gas boundary layer is normally expressed in terms of an overall mass transfer coefficient (K, cm/s) and the local control volume (V, cm^3), where $R_{gb} = V/K$. Thus, Eq. 5-1 becomes

$$\frac{dC}{dt} = A\left[C_{bulk} - C_{eq}\right](K/V) \quad . \qquad (5\text{-}2)$$

Upon making a change in variables $C' = C_{bulk} - C_{eq}$ (where C_{eq} is a constant within a constant temperature control volume), the above expression can be written as

$$\frac{dC'}{C'} = \frac{KA}{V}\,dt \qquad (5\text{-}3)$$

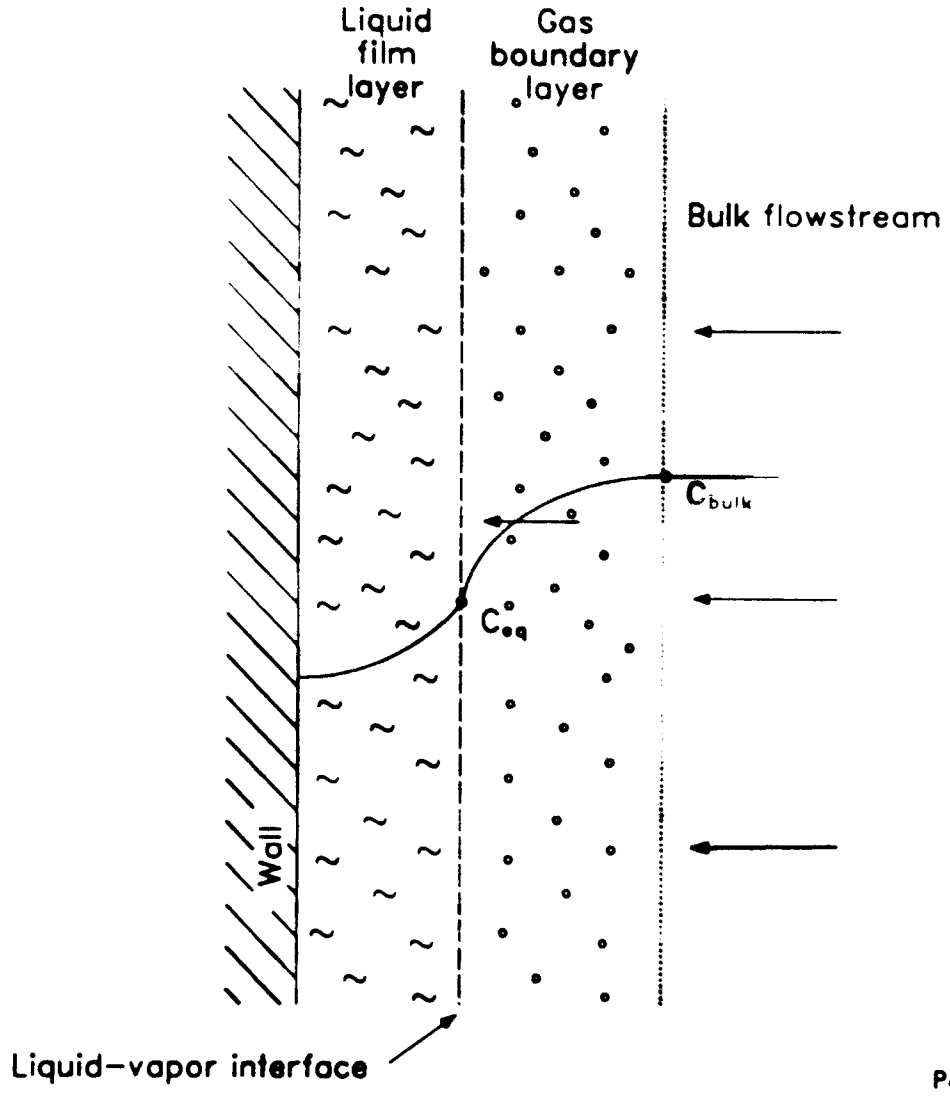

Figure 5-4. Illustration of mass flux conditions through gas boundary and liquid film layers relative to modeling of condensation.

with the general solution of the form

$$C'_{cond} = B \exp (AKt/V) \qquad (5\text{-}4)$$

where B is the constant of integration. For the initial condition that $C'_{cond} = 0$, the above equation, expressed in terms of the bulk and equilibrium concentrations, is

$$C_{cond} = (C_{bulk} - C_{eq}) [\exp (AKt/v) - 1] \quad . \qquad (5\text{-}5)$$

Noting that for an ideal gas the concentration of species-a ($C_a = m/V = P_a/R_aT$) can be written in terms of temperature and pressure, the above equation becomes

$$C_{cond} = \left[\frac{1}{T_{bulk}} - \frac{1}{T_{eq}}\right] (P_aV/R) [\exp (AKt/V) - 1] \qquad (5\text{-}6)$$

where P_a is the partial pressure of species-a in the gas mixture. If the bulk gas temperature (T_{bulk}) is less than the liquid-vapor equilibrium temperature (T_{eq}) of species-a at its partial pressure, condensation of that species is predicted. Using the above expression and the equation-of-state correlations presented in Table 5-2 for cesium and iodine species, the effects of CsI and CsOH condensation can be assessed for the TMI-2 upper plenum and hot leg temperature and surface area conditions.

A qualitative guide to the conditions at which condensation of various fission product species will occur at atmospheric pressure (10^5 Pa) can be obtained from inspection of Figure 5-5, which presents a logarithmic plot of the equilibrium concentration versus wall temperature results based upon the vapor pressure correlations given in Table 5-2. For example, at a surface temperature of 800 K, condensation of CsI is indicated at bulk concentration conditions in excess of 3.2 E-05 kg/m^3 (antilog of -4.5), while condensation of CsOH occurs at concentrations greater then 7.9 E-04 kg/m^3 (antilog of -3.1). At 800 K and atmospheric pressure, no condensation of I_2 and H_2O is indicated.

TABLE 5-2. VAPOR PRESSURE CORRELATIONS FOR Cs AND I FISSION PRODUCT SPECIES

Coefficients for the equation

$$\log P(\text{mmHg}) = -\frac{A}{T} + B + C \log T$$

where T is in degrees kelvin.

Compound	A	B	C	Temperature Range (K)	Reference
I_2	3,578	17.72	-2.51	298-387	a
	3,205	23.65	-5.18	387-457	a
CsI	10,420	19.70	-3.02	600-894	a
	9,678	20.35	-3.52	894-1553	a
HI	Critical temperature = 424K (always gaseous)				
Cs	4,075	11.38	-1.45	280-1000	a
CsOH	logP(Pa) = 9.92 - 6700/T			770-1200	b

a. J. A. Gieseke, et al., Analysis of Fission Product Transport Under Terminated LOCA Conditions, BMI-NUREG-1990, December 1977.

b. J. C. Cummings, R. M. Elrick, and R. A. Sallach, Status Report on Fission-Product Research Program, NUREG/CR-1820, SAND 80-2662, March 1982.

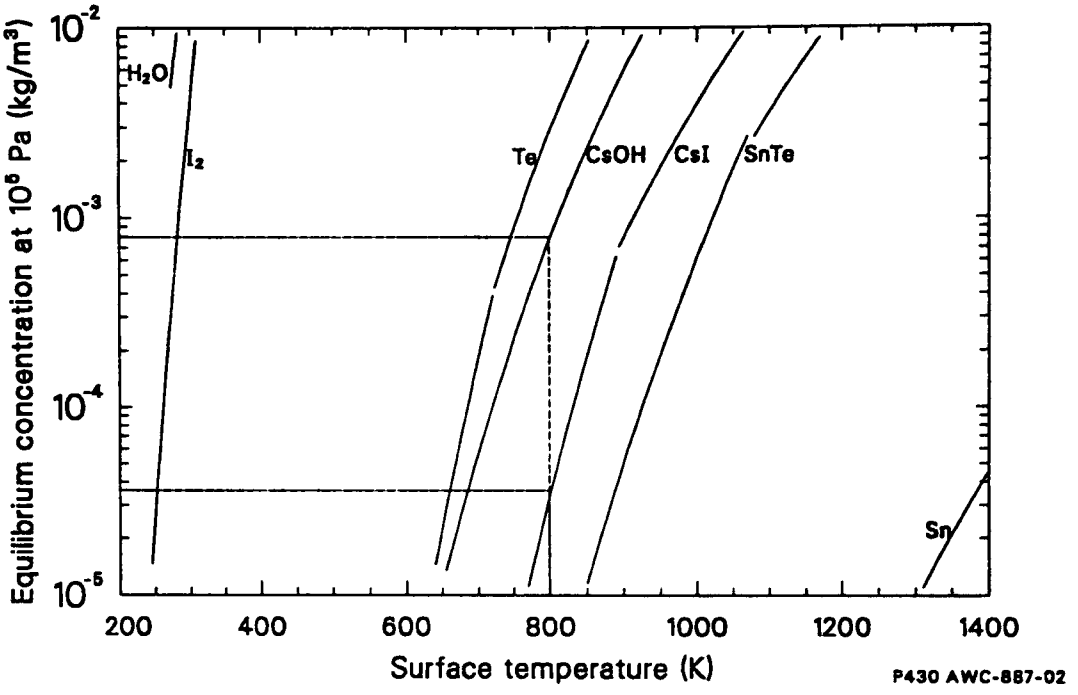

Figure 5-5. Log of equilibrium vapor concentration versus wall surface temperature.

Condensation of a particular chemical species can influence not only the concentration of that species, but other species that are in chemical equilibrium with the gas mixture. According to Le Chatelier's principle, if a stress which alters the concentration of one species is brought to bear on a mixture of chemical species in thermochemical equilibrium, a reaction occurs which tends to undo the effect of the stress and return the mixture to equilibrium. For example, condensation of CsOH will impact the concentration of CsI in the mixture, as revealed by the following chemical balance:

$$2CsI + CsOH + 2H_2O \rightarrow CsOH + CsI + HI + H_2O$$

$$\downarrow$$

$$CsOH\ (Condensed)$$

Thus, if CsOH is removed by condensation from a mixture that is in thermochemical equilibrium, a CsOH replacement reaction will occur which tends to return the system to equilibrium. In the above example, the CsI molecule is destabilized to replace the lost CsOH. The same principle applies if the CsI molecule is removed from the mixture; the CsOH molecule may be destabilized to replace the CsI lost from the mixture. Thus, condensation can have a significant impact on the chemical form of iodine and cesium transport.

5.2.2 Upper Plenum Condensation

Assessment of the condensation potential of CsI and CsOH requires knowledge of the condensation surface area (A), the plenum control volume (V), the mass transfer coefficient (K), and the effective residence time (t_R) of the fluid in each control volume illustrated in Figure 5-2. These parameters can be estimated as follows.

5.2.2.1 Parameter Estimates. For present purposes, steam flow and ideal gas behavior can be assumed. The cross-sectional plenum flow area (A_f), the velocity (V_R) and effective residence time (t_R) in each control volume are estimated in Table 5-3, indicating an approximate residence time of 100 seconds for each of the three volumes indicated in

TABLE 5-3. ESTIMATION OF VAPOR MIXTURE RESIDENCE TIME IN UPPER PLENUM CONTROL VOLUME ELEMENTS

Control Volume-1

T_{ave} = 1255 K (1800 F)

R = steam gas constant = 85.8 lb_f-ft/lb_m-R

$$\rho = P/RT = \left(\frac{1500\ lb_f}{in^2}\right) \times \left(\frac{144\ in^2}{ft^2}\right) \Big/ (85.8\ lb_f - ft/lb_m - R)(1800\ F + 459.7\ R)$$

$$\rho = 1.11\ lb_m/ft^3 = 1.8\ E\text{-}02\ g/cm^3$$

$$A_f = \frac{1}{3}\left(\frac{\pi D^2}{4}\right) = 3.3\ E{+}4\ cm^2$$

m = 2500 g/s

L = control volume height = 1/2 (25 ft) = 380 cm

$$V_R = \left(\frac{2500\ g}{s}\right)\left(\frac{cm^3}{1.8\ E\text{-}02\ g}\right)\left(\frac{1}{3.3\ E{+}4\ cm^2}\right) = 4.2\ cm/s$$

Noting that control volume-1 has an approximate height of 380 cm, the effective residence time in the control volume element is approximately

$$t_R = 380\ cm\left(\frac{s}{4.2\ cm}\right) = 90\ seconds\ .$$

The effective residence time in each of the other plenum control volumes are estimated in a similar manner.

Control Volume-2

T_{ave} = 1033 K (1400 F)

$$\rho = P/RT = \left(\frac{1500\ lb_f}{in^2}\right) \times \left(\frac{144\ in^2}{ft^2}\right) \Big/ (85.8\ lb_f - ft/lb_m - R)\ (1400F + 459.7\ R)$$

$$\rho = 1.35\ lb_m/ft^3 = 2.17\ E\text{-}02\ g/cm^3$$

$A_f = 3.3\ E{+}4\ cm^2$

m_H = 2500 g/s

L = 380 cm

TABLE 5-3. (continued)

$$V_R = \left(\frac{2500\ g}{s}\right)\left(\frac{cm^3}{2.17\ E\text{-}2\ g}\right)\left(\frac{1}{3.3\ E\text{+}4\ cm^2}\right) = 3.5\ cm/s$$

$$t_R = 380\ cm\left(\frac{s}{3.5\ cm}\right) = 110\ seconds$$

Control Volume-3

$T_{ave} = 700\ K\ (800\ F)$

$$\rho = P/RT = \left(\frac{1500\ lb_f}{in^2}\right) x \left(\frac{144\ in^2}{ft^2}\right) / (85.8\ lb_f - ft/lb_m - R)(800\ F + 459.7\ R)$$

$$\rho = 0.5\ lb_m\ ft^3 = 8.0\ E\text{-}03\ g/cm^3$$

$A_f = 10.0\ E\text{+}4\ cm^2$

$\dot{m}_H = 2500\ g/s$

$L = 380\ cm$

$$V_R = \left(\frac{2500\ g}{s}\right)\left(\frac{cm^3}{8.0\ E\text{-}3\ g}\right)\left(\frac{1}{10.0\ E\text{+}4\ cm^2}\right) = 3.1\ cm/s$$

$$t_R = 380\ cm\left(\frac{s}{3.1\ cm}\right) = 122\ seconds$$

Figure 5-2. Knowing the residence time, volume, and the effective stainless-steel surface area for deposition in each volume element, the amount of condensation can then be estimated once the mass transfer coefficient (K) has been specified.

The mass transfer coefficient (K) can be assessed from the dimensionless Sherwood number (Sh), which has been alternatively called the mass-transfer Nusselt number, i.e.,

$$Sh = K(z/d)$$

where z is the equivalent diameter of the flow channel (cm) and D is the diffusion coefficient (cm^2/s). Based upon emperical evidence, the following correlation can be used to estimate the Sherwood number for forced convection:

$$Sh = 0.69 \left(\frac{zv}{D}\right)^{0.5}$$

where v is velocity. Thus, the overall or "effective" mass transfer coefficient for condensation can be expressed as

$$K(cm/s) = 0.69 \left(\frac{zv}{D}\right)^{0.5} \left(\frac{D}{z}\right) = 0.69 \left(\frac{vD}{z}\right)^{0.5}$$

Assuming a diffusivity of $\simeq 1.0$ cm^2/s for simple gases (see Ref. 9), Table 5-4 presents the estimated mass transfer coefficient for each control volume, indicating an average value of 0.1 cm/s. Knowing the mass transfer coefficient (K), the bulk temperature of the gas (T_{bulk}), the liquid-vapor equilibrium temperature (T_{eq}), and the effective residence time (t_R), the amount of condensation of CsI and CsOH in each control volume element can be calculated.

5.2.2.2 Condensation Estimate. Tables 5-5 and 5-6 give the equilibrium temperatures at the TMI-2 CsI and CsOH concentration conditions, indicating condensation at temperatures below about 880 K for

TABLE 5-4. ESTIMATION OF MASS TRANSFER COEFFICIENT FOR CONDENSATION IN EACH PLENUM CONTROL VOLUME

Governing Equation:

$$K(cm/s) = 0.69 \left(\frac{vD}{z}\right)^{0.5}$$

Control Volume 1

v = 4.2 cm/s

z = 1/3 (Plenum diameter) = 110 cm

K (cm/s) = 0.135

Control Volume 2

v = 3.5 cm/s

z = 110 cm

K (cm/s) = 0.123

Control Volume 3

v = 3.1 cm/s

z = Plenum diameter = 355 cm

K (cm/s) = 0.065

TABLE 5-5. EQUILIBRIUM TEMPERATURE FOR CsI CONDENSATION AT THE TMI-2 CONCENTRATION AND PRESSURE CONDITIONS, AT H_2/H_2O = 4.3

Partial Pressure of CsI; $P'(CsI)$

- Essentially all I exists as CsI, thus the mole ratio is $I/H_2O = CsI/H_2O = 5.536\ E\text{-}6$

- The total pressure (P_T) of the gas mixture is essentially equal to the sum of the H_2 and H_2O partial pressures, thus the partial pressure of steam, $P'(H_2O)$ at H_2/H_2O mole ratio of 4.3 is:

  $$P'(H_2O) = \frac{1}{5.3}\ (1500\ psi) = 283\ psi$$

- The partial pressure of CsI is:

  $$P'_{CsI} = 5.536\ E\text{-}6\ (283\ psi) = 1.57\ E\text{-}3\ psi = 0.081\ mmHg$$

Vapor Pressure of CsI

$$\log\ (mm\ Hg) = \frac{-10,420}{T} + 19.7 - 3.2\ \log(T)$$

Temperature at Which $P_v\ (CsI) = P'(CsI)$

$$\log\ (0.081) - -1.09 = \frac{-10,420}{T} + 19.7 - 3.02\ \log(T)$$

$$20.79 = \frac{-10,420}{T} - 3.02\ lot\ (T)$$

$$T \simeq 880\ K$$

NOTE: 51.715 mm Hg equals 1.0 psi

TABLE 5-6 EQUILIBRIUM TEMPERATURE FOR CsOH CONDENSATION AT IMI 2 CONCENTRATION AND PRESSURE CONDITIONS, AT H_2/H_2O = 4.3

Partial Pressure of CsOH; P'(CsOH)

- Essentially all Cs exists as CsOH except for that amount of Cs as CsI, thus the mole ratio of CsOH is

  $CsOH/H_2O$ = 4.89 E-05 - 5.536 E-06 = 4.436 E-05

- The total pressure (P_T) of the gas mixture is essentially equal to the sum of the H_2 and H_2O partial pressures, thus the partial pressure of steam, $P'(H_2O)$ at H_2/H_2O mole ratio of 4.3 is:

  $$P'(H_2O) = \frac{1}{5.3}\ (1500\ psi) - 283\ psi$$

- The partial pressure of CsOH is:

  $$P'_{CsOH} = 4.436\ E\text{-}05\ (283\ psi) = 0.0125\ psi = 0.0125\ psi = 86.185\ Pa$$

Vapor Pressure of CsOH

See Table 5-2

$\log (Pa) = 9.92 - 6700/T$

Temperature at Which P_v (CsOH) = P'(CsOH)

$\log (86.185) = 1.935 = 9.92 - 6700/T$

$-7.985 = -6700/T$

$T = 839\ K$

CsI and below 839 K for CsOH. Based on the plenum temperatures indicated in Figure 5-2, the upper half of the plenum is indicated to have been cool enough (700 K) to induce condensation of both CsI and CsOH, with an effective condensation surface area of about $1.5(10^6)$ cm^2. Table 5-7 presents results where the fractional amount (F) of condensation is indicated to be approximately 14% for CsI and about 12% for CsOH, at a residence time of about 100 seconds. The indication of such results is that partial CsI and CsOH condensation could have occurred on upper plenum structures during the high-temperature phase of the accident. However, such condensate would have been washed from the surface when system conditions were such as to ensure steam condensation in the plenum (at elevated pressures and/or lower effluent temperatures) and upon vessel reflood.

Figure 5-4 can also be used as a check of the wall temperatures at which condensation of CsI and CsOH can be expected. At an effluent density of 0.008 g/cm^3 (see Table 5-3), which is assumed to be primarily steam, the concentrations of CsI and CsOH are:

$$CsOH = \frac{4.44\ E\text{-}05\ \text{moles - CsOH}}{\text{mole } H_2O} \times \frac{1\ \text{mole - } H_2O}{18\ \text{g - } H_2O} \times \frac{154\ \text{g - CsOH}}{\text{mole - CsOH}} \times \frac{0.008\ \text{g } H_2O}{cm^3}$$

$$= 3.04\ E\text{-}06\ g/cm^3 = 3.04\ E\text{-}03\ kg/m^3$$

$$CsI = \frac{5.54\ E\text{-}6\ \text{moles - CsI}}{\text{mole - } H_2O} \times \frac{1\ \text{mole - } H_2O}{18\ \text{g - } H_2O} \times \frac{271\ \text{g - CsI}}{\text{mole - CsI}} \times \frac{0.0008\ \text{g } H_2O}{cm^3}$$

$$= 6.67\ E\text{-}07\ g/cm^3 = 6.67\ E\text{-}04\ kg/m^3 \quad .$$

Noting that the logarithms are -2.5 for CsOH and -3.18 for CsI, the respective wall temperatures at which condensation occurs, based on Figure 5-4, are ≈860 K for CsOH and ≈900 K for CsI, at a system pressure of 0.1 MPa (one atm). These condensation temperatures compare

TABLE 5-7. CALCULATED WALL CONDENSATION OF CESIUM (CsI and CsOH) IN CONTROL VOLUME 3 OF UPPER PLENUM

Governing Equation:

$$C_{cond} = \left[\frac{1}{T_{bulk}} - \frac{1}{T_{eq}}\right] (P_a V/R) \left[\exp (AKt/V) - 1\right]$$

$$= [C_{bulk} - C_{eq}] \left[\exp (AKt/V) - 1\right]$$

Parameter Values:

A = condensation surface area = 2.0 E+6 cm^2

K = mass transfer coefficient = 0.1 cm/s

t = residence time = 100 sec

V = control volume = 3.75 E+7 cm^3

B = AKt/V = 0.533

exp (B) = 1.7

T_{bulk} = 700 K

P'(CsI) = 1.93 E-3 psi = 1.3 E-4 atm

P'(CsOH) = 1.55 E-2 psi = 1.1 E-3 atm

R_u = 82 atm cm^3/mole K

R(CsI) = 82/268 = 0.306 atm cm^3/g K

R(CsOH) = 82/154 = 0.53 atm-cm^3/g K

$P_a V/R$ for CsI = 1.6 E+4 g K

$P_a V/R$ for CsOH = 7.8 E+4 g K

Calculation

Parameter	CsI	CsOH
B = AKt/V	0.533	0.533
exp (B)	1.7	1.7
$C_{bulk} = P'V/R\ T_{bulk}$	22.8	111.4
T_{eq}, K	880	839
$C_{eq} = P'V/R\ T_{eq}$, g	18.2	91.7
C_{cond}, g	3.2	13.8
$F = C_{cond}/C_{bulk}$	0.14	0.12

favorably with the equilibrium temperatures predicted in Table 5-5 and 5-6, (that is, 849 K for CsOH and 800 K for CsI) at a system pressure of 10.3 MPa (1500 psi).

5.2.3 Hot Leg Condensation

The temperature of the hot-leg pipe is estimated at 1000 K during the high-temperature/fission-product release phase of the TMI-2 accident. Since temperatures of less than 880 K for CsI and 849 K for CsOH are required to induce condensation at their respective concentrations, essentially no condensation of these species is predicted for the hot leg during the high-temperature phase of the accident. However, as discussed in the following section, chemisorption of such species is predicted for both CsOH and CsI.

5.3 Chemical Reactions With Surfaces

A second process that can diminish the amount of a reactive species in a gas mixture is chemisorption, where chemical bonding with a surface occurs. For example, CsOH is known to react with stainless steel surfaces.[10-12] For a gas mixture of CsOH, CsI, and steam, the reaction of CsOH with stainless steel will result in a shift in its vapor concentration to lower levels, which in turn may alter the concentration of other cesium bearing species (e.g. CsI) so that thermochemical equilibrium is maintained. Chemisorption is assessed for both CsOH and CsI species in terms of the TMI-2 conditions. A brief overview is first presented on the modeling of chemisorption, followed by calculations performed for the TMI-2 upper plenum and hot leg piping conditions.

5.3.1 Chemisorption Model

Similar to the modeling of condensation, the time-rate-of-change of species-a in the control volume can be written in terms of a mass-transfer flux (J; g/cm^2 s), i.e.,

$\frac{dC_a}{dt}$ = Rate of mass chemisorbed in the control volume = JA

where A is the deposition surface area (cm^2) and C_a is the amount of chemisorption of species-a (grams). To explicitly express the amount of chemisorption, the spatial and time dependence of the concentration profile C_a needs to be specified, which is a complex function of diffusional and reactivity properties, and generally unknown. The usual procedure is to model chemisorption as an irreversible mass transfer process in terms of an "effective" deposition velocity (v_d), where v_d accounts for both diffusional properties through the gas boundary layer and a reactivity factor for irreversible bonding to the wall surface. The resulting expression for the rate of mass transfer due to chemisorption can therefore be formulated as

$$\frac{dC}{dt} = \frac{A\, v_d}{V} C$$

which upon integration becomes:

$$C_{chem} = C_o \left[\exp\left(Av_c t/V\right) - 1\right]$$

where

v_d = deposition velocity (cm/s)

C = initial species concentration (g/cm^3)

A = reaction surface area (cm^2)

V = volume (cm^3)

t = time (s).

The above equations indicate that the amount of chemisorption increases exponentially with an increase in deposition velocity (v_d), surface area (A), and residence time (t), and decreases exponentially with an increase in control volume (V). Standard deposition velocity (v_d) correlations for various I and Cs species are given in Table 5-8. These correlations are used to assess CsOH and CsI chemisorption potential for the TMI-2 reactor plenum temperature and surface area conditions illustrated in Figure 5-2.

5.3.2 Upper Plenum Chemisorption

Unlike condensation, chemisorption can occur over a wide range of temperatures. For both CsI and CsOH, the deposition correlations given in Table 5-8 indicate that the reaction of these cesium bearing species with stainless steel is essentially temperature independent, where v_d = 1.0 E-02 cm/s. Thus, chemisorption would be permitted within all volume elements of the upper plenum. Knowing the residence time, volume, and the effective stainless steel surface area for deposition (see Section 5.2), the amount of chemisorption of each chemical species in each control element can be estimated. Deposition by chemisorption for CsI and CsOH are estimated in Table 5-9.

Note that for a similar surface-to-volume ratio and similar v_d and t_R values in each control volume, the argument of the exponent is the same and thus the amount of chemisorption would be the same. As indicated, 70% chemisorption of CsI and CsOH on stainless steel surfaces is predicted for each of the control volumes.

5.3.3 Hot Leg Chemisorption

Similar chemisorption calculations were performed for the hot leg, based upon the pipe dimensional characteristics illustrated in Figure 5-3 and associated thermalhydraulic parameters estimated in Table 5-10.

Table 5-11 presents chemisorption estimates for effluent flow through one hot-leg pipe. As indicated, because of the relative low

TABLE 5-8. VAPOR DEPOSITION VELOCITIES FOR CESIUM AND IODINE BEARING COMPOUNDS ON STAINLESS STEEL AND ZIRCALOY[a]

Vapor	Substrate	Deposition Velocity, v_d (cm/s)	v_d at 1000k (cm/s)
I_2; HI	Stainless steel	9.0 E-08 exp (4076/T)	5.3 E-06
CsI	Stainless steel	Same as CsOH	1.0 E-02
CsOH; Cs_2	Stainless steel	E-02	1.0 E-02
I_2; HI	Zircaloy	1.2 E-07 exp (3955/T)	6.3 E-06
CsI	Zircaloy	0	0
CsOH; Cs_2	Zircaloy	0	0

a. J. A. Gieseke, et al., Analysis of Fission Product Transport Under Terminated LOCA Conditions, BMI-NUREG-1990, December 1977.

TABLE 5-9. CALCULATED WALL CHEMISORPTION DISTRIBUTION OF CESIUM (CsI and CsOH) IN CONTROL VOLUMES 1 THROUGH 3 OF UPPER TMI-2 PLENUM

Governing Equation:

$C_{chemi} = C_o [\exp (Av_d t/V) - 1]$

A_W = stainless steel surface area, cm^2

v_d = vapor deposition velocity, cm^2/s

t_R = residence time, s

V = control volume, cm^3

Deposition Correlations:

v_d (stainless steel) = 1.0 E-02, cm/s

Calculation of Deposition:

	Control Volume		
Parameter	1	2	3
Wall Material	SS	SS	SS
V, cm^3	1.25 E+7	2.5 E+7	3.75 E+7
A_W, cm^2	0.67 E+6	1.33 E+6	2.0 E+6
Wall Temp, K	1255	1033	700
t_R, s	100	100	100
v_d, cm/s	1.0 E-2	1.0 E-2	1.0 E-2
$B = A_W v_d t_R/V$	0.533	0.533	0.533
exp (B)	1.7	1.7	1.7
$F = C_{chemi}/C_o$	0.7	0.7	0.7

TABLE 5-10. ESTIMATION OF THERMALHYDRAULIC CHARACTERISTICS OF HOT LEG PIPING

Dimensions:

A_f = flow area = $\frac{\pi}{4}(ID^2) = \frac{\pi}{4}(36\ in.)^2 = 1017\ in.^2 = 6.6\ E{+}3\ cm^2$

L = pipe length = 60 ft = 1829 cm

V = pipe volume = 1.2 E+7 cm^3

Calculation of Residence Time, t_R:

T = steam temperature = 1000K

ρ = steam density

$$\rho = P/RT = \left(\frac{1500\ lb_f}{in.^2}\right) \times \frac{144\ in.^2}{ft^2} \Big/ (85.8\ lb_f - ft/lb_m - R)\ (1800\ F + 459.7\ R)$$

$\rho = 1.72\ lb_m/ft^3 = 2.8\ E{-}02\ g/cm^3$

m = core exit mass flow rate = 2500 g/s

V_R = steam velocity in hot-leg pipe

$$V_r = \left(\frac{2500\ g}{s}\right)\left(\frac{cm^3}{2.8\ E{-}02\ g}\right)\left(\frac{1}{6.6\ E{+}3\ cm^2}\right) = 13.7\ cm/s$$

Noting that the hot-leg pipe has an approximate length of 2063 cm, the effective residence time in the control volume element is approximately

$$t_R = 2063\ cm\left(\frac{s}{13.7\ cm}\right) = 150\ seconds$$

Calculation of Deposition Surface Area, A_w:

$A_w = \pi(ID)L = 5.25\ E{+}5\ cm^2$

TABLE 5-11. CALCULATED WALL CHEMISORPTION DISTRIBUTION OF CESIUM (CsI and CsOH) IN HOT LEG PIPE

Governing Equation:

$C_{chemi} = C_o [\exp (Av_d t/V) - 1]$

A_W = stainless steel surface area, cm^2

v_d = vapor deposition velocity, cm^2/s

t_R = residence time, s

V = control volume, cm^3

Deposition Correlations:

v_d (stainless-steel) = 1.0 E-02, cm/s

Calculation of Deposition:

Parameter	Value
Wall Material	Stainless steel
V, cm^3	1.2 E+7
A_W, cm^2	5.25 E+5
Wall Temp, K	1000K
t_R, s	150
v_d, cm/s	1.0 E-02
$B = A_W v_d t_R/V$	0.0656
exp (B)	1.07
$F = C_{chemi}/C_o$	0.07

surface-area-to volume ratio (5.25 E+5 cm^2/1.2 E+7 cm^3 = 0.044 cm^{-1}) for this 3-ft (36 in.) diameter pipe, only 7% chemisorb is predicted. This result is in contrast to the rather high surface-to-volume conditions of the plenum.

5.3.4 Discussion

The above estimates indicate that significant chemisorption of CsOH and CsI would be expected in the upper plenum. However, most fission product iodine and cesium at TMI-2 has been found in water samples, with only a small fraction of the cesium and iodine inventories attributed to chemisorption in the reactor plenum, based upon leadscrew data. Thus, a significant discrepancy exists in predicted versus observed chemisorption behavior, using the temperature-independent correlation suggested in Ref. 7 (i.e., v_d = 0.01 cm/s). A similar overestimate of CsOH chemisorption has also been noted in Ref. 13 using this vapor deposition correlation, relative to assessment of fission product transport and deposition behavior in the PBF-SFD Scoping test. Calculated results in Ref. 13 indicated complete chemisorption of CsOH in the steam line between the test bundle and condenser, while measured activities of Cs indicated little irreversible deposition (chemisorption). As discussed in Ref. 13, the use of a constant deposition velocity, that is neither temperature dependent nor accounts for steel oxidation or the buildup of a reaction layer, is probably erroneous. The TMI-2 results also indicate the inadequacy of present chemisorption modeling of CsI and CsOH using v_d = 0.01 cm/s.

5.4 Effect of Borated Water

In addition to condensation and chemisorption effects, the transport chemistry of iodine and cesium can also be influenced by chemical reactions with borated water released to the primary system during the TMI-2 accident. The influence of potential boron reactions are summarized in this section.

As discussed by Ardon and Cain,[14] the Borated Water Storage Tank (BWST), with a total capacity of 4.73 (10^5) gals, provides a boron poison

to the core during operation of the engineered safeguards system. Orthoboric acid (H_3BO_3), metaboric acid (HBO_2), and boric-oxide (B_2O_3) crystals in the ECCS water, constitute the primary chemical forms of the dissolved boron. Boric acid is an extremely weak acid, and therefore does not exhibit excessive corrosive behavior with primary system iron-based materials. During the TMI-2 accident period between 0-200 min, about 5.5 E+4 kg (14,800 gals) of water is thought to have entered the reactor coolant system from the BWST.[14] Output from the alarm printer indicates that the BWST makeup system operated for a total of about 10 min during this period. Assuming the safety injection system operated at its full design capacity of 63 kg/s (1000 gpm), this implies a total injection from the BWST of 3.8 E+4 kg (10,000 gals) during this period of recorded operation. The remaining 1.8 E+4 kg (4800 gals) was presumably injected from 73-166 min, when the alarm printer was out of action.

An additional source of boron during the TMI-2 accident may have been derived from decomposition of the B_4C Zircaloy-clad burnable poison rods. Besides full- and part-length AgInCd (stainless-steel clad) movable control rods, the TMI-2 core contained 68 fuel assemblies, each containing 16 burnable poison rods. These rods incorporate ceramic pellets containing B_4C suspended in cylindrical alumina (Al_2O_3) pellets. Decomposition of B_4C by steam during core meltdown can occur via the following reaction:[12]

$$B_4C + 6H_2O = 2B_2O_3 + 6H_2$$

Subsequent reactions of the boric-oxide product with water would result in boric acid formation; i.e.,

$$B_2O_3 + H_2O = 2\ HBO_2 \text{ (metaboric acid)} \quad , \text{ and}$$

$$HBO_2 + H_2O = H_3BO_3 \text{ (orthoboric acid)} \quad .$$

these sources of boric acid can impact cesium and iodine chemistry via the following reactions:[15]

$$CsI + HBO_2 = CsBO_2 + HI$$

$$CsI + H_3BO_3 = CsBO_2 + H_2O + HI$$

$$CsOH + HBO_2 = CsBO_2 + H_2O$$

$$CsOH + H_3BO_3 = CsBO_2 + 2H_2O \quad .$$

In this section, the potential for alteration of iodine and cesium transport chemistry due to boron addition is considered with respect to TMI-2 conditions. A brief discussion is first presented on boron-cesium chemistry, followed by an evaluation of the TMI-2 boron concentration levels necessary for significant sequestering of fission product cesium.

5.4.1 B-Cs Chemistry

Small-scale laboratory studies at Sandia Laboratories[12] have shown that CsI reacts with boron carbide in steam at ≈1000 K, generating a volatile iodine species. This observation prompted studies (at the U.K. Winfrith Laboratories) on the reaction between boric acid and CsI at temperatures typical of severe reactor accident conditions.[15] It was found that significant interaction occurred when the reactants were heated together in the range 700 K to 1300 K, producing a volatile iodine species and complex cesium borates. Mass-spectrometer studies of the system identified the volatile iodine species as HI. Additionally, the Winfrith studies showed that the reaction occurred at temperatures as low as 400 K, although significant HI release occurred only above 700 K. Additional studies have also demonstrated that iodine is volatilized from evaporating aqueous solutions of cesium iodide and boric acid,[16] in the temperature range of ≈400 K.

The Winfrith studies[15] demonstrated that the primary reaction between CsI and metaboric acid can be described by the following simple reaction:

$$CsI + HBO_2 = CsBO_2 + HI \quad .$$

The above reaction occurred whether the reactants were in a condensed or vapor phase. However, the most reactive mixture occurred when both reactants were present in a vapor phase, where essentially complete decomposition of CsI was observed. The effect of CsOH vapor on the cesium iodide-boric acid reaction was also considered. Results indicated that the release of the byproduct HI was suppressed somewhat by the addition of CsOH to the reaction mixture. The implication of such results is that the chemical reaction of CsOH with boric acid is favored over that of CsI, although some HI was always produced.

Alexander[10] recently performed experiments to assess the combined effects of CsI and CsOH reactions with boron oxides in the presence of a reactive stainless surface. Results indicated that the stainless steel surface served as a strong bettering agent for depletion of both CsOH and CsI vapor. The effect of boron addition was found to be secondary, where trace amounts of boron components (B_2O_3, $CsBO_2$, and H_3BO_3) had little impact on CsOH and CsI behavior. Alexander[10] concluded that a CsOH/CsI/steam mixture, in the presence of both stainless steel and boric acid, exhibits a stronger reaction for Cs-SS chemisorption and release of HI in the process than for cesium-boron reactions. However, in the absence of reactive stainless-steel surfaces, cesium borate compounds should form, so that the CsI molecule is destabilized, releasing HI in the process.

In the following subsection, such results are assessed relative to conditions that occurred during the TMI-2 accident. The principal concern is whether conditions existed which would have resulted in boric acid destabilization of the CsI molecule, resulting in HI formation.

5.4.2 TMI-2 B/Cs Concentration Conditions

To assess the potential for HI formation by CsI reaction with borated water, an estimate is made of B/Cs concentration conditions for the TMI-2 accident conditions. The principal sources of boron addition to the TMI-2 core are the borated water released during ECC injection and that due to decomposition of the B_4C-Al_2O_3 burnable poison rods.

The ECC contribution can be estimated, based on a solubility of 27.6 g of H_3BO_3 per 100 cc of water (Ref. 16) and a total injection of about 5.5 E+4 kg of borated water to the core during the accident (Ref. 14). Thus, the ECC contribution of boron is estimated to be:

$$\text{Ecc - boron} = \frac{0.276 \text{ g - } H_3BO_3}{1.0 \text{ g - } H_2O} \times 5.5 \text{ E+7 g } H_2O \times \frac{11 \text{ g - B}}{62 \text{ g - } H_3BO_3} = 2.69 \text{ E+6 g} \quad .$$

Most of the burnable poison in the TMI-2 core is a B_4C compound dispersed in ceramic Al_2O_3 of which approximately 1 to 1.4 wt% is B_4C. Noting that a total of 380 lb (Ref. 5) or 1.73 E+5 g of such material was present in the TMI-2 core, the contribution of boron from complete decomposition of the burnable poison material is estimated to be:

$$B_4C \text{ - boron} = \frac{0.012 \text{ g - } B_4C}{1.0 \text{ g - } B_4C/Al_2O_3} \times \frac{1.73 \text{ E+5 g - } B_4C/Al_2O_3}{\text{core}} \times \frac{44 \text{ g - } B_4}{56 \text{ g - } B_4C}$$

$$= 1630 \text{ g} \quad .$$

Because the boron contribution from B_4C decomposition is small compared to that released by ECC injection, the B_4C contribution can be neglected.

Because the total fission product inventory of cesium at the time of TMI-2 shutdown is estimated to be approximately (see Chapter 3) 2.25 E+4 g, the B/Cs mass ratio is:

$$\text{B/Cs mass ratio} = \frac{2.69 \text{ E+6}}{2.25 \text{ E+4}} = 120$$

with a corresponding B/Cs atom ratio of about 1500. Clearly a sufficient quantity of boron would have been present in the TMI-2 coolant for the reaction of both CsI and CsOH to cesium-borate compounds, with resultant release of HI from the CsI-H_3BO_3 reaction. The implication of this result is that HI may have been the primary chemical form of iodine vapor transport in the TMI-2 primary coolant system. Upon contact with water, either in the pressurizer or steam generators, such HI would then have formed a water soluble species.

5.5 Summary

Results of analyses described in this section indicate that although the predominant forms of iodine and cesium transport with the steam/hydrogen effluent exiting the core are predicted to be CsI and CsOH, changes in chemical form can occur as these species interact with either reactive/cool surfaces or boric acid released by ECC injection. Condensation and chemisorption of CsOH and CsI in the upper plenum both tend to increase the concentrations of HI in order for chemical equilibrium to be maintained. An assessment of the TMI Cs/B concentration conditions also indicates that a sufficient quantity of boron would have been present in the TMI-2 core (due to ECC injection) for complete reaction of both CsI and CsOH to cesium-borate compounds, with the resultant release of HI. Gas-phase iodine transport in the TMI-2 primary coolant system is therefore assessed to have been primarily in the form of HI, which, when scrubbed through water, would have resulted in a stable solution containing iodide ions. Although there is no direct evidence of chemical form from the TMI-2 water samples, the measured concentrations in sump water samples are as consistent with HI chemical form as with CsI.

5.6 References

1. R. A. Lorenz, et al., The Behavior of Fission Product Cesium in the TMI-w Accident, ORNL/TM-9666, 1986.

2. D. O. Campbell, A. P. Mallinauskas, and W. R. Stratton, "The Chemical Behavior of Fission Product Iodine in Light Water Reactor Accidents," Nuclear Technology, 53, 1981, pp. 111-119.

3. K. Vinjamuri, D. W. Akers, and R. R. Hobbins, Examination of H8 and B8 Leadscrews from Three Mile Island Unit 2 (TMI-2), EGG-TMI-6685, April 1985.

4. R. R. Hobbins, A. W. Cronenberg, S. Langer, D. E. Owen, and D. W. Akers, "Insights on Severe Accident Chemistry from TMI-2," Proc. Am. Chemical Soc. Mtg., Anaheim, CA, September 8-12, 1986.

5. D. W. Golden, TMI-2 Standard Problem Package, EGG-TMI-7382, September 1986.

6. S. Langer, S. Croney, D. Akers, and M. Russell, Fission Product Inventory Program FY-85 Status Report, EGG-2407, July 1985.

7. J. A. Gieseke, et al., Analysis of Fission Product Transport Under Terminated LOCA Conditions, BMI-NUREG-1990, December 1977.

8. J. C. Cummings, R. M. Elrick, and R. A. Sallach, Status Report on Fission-Product Research Program, NUREG/CR-1820, SAND 80-2662, March 1982.

9. R. Bird, W. Stewart, and E. Lightfoot, Transport Phenomena, J. Wiley and Son, Inc., New York, 1960, pp. 508-513.

10. C. A. Alexander and J. S. Ogen, "CsI-H_2O-Stainless Steel Chemistry," Proc. NRC Severe Damage Partners Meeting, Rockville, MD, October 21-24, 1986).

11. O. Gotzmann, C. E. Johnson, and D. C. Fee, "Attack of Stainless Steel by Liquid and Vaporized CsOH," J. Nucl. Matl., 74, 1978, pp. 68-75.

12. R. M. Elrick and R. A. Sallach, "Fission Product Chemistry in The Primary System," Proc. Intern. Mtg on LWR Severe Accident Evaluation, Cambridge, Mass., August 28-September 1, 1983, pp. 4.6-1 to 4.6-5.

13. A. W. Cronenberg, et al., Fission Product Behavior During the PBF Severe Fuel Damage Scoping Test, Draft EGG Report, Fin. No. A-6321, June 1985.

14. K. H. Ardon and D. G. Cain, TMI-2 Accident Core Heatup Analysis, EPRI Report: NSAC-24, 1981.

15. B. R. Bowsher and S. Dickinson, The Interaction of Cesium Iodide with Boric Acid: Vapor Phase and Vapor-Condensed Phase Reactions, Winfrith Lab Report AEEW-R2102, May 1986.

16. B. J. Handy, "CSNI Specialists' Workshop on Iodine Chemistry in Reactor Safety," September 11-12, 1985, Harwell Labs, AERE-R 11974, 1986.

17. R. C. Weast and S. M. Selby, Handbook of Chemistry and Physics, 47 Edition, The Chemical Rubber Co., Cleveland, OH, 1966, p. B-160.

6. CONCLUSIONS

Although water samples from the TMI-2 accident indicate that the majority of iodine and cesium were retained in aqueous solution within the plant, there is little evidence from water sample analysis that indicates what the true chemical form was during transport. The release to the containment was at all times scrubbed through a pool of water in the pressurizer and steam generators. The only evidence for iodine chemical form was deduced from sump water samples showing high concentrations of ionic species. These results were interpreted as indicating iodine was in the form of CsI salt before entering solution, but HI would also form an ionic solution when exposed to water. However, HI is more volatile than CsI and would transport as a vapor through much of the RCS system before condensing, while CsI would condense at much higher temperatures. The purpose of this investigation was to reevaluate the TMI-2 findings on I and Cs behavior, where in-depth consideration was given concerning internal fuel morphology/microstructural effects on fission product release behavior from fuel, and fission product/steam/hydrogen concentration conditions which govern transport chemistry.

With respect to the question of fission product I and Cs release from fuel, evidence indicates that burnup-related fuel-morphology conditions exert a pronounced effect on release behavior. For the relatively low-burnup (~3200 MWd/t) TMI-2 fuel, I and Cs can be expected to be released from the fuel in atomic form rather than as molecular CsI.

Once released from fuel, I and Cs mix in the high-temperature steam/hydrogen gaseous effluent. In this gas mixture, molecular collision probabilities and reaction kinetics are strongly influenced by concentration conditions. Thermochemical equilibrium predictions, supported by reaction kinetics calculations, were used to describe I and Cs behavior for the TMI-2 environmental conditions. Analysis indicates that CsI would be the major form of iodine generated in the steam and H_2 effluent, where exact partitioning between HI and CsI is highly dependent on concentration conditions. In general, CsI is predicted to be the predominant form of iodine over a wide range of system conditions, while

CsOH is the predominant cesium species. The kinetics results also indicate that chemical equilibrium would be established quickly ($<10^{-2}$ seconds) during effluent transport.

Although the effluent chemical environment would favor predominantly CsOH(g) and CsI(g) species during vapor transport through the core, subsequent CsI reaction with boric acid released from ECC water would have resulted in conversion of CsI to Cs-borate and HI. Transport of CsI(g) and CsOH(g) from the core is also predicted to condense and chemisorb in the upper reactor plenum, forming additional HI(g) in the process. HI(g) is therefore assessed to be the principal form of iodine transport leaving the reactor vessel during core degradation, which was subsequently dissolved in water to produce iodide ions in solution with coolant. Such chemical and physical processes, in conjunction with containment isolation, are considered largely responsible for plant retention of I and Cs during the TMI-2 accident.

APPENDIX A
CHEMICAL KINETICS CONSIDERATIONS

APPENDIX A
CHEMICAL KINETICS CONSIDERATIONS

In Section 4, estimates of I and Cs chemical forms in the steam/hydrogen effluent were based on a thermochemical equilibrium analyses. Such thermodynamic predictions are valid only if the system has reached equilibrium. However, for dilute mixtures, collision probabilities are reduced so that the time required to reach equilibrium is increased. In this appendix the applicability of such thermodynamic predictions for the TMI-2 fission product concentration conditions is assessed by examining reaction rates. Estimates are made of a characteristic collision time as well as a detailed assessment of the primary reaction mechanisms controlling overall reaction kinetics.

A.1 Collision Rate Predictions

The assumption of thermochemical equilibrium is based on the fact that the number of collisions in a gas mixture is typically on the order of 10^{+28} collisions/s-cm^3 at standard temperature and pressure. However, for a low-inventory of reactive fission products in a gas mixture dominated by steam, the collision frequency between individual fission products may be low. This can be seen through inspection of the collision frequency ($Z_{I\text{-}Cs}$) for I and Cs in a gas mixture, which from kinetic theory can be expressed as:

$$Z_{I\text{-}Cs} = n_I n_{Cs} \sigma^2_{I\text{-}Cs} \left(8\pi RT \frac{M_I + M_{Cs}}{M_I M_{Cs}} \right)^{1/2}$$

where n = number atoms of reactant per cc, M = atomic or molecular weight, R = gas constant, T = absolute temperature, $Z_{I\text{-}Cs}$ = collision rate between I and Cs per cubic centimeters, and $\sigma_{I\text{-}Cs}$ = mean molecular collision diameter. As indicated, the collision frequency is proportional to the product density of interacting species.

An evaluation of the collision frequency between I and Cs atoms at the "Nominal TMI-2" effluent is presented in Table A-1. For present purposes, the collision diameter σ_{AB} can be estimated from atomic diameters. The concentrations of I and Cs are at the "Nominal TMI-2" conditions used in the SOLGASMIX calculations (see Table 4-2). The pressure and temperature conditions are the same as those used in the thermoequilibrium calculations (that is, 10.3 MPa and 1500 K, respectively). For such conditions, the I-Cs collision frequency is:

$$Z_{I\text{-}Cs} \cong 2.8\ E{+}21 \text{ collisions/cm}^3 \text{ s} \quad .$$

Dividing the concentration density (atoms/cm^3) of the most dilute species by the collision frequency (collisions/cm^3 s) gives the mean time between collisions (t_c)

$$t_c = m_I/Z_{I\text{-}Cs} = 2.07\ E{+}1/2.8\ E{+}21 = 7.04\ E{-}07 \text{ seconds} \quad .$$

If the collision time is short compared to the time period over which molecules can interact, thermoequilibrium can be assumed. For present purposes, the period for interaction can be represented by the transport time (t_b) through the core half-height, which is estimated in Table A-2 to be

$$t_b = A_f\ L/\dot{m} = 204 \text{ s} \quad .$$

Since t_c is about 9 orders-of-magnitude less than t_b, the assumption of thermochemical equilibrium for I-Cs reaction appears satisfactory. However, in general only a small fraction of molecular collisions will result in compound formation. Thus, a detailed investigation of the kinetics of the actual reaction processes involved is necessary to establish, with assurance, the time when equilibrium is achieved. Such reaction kinetics is investigated in the following section.

TABLE A-1. ESTIMATION OF THE COLLISION FREQUENCY BETWEEN FISSION PRODUCT I AND Cs ATOMS IN THE TMI-2 CORE EFFLUENT

Governing Equation:

$$Z_{I\text{-}Cs} = n_I n_{Cs} \sigma^2_{I,Cs} \left(8\pi RT \frac{M_I + M_{Cs}}{M_I M_{Cs}} \right)^{1/2}$$

Parameter Values:

P = 10.3MPa = 10.3 E+06Pa = 103 E+06 dy/cm^2

T = 1500 K

M_I = 3.43 E-09 moles-I/cm^3 = 2.065 E+15 atoms-I/cm^3

n_{Cs} = 3.03 E-08 moles-Cs/cm^3 = 1.824 E+16 atoms-Cs/cm^3

R = 1.986 cal/mole K

M_I = mass iodine atome = 127

M_{Cs} = mass cesium atom = 133

σ_I = atomic diameter iodine = 1.33 Å

σ_{Cs} = atomic diameter cesium = 2.35 Å

$\sigma_{I\text{-}Cs}$ = $(\sigma_I + \sigma_{Cs})/2$ = 1.84 A = 1.84 E-08 cm

Calculation of Parameters:

$(M_I + M_{Cs})/M_I M_{Cs}$ = (127 + 133)/127(133) = 0.0154 mole/g

$8\pi RT$ = 74.87 E+03 cal/mole = 3.13 E+12 ergs/mole
= 3.13 E+12 g-cm^2/s^2 mole

$$\left(8\pi RT \frac{M_I + M_{Cs}}{M_I M_{Cs}} \right) = (0.0154 \text{ mole/g} \times 3.13 \text{ E+12 g - cm}^2/\text{s}^2 \text{ - mole})^{0.5}$$

= 2.19 E+05 cm/s

$n_I n_{Cs}$ = 2.07 E+15 x 1.82 E+16 = 3.77 E+31 cm^{-6}

$s^2_{I\text{-}Cs}$ = [1.84 E-04 cm]^2 = 3.386 E-16 cm^2

Calculation of Collision Frequency:

$Z_{I\text{-}Cs}$ = [3.77 E+31 cm^{-6}] [3.386 E-16 cm^2] [2.19 E + 05 cm/s]
= 2.8 E+21 collisions/cm^3 s

TABLE A-2. ESTIMATION OF EFFLUENT TRANSPORT TIME THROUGH TMI-2 CORE HALF-HEIGHT

System Parameters:

P	=	Pressure	=	1500 psi (10.3MPa)
A_f	=	Core Flow Area	=	52 ft^2 = 7488 in^2
L	=	Core 1/2-Height	=	6 ft = 72 in
M	=	Mass Flow Rate (see Chapter 4)	=	2500 g/s = 5.5 lb/s
ρ	=	Saturated Steam Density (1500 psi)	=	3.6 lb_m/ft^3 = 2.08 E-03 lb_m/in^3

Calculation of Transport Time (t_D):

$t_D = \rho A_f L/M = 204$ sec

A.2 Reaction Kinetics Predictions

For any chemical reaction, the rate of change in concentration of a particular component in a reacting mixture can be expressed in terms of its generation minus consumption rates. Thus, for a reaction of the form:

$$A + B \underset{k_d}{\overset{k_r}{=}} C + D$$

the rates of change in concentrations for species A and C can be expressed as:

$$\frac{dA}{dt} = -k_r [A] [B] + k_d [C] [D]$$

$$\frac{dC}{dt} = +kr [A] [B] - k_d [C] [D]$$

In the above expressions, k_r and k_d are the reaction and dissociation rate constants, respectively, and the brackets [ ] denote concentration in molecules or atoms per cubic centimeter.

For a multicomponent system involving any number of reactions, the time-dependent concentration [C] of a particular component (i), requires the solution to the coupled differential rate equations of the general form:

$$\frac{dC_i}{dt} = \sum_j k_j C_j + \sum_{j,k} k_{jk} C_j C_k + \sum_{j,k,l} k_{jkl} C_m C_k C_l$$

where C_j, C_k, and C_l are the concentrations of the various reaction species affecting the concentration of species (i), and k_j, k_{jk}, k_{jkl} are first-, second-, and third-order rate constants. A solution to the above equation will yield information on the change in concentration of a

particular species with time. When the concentration is constant, chemical equilibrium for that species is achieved. A kinetics model for a multicomponent system requires as input not only the concentrations of all participants but also the respective rate constants, which are generally strong Arrhenius type functions of temperature, i.e.

$$k = A \exp(-Q/RT)$$

where A is a pre-exponential factor and Q is the activation energy. For a Q value of ≈40 kcal/mole K and temperatures in the range of ≈1000 K, the rate constant approximately doubles with a temperature increase of ≈35 K.

In a recent study by Wren,[A.1] the gas-phase kinetics of cesium and iodine reactions in steam and steam/hydrogen atmospheres were studied. Over 150 potential reaction and dissociation equations were postulated. However, results indicated that I and Cs chemistry in a H_2/steam atmosphere are governed by only a few primary reactions. In Refs. A.2 and A.3, the kinetics of Cs-I-C-O-H system was studied with respect to interpretation of fission product chemistry for the PBF Severe Fuel Damage (SFD) Scoping and 1-1 tests. Results indicated that the following system of chemical equations governs overall I/Cs/H_2/H_2O reaction behavior:

$$Cs + I + X \underset{k_{d1}}{\overset{k_{r1}}{=}} CsI + X \qquad I + I + X \underset{k_{r6}}{\overset{k_{r6}}{=}} I_2 + X$$

$$Cs + H_2O \underset{k_{d2}}{\overset{k_{r2}}{=}} CsOH + H \qquad CH_4 + I_2 \underset{k_{d7}}{\overset{k_{r7}}{=}} CH_3I + HI$$

$$I + H_2 \underset{k_{d3}}{\overset{k_{r3}}{=}} HI + H \qquad Cs + HI \underset{k_{d8}}{\overset{k_{r8}}{=}} CsI + H$$

$$I + H + X \underset{k_{d4}}{\overset{k_{r4}}{=}} HI + X \qquad CsOH + HI \underset{k_{d9}}{\overset{k_{r9}}{=}} CsI + H_2O$$

$$H + H_2O \underset{k_{d5}}{\overset{k_{r5}}{=}} HOI + H \qquad H + H + X \underset{k_{d10}}{\overset{k_{r10}}{=}} H_2 + X$$

where k_r and k_d are the reaction and dissociation rate constants, respectively. Although methyl-iodide (CH_3I) formation is possible due to the potential for carbon release from structural materials at high temperatures, previous studies[A.3] indicate little potential for CH_3I formation. In this analysis, methyl-iodide formation is neglected.[A.4,A.5]

Second- and third-order reactions were chosen to provide an excited secondary product that stabilizes each reaction. For this system of ten chemical equations, there are 12 reaction species (Cs, I, CsI, H_2O, CsOH, H, H_2, HOI, HI CH_4, I_2, and CH_3I) for which twelve rate equations must be written. Since the molecule X is nonreactive, its concentration is constant.[a] Two example rate equations for I and CsI are:

$$\frac{d[I]}{dt} = -k_{r1}[Cs][I][X] + k_{d1}[CsI][X]$$

$$-k_{r3}[I][H_2] + k_{c3}[HI][H]$$

$$-k_{r4}[I][H][X] + k_{d4}[HI][X]$$

$$-k_{r5}[I][H_2O] + k_{d5}[HOI][H]$$

$$-k_{r6}[I][I][X] + k_{d6}[I_2][X] \quad , \text{ and}$$

---

a. In the present analysis the concentration of the collision molecule (X) that carries the reaction energy is considered to be H_2.

$$\frac{d[CsI]}{dt} = +k_{r1}[Cs][I][X] - k_{d1}[CsI][X]$$

$$+k_{r8}[Cs][HI] - k_{d8}[CsI][H]$$

$$+k_{r9}[CsOH][HI] - k_{d9}[CsI][H_2O] \quad .$$

The rate constants k_r were taken from Wren[A.1] at T = 1500 K and 1000 K, while k_d was estimated from the equilibrium relationship $K_{eq} = k_r/k_d$, where $K_{eq} = \exp(-\Delta G/RT)$, R is the gas constant (8.314 J/mole K), T is absolute temperature (K), and ΔG is the net free energy of formation (J/mole) which is expressed as:

$$\Delta G = \sum \Delta G_f^{\circ} \text{ (products} - \sum \Delta G_f^{\circ} \text{ (reactants)} \quad .$$

The free energies were taken from the SOLGASMIX[A.6] data base.

Basically two sets of calculational results are presented, one representative of the estimated TMI-2 core conditions and the other for the colder upper plenum environment. Table A-3 presents the kinetics data at 1500 K and 1000 K. It should be noted that although a steam temperature of 2000 K was assumed in the calculation of concentration conditions, the Wren[A.1] kinetics data are for a maximum temperature of 1500 K. For the sake of simplification the kinetics data (k_r and k_d) are based on values at 1500 K (core conditions) and at 1000 K (plenum conditions), while the concentrations are estimated from ideal gas behavior at the quoted temperature (core = 2000 K; plenum = 1000 K) and pressure (10.3 MPa) conditions cited in Table A-3.

A.2.1 Core Conditions

Figure A-1 presents a numerical solution for the TMI-2 estimated core conditions. Concentration versus time results are plotted on a logarithmic scale, assuming zero initial concentration of methane. As indicated, I and

TABLE A-3. SUMMARY OF KINETICS DATA AND INITIAL CONDITIONS

Kinetics Data at 1500 K	k_{r1} = 1.65 E-30[b] k_{d1} = 5.52 E-38[a]	k_{r2} = 6.57 E-14[a] k_{d2} = 1.42 E-10[a]	k_{r3} = 2.47 E-15[a] k_{d3} = 4.19 E-11[a]
	k_{r4} = 1.30 E-29[b] k_{d4} = 7.06 E-35[a]	k_{r5} = 1.56 E-16[a] k_{d5} = 9.40 E-11[a]	k_{r6} = 4.10 E-31[b] k_{d6} = 1.00 E-80[a]
	k_{r7} = 1.66 E-11[a] k_{d7} = 2.77 E-10[a]	k_{r8} = 5.10 E-11[a] k_{d8} = 3.14 E-13[a]	k_{r9} = 6.90 E-14[a] k_{d9} = 1.97 E-19[a]
	k_{r10} = 1.07 E-29[b] k_{d10} = 3.46 E-39[a]		
Kinetics Data at 1000 K	k_{r1} = 7.66 E-32[b] k_{d1} = 2.43 E-45[a]	k_{r2} = 1.76 E-16[a] k_{d2} = 1.16 E-10[a]	k_{r3} = 1.46 E-17[a] k_{d3} = 6.91 E-11[a]
	k_{r4} = 1.24 E-30[b] k_{d4} = 2.57 E-41[a]	k_{r5} = 4.12 E-21[a] k_{d5} = 8.50 E-12[a]	k_{r6} = 1.00 E-30[b] k_{d6} = 1.00 E-107[a]
	k_{r7} = 1.66 E-11[a] k_{d7} = 3.36 E-9[a]	k_{r8} = 2.00 E-11[a] k_{d8} = 3.06 E-14[a]	k_{r9} = 1.00 E-15[a] k_{d9} = 2.32 E-24[a]
	k_{r10} = 1.03 E-32[b] k_{d10} = 4.53 E-50[a]		

Note: a = cm^3/molecule s
b = cm^6/molecule^2 s

TMI-2 Initial Conditions	T = 1000 K (plenum) T = 2000 K (core) H_2/H_2O Mole Ratio = 4.3 P = 10.3 MPa Nominal Boiloff Rate = 2500 g/s I = 2.06 E+15 atoms/cm^3 Cs = 1.82 E+16 atoms/cm^3 H_2 = 3.018 E+20 molecules/cm^3 H_2O = 7.080 E+19 molecules/cm^3

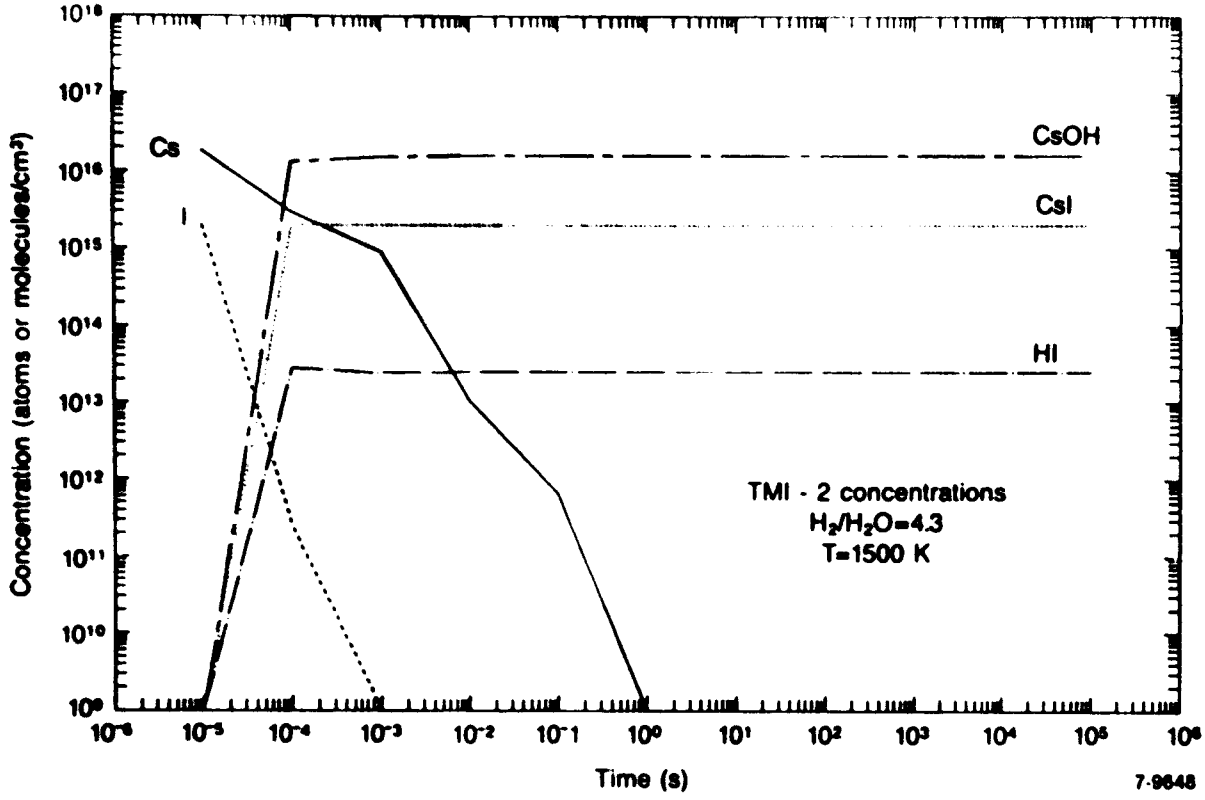

Figure A-1. Illustration of I and Cs gas-phase reaction behavior in the TMI-2 core effluent at t = 180 min.

Cs are shown to react quickly to form CsOH, CsI, and HI, where equilibrium is attained in approximately 10^{-2} seconds for these species. Essentially no formation of HOI (hypoiodous acid) is predicted. The ultimate (steady-state) partitioning of iodine between CsI and HI, as predicted for the TMI-2 environmental conditions, is CsI = 98.5% and HI = 1.5%. As shown in Table A-4, this partitioning compares favorably with SOLGASMIX thermochemical equilibrium calculations previously presented in Section 4, indicating approximately 98.5% CsI and 1.4% HI. It should be noted that the kinetics predictions should converge to the same thermochemical equilibrium results, if all reaction mechanisms are included in the kinetics study. The discrepancy of less than 1% is encouraging and indicative that the primary reactions governing I and Cs behavior have been considered.

Figure A-2 illustrates the effects of changing initial I and Cs concentrations. All parameters were the same as used in Figure A-1 except that the I and Cs initial release concentrations were both reduced and increased by a factor of 10. Table A-4 summarizes the results. As indicted, a change in concentration affects both species partitioning and the time to reach chemical equilibrium. As the concentration is decreased, the partitioning of iodine changes from one of 98.5% CsI at the nominal concentration TMI-2 conditions, to about 89% CsI and 11% HI when the concentrations are reduced by an order of magnitude. A reduction in concentration level also results in an increased time to reach equilibrium, although at 1500 K this effect is not large. On the other hand, an increase in concentration by a factor of 10 above the TMI-2 estimated core conditions results in almost total reaction of I with Cs.

As discussed in Section 2, the hydrogen generation rate and coolant inlet flow (which influenced the steam production process) varied widely during the course of the accident, so that at certain times a hydrogen-rich environment existed while at other times the atmosphere may have been steam-rich. Uncertainty thus exists relative to definition of a characteristic H_2/H_2O molar ratio, particularly at the time just after core reflooding, when the boiloff and the zircaloy oxidation induced hydrogen production rate were probably maximized. Because of such

TABLE A 4 SUMMARY OF TMI-2 KINETICS PREDICTIONS AND COMPARISON WITH SOLGASMIX THERMOCHEMICAL EQUILIBRIUM RESULTS AT 180 MIN

Initial I/Cs Concentration Conditions	H_2/H_2O Mole Ratio	Kinetics Data at Temperature (K)	Iodine Species Partitioning (%) SOLGASMIX Predictions	Kinetics Predictions	Equilibrium Time (s)
TMI-2	4.3	1500	I = 0 HI = 1.4 CsI = 98.6	I = 0 HI = 1.5 CsI = 98.5	10^{-3}
10 x TMI-2	4.3	1500	- -- --	I = 0 HI = 0 CsI = 100	10^{-2}
1/10 x TMI-2	4.3	1500	I = 0 HI = 11.4 CsI = 88.6	I = 0 HI = 11 CsI = 89	10^{-1}
TMI-2	1.0	1500	I = 0 HI = 3.3 CsI = 96.7	I = 0 HI = 3.2 CsI = 96.8	10^{-2}
TMI-2	4.3	1000	I = 0 HI = 0 CsI = 96.2 Cs_2I_2 = 3.8	I = 0 HI = 0 CsI = 100 Cs_2I_2 = N/C	10^{+2}
TMI-2	1.0	1000	I = 0 HI = 0 CsI = 97.6 Cs_2I_2 = 2.4	I = 0 HI = 0 CsI = 100 Cs_2I_2 = N/C	10^{+2}

N/C = Not Considered

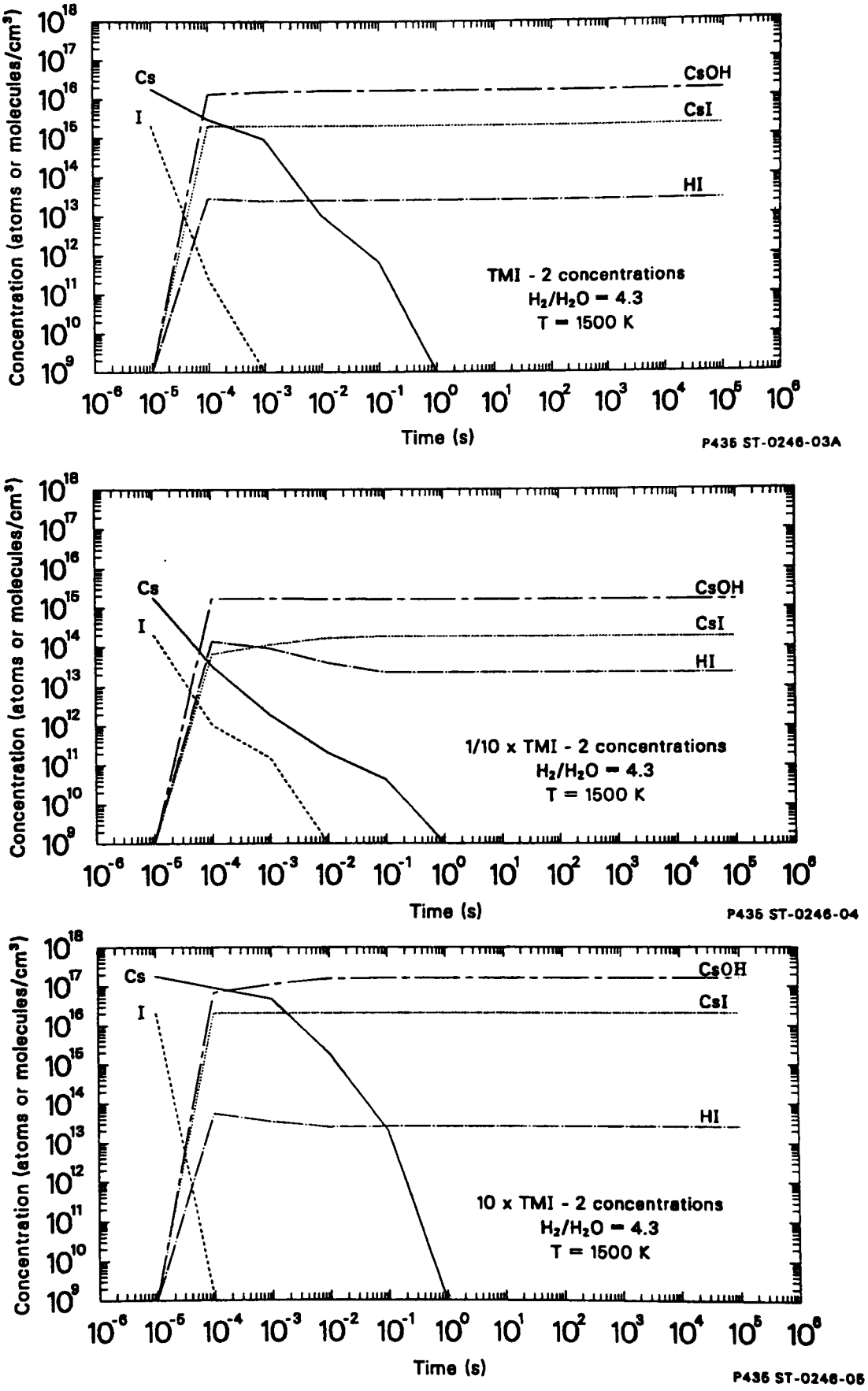

Figure A-2. Illustration of the effect of a change in I and Cs concentration on reaction kinetics and species partitioning.

uncertainties, the effect of a variation in H_2/H_2O mole ratio was also assessed, namely at a ratio of 4.3 (estimated condition at reflood) and at 1.0 (neutral environment). Figure A-3 illustrates results where all parameters were the same as used in Figure A-1, except the H_2/H_2O mole ratio was varied to 1.0. Calculational results indicate essentially no effect on reaction kinetics and only a minor effect on iodine chemical form. At a H_2/H_2O molar ratio of 4.3, the ultimate partitioning of I is 98.5% CsI and 1.5% HI, while at H_2/H_2O = 1.0 the partitioning is approximately 96.8% CsI and 3.2% HI, as predicted from kinetics.

It is interesting to note that at the higher H_2/H_2O mole ratio, less HI is formed, which is not intuitively expected. This result is due to the complexity of the reactions of Cs and I with each other and with steam and the relative concentrations of these reacting species. Because the concentration of cesium for the TMI-2 conditions is estimated to exceed that of iodine by a factor of approximately 8.8, the reaction of Cs with H_2O to form CsOH largely controls the overall partitioning of cesium species. As the relative concentration of steam is diminished at a higher H_2/H_2O mole ratio, more Cs is available to form CsI, so that the concentration of HI is diminished somewhat. In other words, because Cs is in greater concentration than I, Cs reaction behavior somewhat overrides that of iodine. Thus, if the potential to form CsOH is reduced due to a lower H_2O concentration, then the probability to form CsI is increased, which reduces the potential for HI formation. However, this effect is relatively minor, where a factor of four reduction in the H_2/H_2O ratio results in only a 2% change in the partioning of CsI and HI species.

A.2.2 Plenum Conditions

A simulation of upper plenum conditions was also made, where it was assumed that little steam condensation occurred so that the concentrations of the major carrier species (steam and hydrogen) were the same as in the core. However, the temperature in the lower region of the upper plenum was taken to be 1000 K.

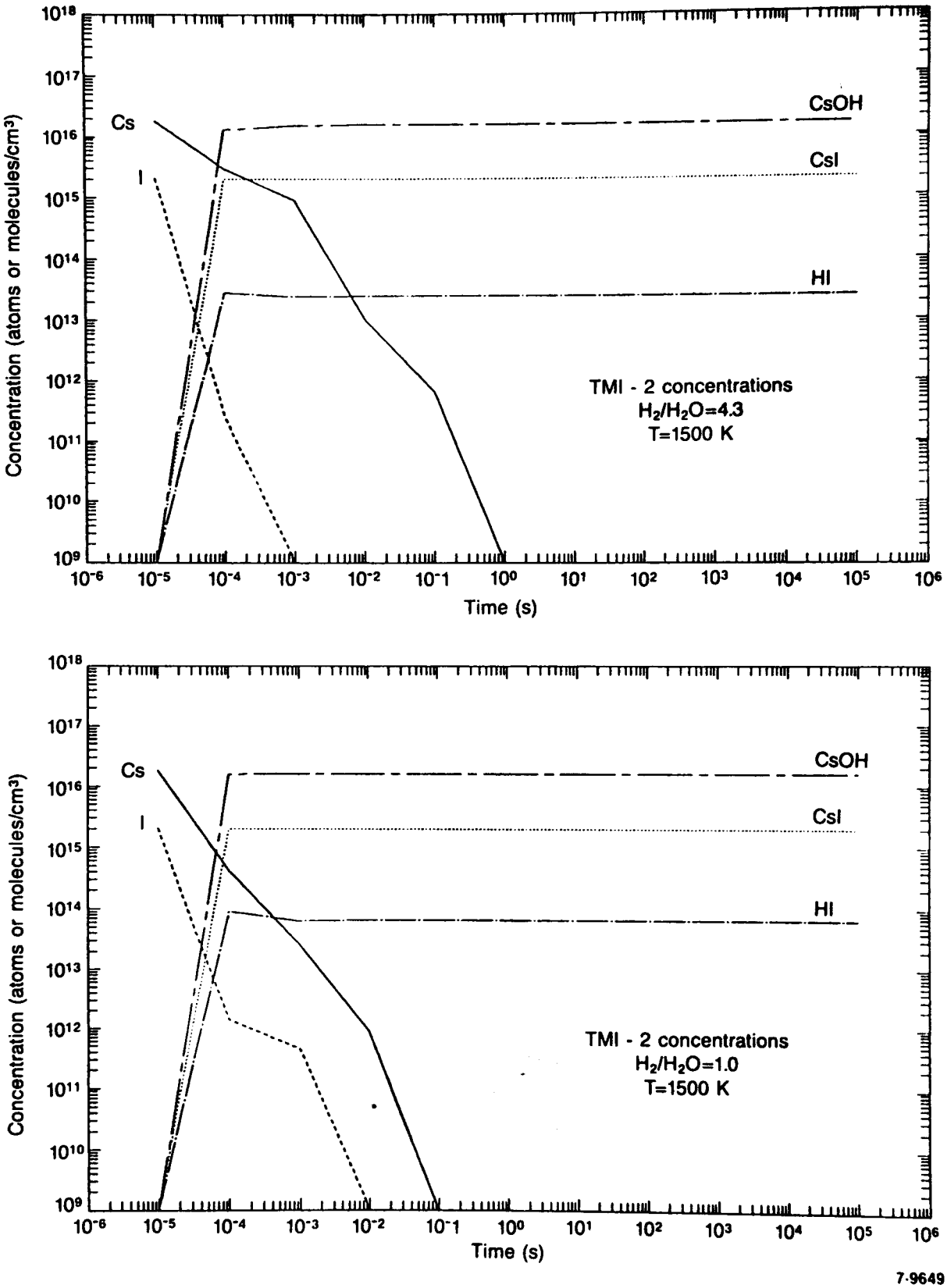

Figure A-3. Illustration of the effect of H_2/H_2O mole ratio on reaction kinetics and I/Cs species partitioning at T = 1500 K.

Figure A-4 illustrates the effect of temperature. All parameters are fixed and equal to the nominal TMI-2 concentration conditions, except the temperature-dependent kinetics rate constants were varied. As indicated, the effect of temperature on the time required to establish equilibrium is significant. At 1500 K the equilibrium of the predominant species (CsOH, CsI, HI) is reached in about 10^{-3} seconds, while at 1000 K the equilibrium of CsOH is not reached until approximately 100 seconds.

The time for the Cs-I-O-H system to reach equilibrium at 1000 K is relatively long. The reason for this behavior can be determined by examining the rate constants for the following reactions:

	1000 K	1500 K	Reaction Order
$Cs + H_2O = CsOH + H$	1.76 E-16	6.57 E-14	2
$Cs + OH + X = CsOH + X$	1.79 E-31	3.84 E-30	3
$H_2O = OH + H$	3.46 E-11	1.77 E-02	2

For the reaction $Cs + H_2O = CsOH + H$, a decrease in temperature from 1500 K to 1000 K results in a 2 order-of-magnitude decrease in the forward rate constant. For the two-stage reaction

$$H_2O = OH + H$$
$$Cs + OH + X = CsOH + X$$

the forward rate constant for the reaction $Cs + OH + X = CsOH + X$ drops only one order of magnitude over the temperature rate 1500 to 1000 K. However, the rate constant for the decomposition of water drops nine orders of magnitude over the same temperature range, indicating that it is quite difficult to dissociate water at 1000 K. As a result, the kinetics data suggest that the formation of CsOH via either mechanism (direct reaction of Cs with water to form CsOH or the two-stage process described earlier) is slow at 1000 K. For either mechanism, water must be dissociated to form CsOH, which is difficult at 1000 K. Likewise, because of the high

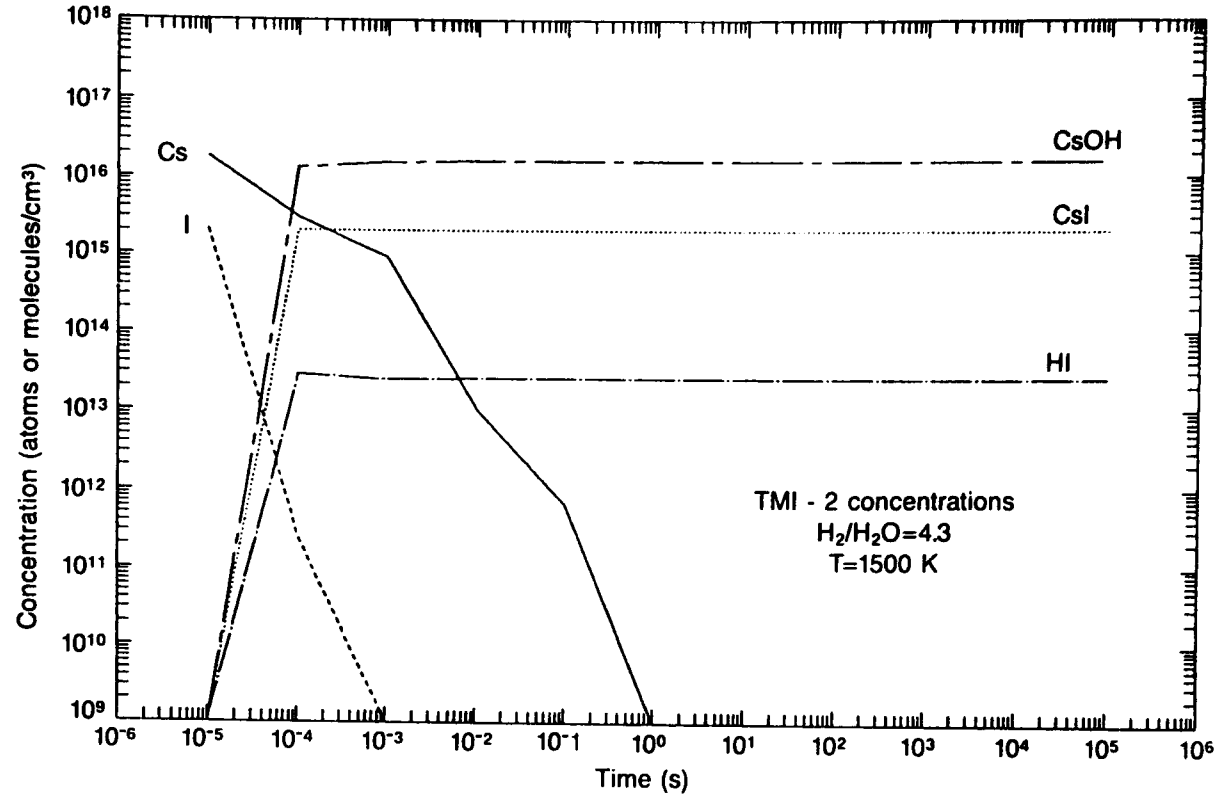

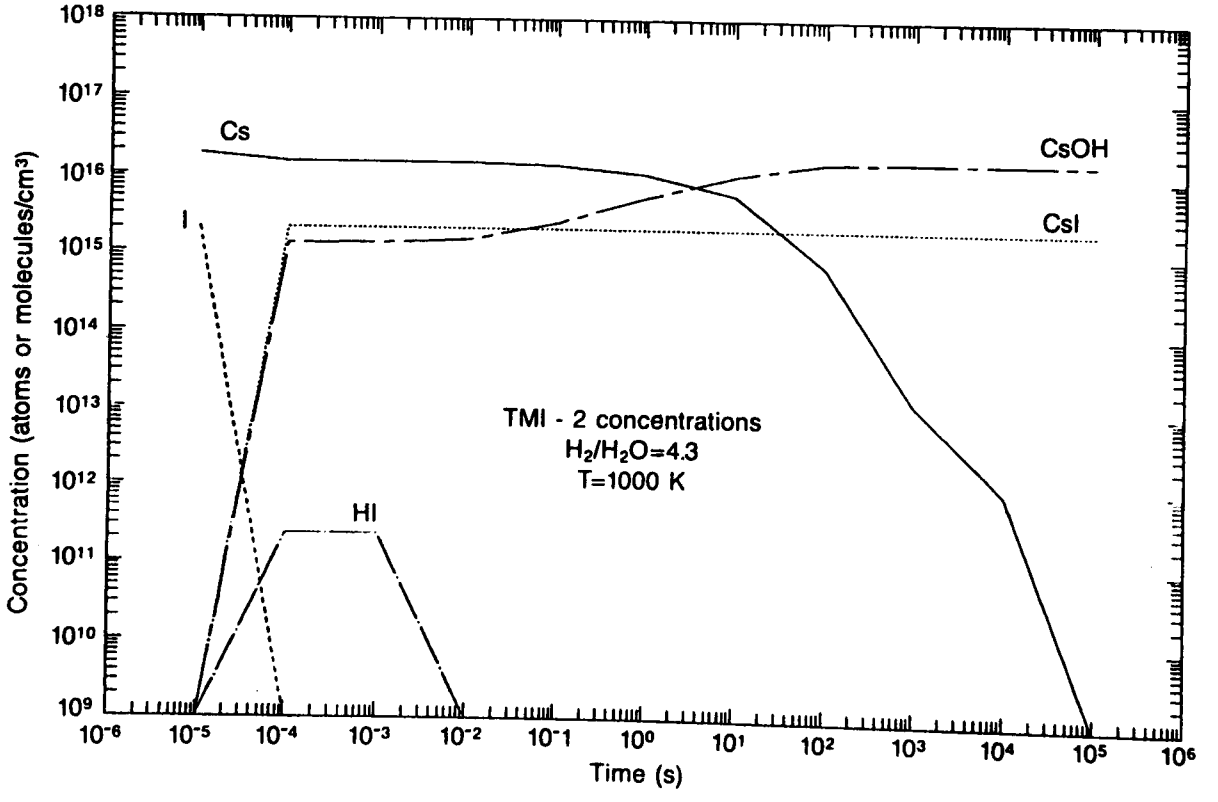

7-9650

Figure A-4. Illustration of the effect of temperature on reaction kinetics and Cs/I species partitioning.

concentration of hydrogen, the probability of free OH combining with H to form water at 1000 K is much greater than the probability of OH reacting with Cs to form CsOH. Hence, the long time to reach CsOH equilibrium is consistent with the kinetics data and intial concentration conditions used in the analysis.

It is also noted that at 1500 K, HI remains stable in the presence of cesium, while at 1000 K, HI is unstable and transformed to CsI. Thus, as the effluent (hydrogen, steam, and fission products) exits the core and cools in the upper plenum, complete transformation of HI to CsI is predicted to occur. The same is true for both hydrogen-rich (e.g., $H_2/H_2O = 4.3$) and neutral ($H_2/H_2O = 1$) environments, as indicated in Figure A-5.

On comparing the time to reach equilibrium for the 10 reaction mechanisms studied here, with the effluent transit time through the core half-height ($t \cong 204$ sec; see previous section), it can be seen that for most conditions the time to reach chemical equilibrium is much shorter than the effluent transit time, particularly at the elevated core temperature ($T>1500$ K). However, this may not be true in the plenum region, where lower temperatures ($T \leq 1000$ K) result in slow kinetics for the CsOH reaction species. Nevertheless, since equilibrium for CsOH would have been established in the core prior to the effluent entering the colder plenum, this effect is minimal.

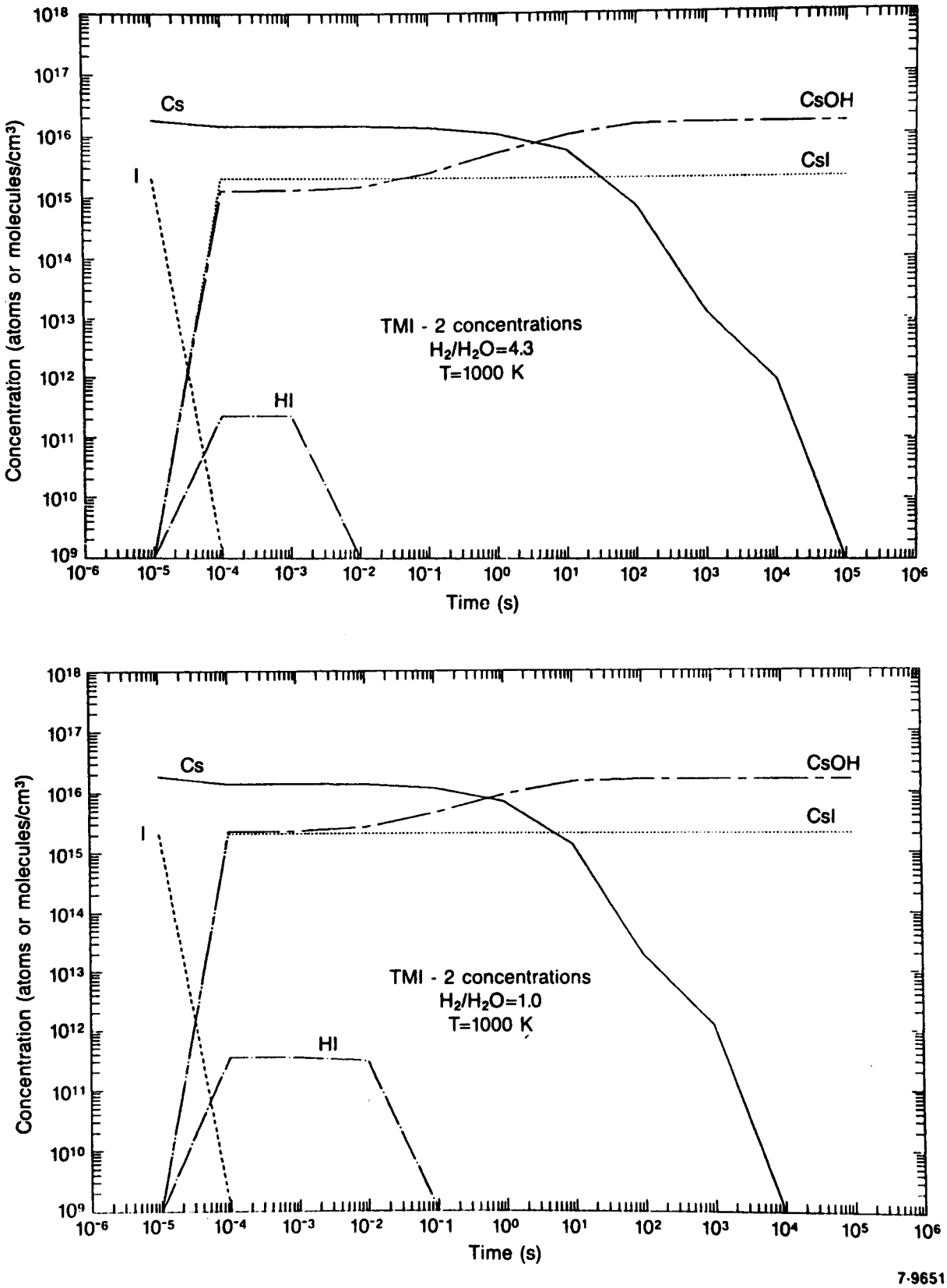

Figure A-5. Illustration of the effect of H_2/H_2O mole ratio on reaction kinetics and I/Cs species partitioning at T = 1000 K.

A.3 References

A.1 D. J. Wren, Kinetics of Iodine and Cesium Reactions in the CANDU Reactor Primary Heat Transport System Under Accident Conditions, AECL-7781, April 1983.

A.2 A. W. Cronenberg, D. J. Osetek, and P. R. Reed, "Analysis of Iodine Chemical Form for Severe Fuel Damage Experiments," Proc. Am Chemical Soc. Mtg; Severe Accident Chemistry Symposium, Anaheim, CA, September 7-12, 1986.

A.3 Z. R. Martinson, D. A. Petti, and B. A. Cook, PBF Severe Fuel Damage Test 1-1: Test Results Report, NUREG/CR-4686, EGG-2463, October 1986.

A.4 E. C. Beahm, W. E. Shockley, and O. L. Culberson, Organic Iodine Formation Following Nuclear Reactor Accidents, NUREG/CR-4327, April 1985.

A.5 A. K. Postma and R. W. Zavadoski, Review of Organic Iodide Formation Under Accident Conditions in Water-Cooled Reactors, WASH-1244, 1972.

A.6 T. M. Besmann, SOLGASMIX-PV, A Computer Program to Calculate Equilibrium Relationship in Complex Chemical Systems, ORNL/TM-5775, 1977.